Genomic dependencies in MYC overexpressing multiple myeloma

Lama Hasan Bou Issa

UNIVERSITE DE LILLE
Ecole doctoral Biologie-Santé de Lille (ED446)

THESE
Pour l'obtention du grade de

DOCTEUR DE BIOLOGIE-SCIENCE DE LA VIE ET DE LA SANTE
DE L'UNIVERSITE DE LILLE

Etude des dépendances génomiques dans le myélome multiple surexprimant *MYC*

Présentée et soutenue publiquement le 25 Mars 2024 par
Lama Hasan Bou Issa

JURY COMPOSE DES MEMBRES

Monsieur le **Professeur Xavier LELEU**	Examinateur/ président du jury
Monsieur le **Professeur Jérome MOREAUX**	Rapporteur
Madame le **Professeur Jill CORRE**	Rapporteur
Madame le **Docteur Audrey VINCENT**	Examinateur
Monsieur le **Professeur Salomon MANIER**	Directeur de thèse

Travail réalisé au sein de l'UMR9020 (CNRS)- U1277 (INSERM) - Le laboratoire CANTHER « Hétérogénéité, Plasticité et Résistance aux Thérapies des Cancers » - ONCOLille.

Equipe : Facteurs de persistance des cellules leucémiques

To Syria, my war-torn homeland, and to the resilient Syrian people—those who left seeking dreams beyond war's shadows, and those who stayed with unparalleled courage.

This thesis is a tribute to your collective strength, perseverance, and unwavering spirit.

Acknowledgements

I extend my deepest gratitude to **ARC foundation** and **Société Française d'Hématologie SFH** for funding this thesis and the **University of Lille** for hosting me during my doctoral studies.

My sincere thanks go to **Professor Philippe Delannoy** and **Professor Michel Salzet** for welcoming me to the institute pour la Recherche sur le Cancer de Lille (IRCL) and **Dr Isabelle Van Seuningen** for welcoming me to the CANTHER research unit.

I'd also like to thank **Professor Bruno Quesnel** who graciously opened the door of this academic opportunity and introduced me to my esteemed supervisor.

My sincere thanks go to **Dr. Audrey Vincent** and **Dr Catherine Pellat- Deceunynck** for their invaluable guidance, support during my yearly CSI meetings.

I extend my sincere and respectful thanks **to the members of the jury** for their interest in this work. I would like to thank **Professor Jérôme Moreaux** and **Professor Jill Corre** for doing me the honour of being the rapporteurs for this thesis. I would like also to thank **Professeur Xavier Leleu and Dr. Audrey Vincent** for agreeing to be examiners for this work.

This work benefitted greatly from the collaboration with **Professor Jérôme Kluza,** It was a pleasure working with you.

I would like to express my sincere gratitude to **Professor Salomon Manier**, my thesis supervisor for his unwavering support, trust, and encouragement throughout four years. You've pushed me to challenge myself and even though it felt tough at times, but it has undoubtedly imparted invaluable experiences and has significantly shaped my academic development and helped me grow into an autonomous researcher. I'd like to thank you sincerely for the enthusiasm you shared with me, your insights when I got carried away too quickly, and your optimism when my spirit dropped.

To my colleagues, **Silvia Gaggero, Adeline Cozzani, Tiziano Ingegnere, Malo Leprohon, Pauline Peyrouze, Hassiba Bouafia, Djohana Laurent, Salim Dekiouk, Melanie Dhayer** and **Lea Fléchon, Meriem Ben Khoud**. I'm immensely grateful for the wonderful bond shared between us and your encouragement during the challenging phases of my doctoral journey.

Heartfelt thanks to the dedicated **William Laine.** Despite the long and tiring experiments with endless conditions we have tested, these moments were enjoyable in your company.

To the future doctors who still on this rollercoster ride, **Marie-Océane Laguillaumie, Julie Vrevin, Axel Chomy, Claire Degand, Benjamin Segain, Pauline Cioffi,** I wish you all the best in your journey, I cannot wait until I celebrate your PhD defences to join the thesis-free world.

To **Nathalie Jouy** and **Emilie Floquet**, thank you for your advice and help with the flow cytometry analysis, your kindness, and your morale support.

I extend my appreciation to the researchers on my team **Dr. Suman Mitra, Dr. Xavier Thuru, Dr. Yasmine Touil, Dr. Meyling Cheok, Dr. Marie-Hélène David-Cordonnier** and **Dr. Thierry Idziorek** for their valuable advice and support provided throughout this thesis.

I want to express my sincerest gratitude to the IRCL family **Micheline Magdelon, Corinne Merckx, Mathias Gerard and Michel Marissal** for their moral and administrative support.

I would like to thank the generous support of **Justine Hannebique** from the animal facility who trained me to start the long and demanding *in vivo* part of this study. I would like also to thank **Aurelie Parmentier** from the animal facility for helping me to find solutions to reduce the stress during heavy-manipulations.

Special thanks to **Veronique Baclet** for her joyful spirit and for her efficacy and productivity.

To all Leukemia team, I extend my heartfelt gratitude **to all of you** for your constant support, genuine concern, and efforts to uplift my spirit when my homeland faced the devastating earthquake. This tragedy put me through an emotional turbulence which I cannot explain, but your collective kindness became a source of strength that kept me going to arrive to this moment of my journey.

To my Friends, **Razan Assaad, Naji Mawaket, Tarek Al Najjar and Hala Abou Daher** who welcomed me as a family when I knew no one in this country, I am in dept to you. I would never forget to thank my lifelong friends **Ali Maroof**, **Alice Mostafa**, **Oula Mansour and Marah Eido.**

To my Family,

Probably the most difficult part to write in this thesis is this, and at this moment I feel that my vocabulary is not enough. To my **Mother Seham** and **Father Abdulhakem**, you have been both the beating heart of my journey, supporting me when I chose a less conventional path, even during challenging times in Syria. Your encouragement has been the wind beneath my wings. It would not have been possible without you.

To my **Brother Housam** and **Sister Leen**, the sunshine of my life and the infusion of joy to my days. Your laughter even through the phone and video calls have been my daily reminder to focus and find my way in the midst of challenges.

It has been a tough six years since I last saw you, and the distance has been a constant ache, but here I am as I promised, coming back with a PhD and I cannot wait to celebrate this, the five of us united again.

To my in-law family,

In the past four years, you've not only welcomed me into your family but embraced me with warmth and love. I am incredibly fortunate to have found such supportive and caring extended family. Thank you, **Franck, Paulina, Nina and Amaury.** You have created a precious family circle that I have missed dearly while being away from my own.

To my love,

I cannot thank enough my darling fiancé **Igor Pollet**, who is my biggest supporter in this long journey. Through all the research-challenges, experiments going wrong, day and night mouse experiment, sleepless nights, weekend-less weeks, and rejection of manuscript, you have been there for me with your endless encouragements. You blessed me with unique gentleness, love and believed in me, making every step of this challenging path a shared triumph.

I am thankful **to God**, the ever-present guiding force who has shaped my path to be who I am and where I am today.

Last but not least, I would like to leave a word **to my future-self**. Whatever challenges future is keeping for us, do not forget the purpose of research and the passion that you've started with and keep going. Remember that, even through homesick, depression, gloomy mornings, rainy evenings, global pandemic, horrific earthquake, endless research struggles, we have made it to the finish line.

Lama

Scientific achievements and participations

Articles

1- **Lama Hasan Bou Issa***, Léa Fléchon, William Laine, Aicha Ouelkdite, Silvia Gaggero, Adeline Cozzani, Remi Tilmont, Paul Chauvet, Nicolas Gower, Romanos Sklavenitis Pistofidis, Carine Brinster, Xavier Thuru, Yasmine Touil, Bruno Quesnel, Suman Mitra, Irene M. Ghobrial, Jérôme Kluza, Salomon Manier. MYC dependency in GLS1 and NAMPT is a therapeutic vulnerability in multiple myeloma. iScience (accepted).

2- Léa Fléchon*, Ines Arib*, Ankit K. Dutta*, **Lama Hasan Bou Issa**, Romanos Sklanvenitis-Pistofidis, Remi Tilmont, Chip Stewart, Romain Dubois, Stéphanie Poulain, Marie-Christine Copin, Sahir Javed, Morgane Nudel, Doriane Cavalieri, Guillaume Escure[2], Nicolas Gower[2], Paul Chauvet, Nicolas Gazeau, Cynthia Saade, Marietou Binta Thiam, Aïcha Ouelkite-Oumouchal, Émeline Cailliau, Sarah Faiz, Olivier Carpentier, Nicolas Duployer, Thierry Idziorek, Laurent Mortier, Martin Figeac, Claude Preudhomme, Bruno Quesnel, Suman Mitra, Franck Morschhauser, Gad Getz, Irene M. Ghobrial, Salomon Manier. Genomic profiling of Mycosis Fungoides identifies patients at high risk of disease progression. Blood advances (accepted).

3- Guillaume Escure*, Elise Fournier, Cynthia Saade, **Lama Hasan Bou Issa**, Inès Arib, Rémi Tilmont, Nicolas Gazeau, Binta M Thiam, Morgane Chovet, Maxime Delforge, Nicolas Gower, Léa Fléchon, Doriane Cavalieri, Paul Chauvet, Morgane Nudel, Laure Goursaud, Céline Berthon, Bruno Quesnel, Thierry Facon, Claude Preudhomme, Nicolas Duployez, Salomon Manier. Small myeloid subclones are present at diagnosis of multiple myeloma in patients who develop secondary myelodysplastic syndromes. Haematologica. 2023 Oct 19. doi: 10.3324/haematol.2023.284050. PMID: 37855058.

4- Cheng W*, Gaggero S*, Ouelkdite A*, Escure G, Cozzani A, Tchantchou Njosse Y, Carlier N, Leprohon M, Kasprowicz A, Groux S, **Hasan Bou Issa L**, Moreau J, Arnulf B, Corre J, Martinet L, Leleu X, Avet-Loiseau H, Facon T, Jin W, Mitra S, Manier S. Inflammatory microenvironment impairs responses to daratumumab in multiple myeloma. In submission to Blood.

Presentations

- **3rd annual global summit on Hematological Malignancies** (2020) Lisbon-Portugal (Poster presentation)
- **41st Société Française d'Hématologie SFH annual congress** (2021) Paris-France (Poster presentation).
- **European Hematology Association EHA2022** (2022) Vienna-Austria (Poster presentation).
- **2nd scientific day Intergroupe Francophone Du Myélome IFM** (2022) Paris-France (Oral presentation)

Prizes

- Best oral presentation of the ONCOLille PhD day 2023
- EHA 2022 travel grant 2022
- Best oral presentation of the ONCOLille PhD day 2022

Table of content

List of tables, figures & tables

List of abbreviations

1,3PG	1,3-bisphosphoglycerate
3PG	3-phosphoglycerate
ACLY	ATP citrate lyase
ACO	Aconitase
ADP	Adenosine diphosphate
AID	Activation-induced cytidine deaminase
a-KG	Alpha-ketoglutarate
ANT	Adenine nucleotide translocase
Asn	Asparagine
Asp	Aspartate
ATARiS	Analytic technique for assessment of RNAi similarity
ATP	Adenosine triphosphate
BCR	B cell receptor
BIM	Bcl2 interacting mediator of cell death
CAD	Carbamoyl-phosphate synthetase
CAF	Cancer associated fibroblasts
CAT	Carnitine translocase
CDK	Cyclin-dependent kinase
CLP	Common lymphoid progenitor
CMP	Common myeloid progenitor
CPT	Carnitine palmitoyltransferase
CS	Citrate synthase
CSR	Class switch recombination
DCA	Dichloroacetate
DepMap	Cancer dependency map
DG	Deaoxyglucose phosphate
DSS	Durie-Salmon staging system
E4P	Erythrose 4-phosphate
EAA	Essential amino acid
EMD	Extramedullary disease
ENO	Enolase
ETC	Electron transport chain
F1,6P	Fructose 1, 6-biphosphate
F6P	Fructose 6-phosphate
FABP	Fatty acid binding protein
FADH	Flavin adenine dinucleotide+ hydrogen (H)
FAT	Fatty acid translocase
FISH	Fluorescent in situ hybridization
G3P	Glycerol-3-phosphate
G6P	Glucose-6-phospahte
G6PD	Glucose-6-phosphate dehydrogenase

GA	Glutaminase
GAC	Glutaminase C
GDH	Glutamate dehydrogenase
GGT	Gamma glutamyl transpeptidase
Gln	Glutamine
Glu	Glutamate
GLUT	Glucose transporter
GMP	Guanosine 5-monophosphate
GMP	Granulocyte-macrophage progenitors
GOT	Aspartate aminotransferase
GPI	Glucose-6-phospahte isomerase
GPNA	Gamma-glutamyl-p-nitroanilide
GPT	Alanine aminotransferase
GR	Glutathione reductase
GSH	Glutathione
GTP	Guanosine triphosphate
HDMM	Hyperdiploid myeloma
HIF-a	Hypoxia-inducible factor
HK2	Hexokinase
HLH	Helix loop helix
HMGCR	Hydroxymethylglutaryl-coa reductase
HMGCS	Hydroxymethylglutaryl-coa synthase
HSC	Hematopoietic stem cells
IDH	Isocitrate dehydrogenase
Ig	Immunoglobulin
IMP	Inosine 5-monophosphate
ISS	International staging system
KGA	Kidney-type glutaminase
L-ases	Asparaginase
LDH	Lactate dehydrogenase
LGA	Liver-type glutaminase
lncRNA	Long non-coding RNA
LZ	Leucine zipper
MAPK	Mitogen-activated protein kinase
MAS	Malate-aspartate shuttle
MB	Myc box
MCT	Monocarboxylate transporter
MDH1	Malate dehydrogenase
MeAIB	N-metyl-aminoisobutyric acid
MGUS	Monoclonal gammopathey of undetermined significance
MM	Multiple myeloma
MOI	Multiplicity of infection
MPC	Mitochondrial pyruvate carrier
MYC OE	MYC overexpressing cells
NAAD	Nicotiic acid dinucleotide

NADH	Nicotinamide adenine dinucleotide+ hydrogen (H)
NADP	Nicotinamide adenine dinucleotide phosphate
NADPH	Nicotinamide adenine dinucleotide phosphate, reduced
NADS	NAD synthase
NAMN	Nicotninc acid mononucleotide
NAMPT	Nicotinamide phosphoribosyltransferase)
NCL	Nucleolin
NEAA	Non-essential amino acid
NHDMM	Non-hyperdiploid myeloma
NMN	Nicotinamide mononucleotide
NMNAT	Nicotninc-acid-specific mononucleotide adenylyltransferase
NMNAT	Nicotinamide mononucleotide adenylyltransferase
NPM1	Nucleophosmin
NR	Nicotinamide riboside
NRF	Nuclear respiratory factor
NRk	Nicotinamide riboside specific kinase
PARP	Poly ADP -ribose polymerase
PC	Pyruvate carboxylase
PCL	Plasma cell leukemia
PDH	Pyruvate dehydrogenase
PDK	Pyruvate dehydrogenase kinase
PDP	Pyruvate dehydrogenase phosphate
PFK	Phosphofructokinase
PGC	Peroxisome proliferator activated receptor
PGK	Phosphoglycerate kinase
PGM	Phosphoglycerate mutase
PHGDH	Phosphoglycerate dehydrogenase
PK	Pyruvate kinase
PPP	Pentose phosphate pathway
PRPS	Phosphoribosyl pyrophosphate synthetase
PSAT1	Phosphoserine aminotransferase
PSPH	Phosphoserine phosphatase
R5P	Ribose-5-phosphate
RPL	Large ribosomal subunit
RPS	Small ribosomal subunit
SCS	Succinyll-coa synthetase
Sel	Selenazofurin
SHM	Somatic hypermutation machinery
SHMT2	Serine hydroxymethyltransferase 2
SL1	Selectivity factor 1

SLC Soluble linked carrier

SMM Smoldering multiple myeloma

SV Structure variant

TAZ Tiazofurin

TNBC Trip negative breast cancer

TTD Terminal tandem duplication

UBF Upstream binding factor

UTR Untranslated region

VAD Vacor adenine dinucleotide

Résumé

Le myélome multiple (MM), une hémopathie maligne qui représente environ 13% des cancers hématologiques, est caractérisée par la prolifération de plasma cells tumoraux au niveau de la moelle osseuse. Le MM évolue à partir de stades précurseurs, à savoir la gammapathie monoclonale de signification indéterminée (MGUS) et le myélome multiple asymptomatique (SMM), vers la forme symptomatique, le MM. C'est une hémopathie maligne incurable dont l'hétérogénéité et l'évolution clonale permettent l'échappement aux traitements et la progression de la maladie. Les altérations de MYC ont un rôle essentiel dans cette progression. Cependant, MYC n'est pas ciblable thérapeutiquement en raison de sa localisation nucléaire et de la courte demi-vie de la protéine.

Pour surmonter cela, nous avons fait l'hypothèse que l'avantage prolifératif induit par la surexpression de MYC crée des dépendances des cellules tumorales vis-à-vis d'autres voies de signalisation qui deviennent indispensables à la survie de ces cellules. Pour tester cette hypothèse, nous avons appliqué une nouvelle méthodologie utilisant la carte de dépendance (Achilles) et effectué un screening de 2000 petites molécules afin d'identifier les vulnérabilités génomiques induites par MYC. Si elles sont identifiées, ces vulnérabilités offrent une possibilité de traitement ciblé des cancers ayant une surexpression de MYC. Nos analyses démontrent la dépendance des lignées cellulaires surexprimant MYC pour le métabolisme de la glutamine, spécifiquement les gène GLS1 (glutaminase). Nous avons validé et délimité fonctionnellement cette dépendance *in vitro* à partir des différentes approches.

Par l'analyse de notre criblage de 1869 composés chimiques, nous avons observé que les inhibiteurs de la synthèse de NAD avaient un effet préférentiel sur la prolifération des cellules surexprimant MYC. Considérant que les rôles métaboliques du glutamine sont liés à ceux du NAD, nous avons ensuite exploré un effet synergique potentiel entre les inhibiteurs du GLS1 et du NAMPT. Nous avons démontré l'efficacité de cette nouvelle combinaison synergique pour cibler les cellules MM surexprimant MYC *in vitro* et *in vivo*.

Ces résultats établissent une base méthodologique solide utilisable pour développer de nouvelles approches thérapeutiques afin de répondre à des besoins thérapeutiques non satisfaits pour cibler le MYC dans le MM.

Abstract

Multiple myeloma (MM) is a hematological malignancy that accounts for around 13% of hematological cancers and is characterized by the uncontrolled proliferation of malignant plasma cells in the bone marrow. MM progresses from precursor stages, known as monoclonal gammopathy of undetermined significance (MGUS) and smoldering multiple myeloma (SMM), to the symptomatic form, MM. It is an incurable malignancy in which heterogeneity and clonal evolution allow treatment escape and disease progression. MYC alterations play an essential role in this progression. However, MYC is not therapeutically targetable due to its nuclear localization and the protein's short half-life.

To overcome this, we hypothesized that the proliferative advantage induced by *MYC* overexpression creates genomic dependencies on other signalling pathways that become essential for cell survival. To test this hypothesis, we applied a novel approach by leveraging large-scale loss of function screen (Achilles) and 1869 small molecules screen to identify MYC-induced genomic vulnerabilities. When identified, these vulnerabilities offer an opportunity to selectively target cancer cells harbouring this overexpression and spare normal cells.

Our analyses demonstrate the dependence of MYC overexpressing cells on glutamine metabolism, in particular on the GLS1 (glutaminase). We validated and functionally delineated this dependence *in vitro* using different approaches.

Our small molecule screen highlighted that NAD synthesis inhibitors had a preferential effect on the proliferation of MYC overexpressing cells. Considering that glutamine and NAD have closely interlinked metabolic networks, we investigated the possibility of a potential synergistic effect between GLS1 and NAMPT inhibitors. We demonstrated the effectiveness of this new synergistic combination to target MYC-driven MM cells *in vitro* and *in vivo.*

These results establish a solid methodological basis that can be used to develop new therapeutic approaches to address unmet therapeutic needs to target MYC in MM.

Introduction

Chapter I

Multiple Myeloma (MM)

1. Origin of MM cell

Mammalian B-cell development is a series of continuum stages known as B lymphopoiesis which begins with hematopoietic stem cells (HSCs) in the fetal liver prenatally and in the bone marrow postnatally. HSCs are found within an anatomical and functional structure known as the hematopoietic niche, where HSCs undergo asymmetric division to self-renew and replenish other blood cell progenitors. HSCs give rise to common myeloid and lymphoid progenitors, also known as (CMP) and (CLP). Furthermore, CMP gives rise to megakaryocyte-erythroid progenitors (MEPs), which form erythroid, and megakaryocytic progeny, which will form erythrocytes and platelets, respectively. CMPs also give rise to granulocyte-macrophage progenitors (GMPs), which form granulocytes and monocytes. While CLPs develop into early pro-T cells and pro B-cells [1,2] (Figure 1).

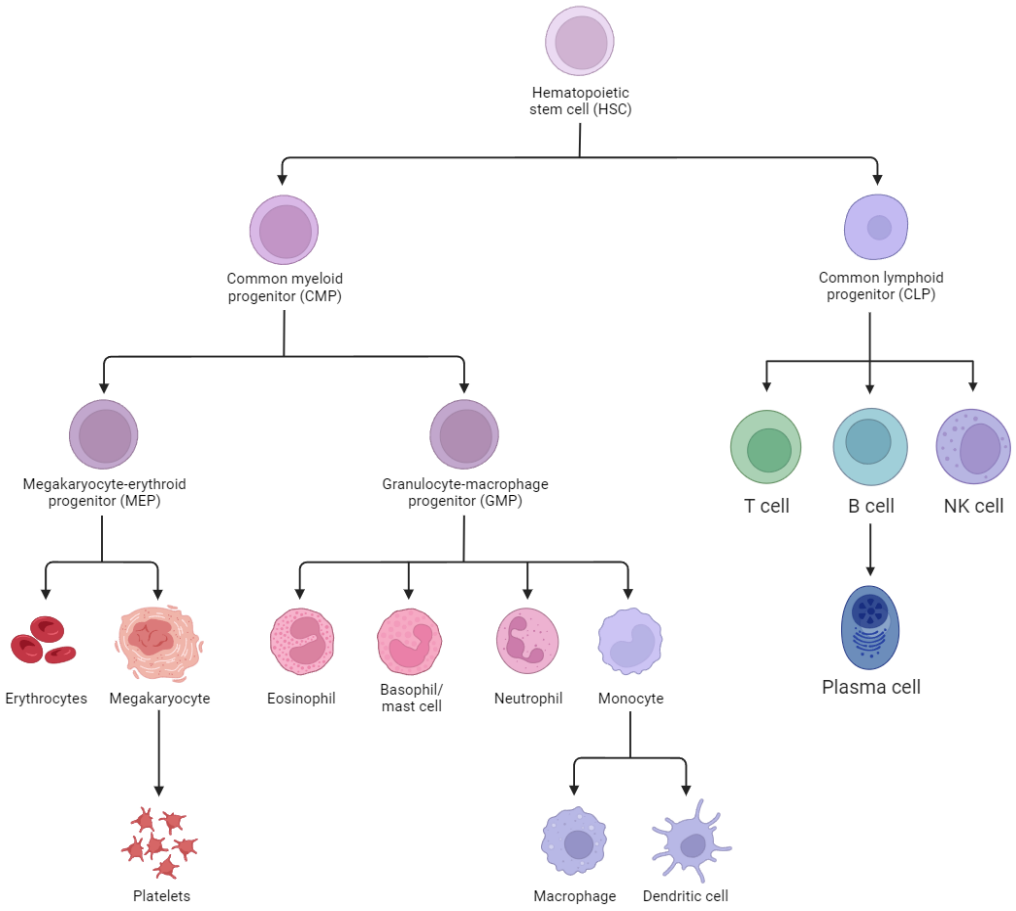

Figure 1| Overview of the hematopoietic stem cells (HSCs) differentiation. CMP: Common myeloid progenitor; CLP: Common lymphoid progenitor; MEP: megakaryocyte-erythroid progenitor; GMP: granulocyte-macrophage progenitor.

Interleukin-7 (IL-7) induces the differentiation of early pro-B cells to late pro-B cells. At this stage, heavy chain rearrangement is initiated by bringing together D and J segments, and then the DJ rearrangement is subsequently joined to a V segment to create a composite exon; this process is known as VDJ recombination. The VDJ recombination is essential for generating a diverse repertoire of immunoglobulins. Late pro-B cells that have assembled functional heavy chains receive a survival signal through the pre BCR, which allows them to develop into pre-B cells. Pre-B cells undergo recombination of their light chain (both Kappa and lambda light chains) before assembling their complete BCR, which consists of both heavy and light chains. Next, these BCRs are expressed on the surface of the B cell with a constant region isotype called IgM, and the cells at this step are classified as immature B cells. Immature B cells are then tested for auto-reactivity to self-antigen; this process is a negative selection known as Central tolerance in which the autoreactive cells will be eliminated from the B-cell pool. Immature B cells encoding non-autoreactive BCR migrate to the secondary lymphoid tissue, where cells undergo a second round of negative selection (Peripheral tolerance) before developing into mature naive B cells, which are characterized by the expression of their BCR on both IgM and IgD isotypes. Mature naive B cells are then differentiated into either plasma cells, specialized in antibody production, or memory B cells for long-term immunity (Figure 2).

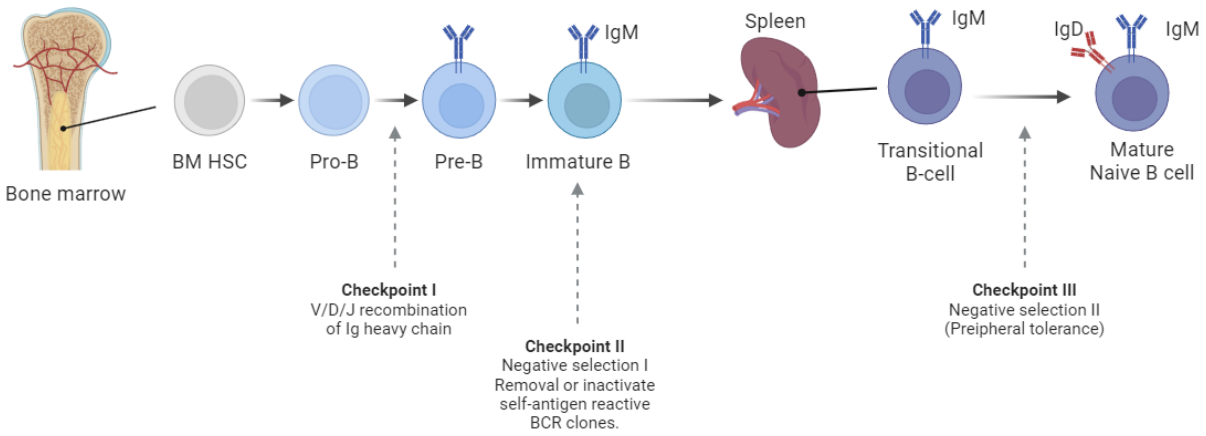

Figure 2| Stages of B cell development. B cell development occurs in both primary lymphoid tissue (the bone marrow) and the peripheral lymphoid tissues such as the spleen. In addition to the organ where development takes place, each stage can be also separated according to whether development is antigen-independent (BM HSC to Pre-B cell) or antigen-dependent (Immature and mature B cells).

Naive B cells then circulate through the peripheral blood and lymphatic system until they encounter antigens in the B cell follicles of the secondary lymphoid tissue. Bretcher and Cohn proposed that B-cell activation required two distinct signals. The first signal occurs upon antigen binding to the BCRs, while the second signal can occur via the thymus-independent (T-independent) or thymus-dependent (T-dependent) mechanism. The thymus-independent (T-independent) mechanism requires no help from T cells. Some antigens, such as polysaccharides or lipopolysaccharides, can directly provide the second B cell activation signal. Alternatively, T-dependent mechanism involves signals from T helper cells. Activated B cells load the internalized antigen on major histocompatibility complex II (MHCII) molecules. Then, T-helper cells recognize MHCII/peptide complexes on the B cells, resulting in T-cell activation. The activated T cell provides a second activation signal to activate the B cell [3,4]. As T-dependent response B lymphocytes proliferate they create microanatomical structures in the secondary lymphoid organs called germinal centers. Within the germinal centers somatic hypermutation (SHM) is induced, which allows random mutation in BCR genes, and these mutations lead to variations in the BCR's antigen-binding region. B cells with the highest affinity to the antigen are selectively favored in the germinal centers in a process known as affinity maturation. Affinity-matured B cells can switch from expressing IgD and IgM to IgG, IgE, or IgA through isotype/class switch recombination (CSR). This change can improve the cells' ability to eliminate the pathogen that induced the response [5,6].

2. Overview of multiple myeloma

Multiple Myeloma (MM) is an incurable plasma cell malignancy characterized by monoclonal plasma cells proliferation in bone marrow. Unlike normal plasma cells, myeloma plasma cells accumulate in the bone marrow and crowd out normal blood-forming cells, leading to bone marrow failure and anaemia. Furthermore, these malignant plasma cells suppress the normal plasma cells' function and produce abnormal and non-functional antibodies known as M-protein. The symptomatic or active MM passes through indolent forms, known as asymptomatic subclinical phases, including monoclonal gammopathy of undetermined significance (MGUS) and smoldering multiple myeloma (SMM) [7,8]. Genetic and microenvironment changes are what evoke the high-state risk. MGUS has a low risk of progression to MM of approximately 1% per year. In comparison, it is 10% per year for patients within the five years following diagnosis with SMM (Figure 3).

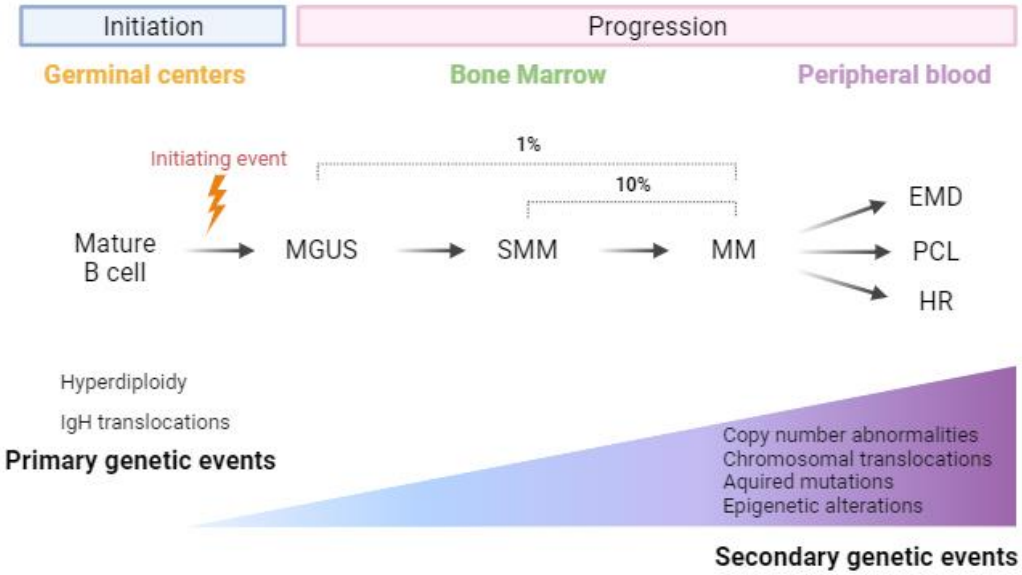

Figure 3| The stages of MM development. Common initiating events including hyperdiploidy or IgH translocations mainly t(4;14), (6;14), (11;14), (14;16) and (14;20), trigger the development of MGUS. Further mutational load transforms the MGUS to SMM before its transformation to MM. Secondary genetic events are responsible for the disease progression. EMD, PCL develop when the myeloma cells are no longer dependent on the survival signals from the BM microenvironment. EMD: extramedullary disease; PCL: plasma cell leukemia; HR: high-risk.

2.1 Diagnosis criteria

Diagnosis of asymptomatic and symptomatic MM is based on several clinical and biological factors. An original criterion was established in 2003 (according to the International Myeloma Working Group, IMWG) known as CRAB criteria, a group of features that describes end-organ damage. Recently, in 2014, the IMWG updated these criteria and added three main biomarkers to diagnose patients with MM without the CRAB features to enable earlier diagnosis and prevent the development of end-organ damage for patients with the highest risk and eventually allow the initiation of effective therapy [9]. The new diagnostic criteria include: This criterion was used to classify cases into three clinical forms: MGUS, SMM, and MM.

- Hyper**C**alcemia, serum calcium >0.25 mmol/L or 11 mg/dl.
- **R**enal insufficiency, with creatinine levels above 177 µmol/l or creatinine clearance <40 mL per minute
- **A**nemia, with hemoglobin below 10 g/dL (100 g/l) or 2g/dl below the lowest limit of normal

- **B**one lesions, one or more osteolytic lesion ≥5 mm in size, revealed by skeletal radiography, CT or PET/CT
- Ratio of involved /uninvolved free light chain ratio (FLC) ≥ 100 while involved FLC must be ≥ 100 mg/L
- ≥60% of clonal bone marrow plasma cells
- One or more focal lesions on MRI that is at ≥ 5mm

MGUS is characterized by serum monoclonal immunoglobulin (IgG or IgA) <30 g/l, <10% clonal bone marrow plasmacytes, and absence of CRAB features or amyloidosis whereas SMM is characterized by the presence of one or both biological criteria (serum monoclonal protein ≥ 30 g/l and/or clonal bone marrow plasma cells ≥10%) and the absence of CRAB criteria. The symptomatic MM is diagnosed by >10% clonal bone marrow plasma cells and >30g/l serum monoclonal immunoglobulin and the presence of at least one of the CRAB criteria. This stage requires immediate specific treatment.

2.2 Classifications and prognosis scores

The median overall survival of myeloma patients is 4 to 5 years. However, different factors such as host factors, tumor burden, and biology can modulate the disease progression and the overall survival rate. Thus, classification and prognosis scores were developed to guide treatment decisions among these systems:

2.2.1 Durie-Salmon staging system (DSS)

One of the earliest staging systems developed to assess the prognosis of individuals with MM was introduced in the 1970s. This system categorizes patients into three stages using the following main. Firstly, the tumor burden is evaluated by the amount of the M protein in the blood and urine, hemoglobin levels and the presence of osteolytic signs. The stages are further subdivided into A and B depending on the renal function (Table 1).

Stage	Criteria
I (low cell mass) $< 0.6x10^{12}$ cells/m^2	Hemoglobin > 10g/dl Normal bone structure or a single bone lesion Urine light chains M-protein <4g/24h Low monoclonal peak: IgG <5g/dl, IgA <3g/dl Normal serum calcium level or <10.5 mg/dL

II (intermediate cell mass) 0.6-1.2 x10^{12} cells/m^2	For MM cases whose criteria fall between stage I and stage III
III (High cell mass) > 1.2 x10^{12} cells/m^2	One or more of the following: Hemoglobin < 8.5 g/dl Multiple lytic bone lesions Urine light chains M-protein >12g/24h Low monoclonal peak: IgG>7g/dl, IgA>5g/dl High serum calcium level > 12 mg/dL
Subclassification	A. relatively normal renal function (serum creatinine value) < 20mg/l
	B. abnormal renal function (serum creatinine value) ≥ 20mg/l

Table 1| Durie-Salmon staging system

This system has its limitations, as it mainly classifies the patients based on the tumor burden and has problems with reproducibility; therefore, new systems were developed.

2.2.2 International Staging System (ISS)

This system was developed by IMWG in 2005 based on an analysis of 10750 patients from 17 healthcare institutions in different continents. This system is based on two key laboratory measurements: The serum β2-microglobulin level and serum albumin level [10]. β2-microglobulin level represents an indicator of the tumor burden while the serum albumin levels indicate the aggressiveness of the tumor clone because myeloma cells secret IL-6, which blocks the secretion of albumin. Based on the ISS system, patients can be categorized into ISS I, ISS II, and ISS III (Table 2). This system is more reproducible than the DSS system, but the albumin level was shown to be affected by other factors that are not disease specific.

Stage	Criteria
ISS I	serum β2-microglobulin < 3.5 mg/L; serum albumin ≥ 3.5 g/dL
ISS II	3,5 ≤ serum β2-microglobulin < 5,5
ISS III	serum β2-microglobulin ≥ 5,5 mg/l

Table 2| International Staging System

2.2.3 Revised international system staging (R-ISS)

A more recent staging system was introduced in 2015 by the IMWG as a revised version of the ISS system based on 4,445 patients newly diagnosed with MM from 11 international trials [11]. This system incorporated two important prognostic parameters: High-risk cytogenic abnormalities determined by interphase fluorescence *in situ* hybridization, including the presence of (t(4;14), t(14;16) and del (17p)) and the serum lactate dehydrogenase (LDH) level (Table 3).

Stage	Criteria
I	serum β2-microglobulin < 3.5 mg/L; serum albumin ≥ 3.5 g/dL Normal LDH No high-risk cytogenic abnormalities
II	For MM cases whose criteria fall between stage I and stage III
III	serum β2-microglobulin ≥ 5,5 mg/l and either The presence of high-risk cytogenic abnormalities or high LDH level

Table 3| Revised international system staging

This system combines the reproducibility of the ISS system and the disease biology represented by genetic factors thus provide a better tool in clinic helping guide treatment decisions.

3. Epidemiology

MM accounts for 1.8% of cancer cases worldwide and about 10% of hematological cancers, ranking among the most common after non-Hodgkin lymphoma and leukemia [12]. This malignancy is more common in men than in women, with an incidence rate of 8.7 per 100,000 in men and 5.8 in women and a median age at diagnosis of 69. Estimated Deaths in 2023 caused by MM were 12,590 accounting for 2.1% of total cancer deaths worldwide. In France, 6967 new MM cases and 3720 deaths were recorded in 2020. Compared to other countries of the European Union, France has the second-highest incidence of MM, with an estimated 10 cases per 100.000 population [13,14].

4. Oncogenic abnormalities in MM

4.1 Primary genetic events

Conventional karyotyping and more recent fluorescent in situ hybridization (FISH) on the chromosomes of $CD138^+$ cells identified primary cytogenetic abnormalities that trigger MM. Based on these recurrent primary cytogenetic abnormalities, two main groups of MM patients were described: hyperdiploid (HDMM) and non-hyperdiploid myeloma (NHDMM). HDMM is observed in 60% of MM cases and is characterized by a trisomy of several odd-numbered chromosomes 3,5,7,9,15,19 and 21. Although the molecular basis of this abnormality is currently unclear due to the lack of model systems for hyperdiploid myeloma. Cell line models used to study MM are driven from patients with extramedullary disease (EMD) or plasma cell leukemia (PCL) when MM is independent of the bone marrow microenvironment; thus, no cell line model can be used to understand the biology of hyperdiploid myeloma [15]. Clinically, HDMM has a good prognosis and a better outcome than NHDMM [16,17]. On the other hand, NHDMM is observed in 40% of MM patients and is characterized by translocations leading to the juxtaposition of the immunoglobulin heavy chains (IgH) control elements to one of the putative oncogenes. Among the most frequent translocations: t(4 ;14), t(6 ;14), t(11 ;14), t(14 ;16) and t(14 ;20). The main oncogenes involved in these translocations are the D-type cyclins, including cyclin D1, D2, and D3 at these loci: 11q13 (*CCND1*) in 15-20% of NHDMM and less frequently 6p21 (*CCND3*) in about 1-4% and possibly D2 on 12p13 but at a lower frequency of ~1%. Moreover, t(4;14) is the second most common NHDMM alteration (15%). In most cases, this translocation results in the deregulation of both Wolf–Hirschhorn syndrome candidate 1 (*WHSC1*), also known as Nuclear Receptor Binding SET Domain Protein 2 (*NSD1*) and the fibroblast growth factor receptor 3 (*FGFR3*). MAF family members are also involved (MafA, MafB, and c-Maf). *c-Maf* located on 16q23 loci was reported in ~5% of the cases results from t(14;16) while translocations in *MafB* t(14;20) were observed less frequently [17–19]. Both, Hyperdiploid myeloma and IgH translocations are large genetic alterations that are necessary events to initiate MGUS but are not sufficient to trigger symptomatic MM.

4.2 Secondary genetic events

Secondary genetic events include late-onset translocations, copy number abnormalities, single nucleotide mutations, and epigenetic modification, which play a major part in the disease progression and adversely affect the outcome. These abnormalities include del(17p), which is observed in 8% of newly diagnosed MM and found to affect progression free survival and

overall survival. Of note, Corre et al., reported an extreme poor outcome associated with the del(17p) even in the absence of *TP53* mutation [20]. Other deletions were also observed such as del(13q), del (6q), del (8p), and del (12p). Another important cytogenetic alteration is the chr(1q) gain. This gain incident increases from MGUS to relapsed multiple myeloma and is related to prognosis [21–23]. The presence of at least one of the mutations related with poor prognosis, including; gain (1q), deletion (17p) and the frequent translocations t(4 ;14), t(14 ;16), t(14 ;20) and *TP53* mutation is defined as high risk MM. In 2018, Walker et al., defined a subgroup of patients having 2 or more of these adverse high-risk genetic abnormalities as double and triple hit MM which can be related with even poorer outcomes and aggressive presentation. Compared to high-risk MM, these subgroups represent less than 10% of MM patients [24].

At the epigenetic level, altered DNA methylation was observed in MM cells compared to normal plasma cells. Both hypo and hypermethylation were observed in MM, and changes in the methylation profile were associated with MM tumorigenesis. The hypomethylation level was found to be increased in MM compared to MGUS stage, leading to a greater genome instability. Hypermethylation of specific genes was also observed in the CpG islands in the promotor region of tumor suppressor genes, including *RASSF4, p15, p16, p73, TP53, SOCS1, DAPK, SFRP1, SFRP2, VHL*, and *EGLN3* [25,26]. Furthermore, *MYC* structural variants (MYC SVs) are common in MM and promote disease progression. MYC SVs do not appear in MGUS stage while they are present in about 40% of newly diagnosed NHDMM and 57% of HDMM cases [27,28]. MYC role in MM progression from the MGUS stage was demonstrated by a transgenic mouse model called Vk*MYC, which will be discussed in details later [29]. Nine subtypes of MYC SVs were identified by next-generation sequencing (NGS), including translocations (Ig and non-Ig), duplication (of the genomic segment downstream of MYC known as terminal tandem duplications; TTD), deletions (proximal and terminal), amplifications, insertions (Ig and non-Ig) and complex del/gain.

Classic reciprocal translocations, mainly t(8;14) and t(8;22), in which the MYC juxtaposes the Ig loci (IgH>IgL>IgK) enhancer, leading to *MYC* overexpression. These c-MYC karyotypic abnormalities were observed in 5-10% of MM. Whereas the majority of translocations involving MYC are complex, often non-reciprocal, involving many partner chromosomes, and are sometimes associated with insertion, inversion, and duplication [19]. MYC translocations also occur with non-Ig partners such as *FAM46C, FOXO3*, and *BMP6* [30]. This complexity of the rearrangement and the high number of partner loci render the detection of the presence of these

rearrangements challenging. Thus, a targeted sequencing panel that is superior to both FISH and WGS was developed to identify common genomic abnormalities [31]. Clinically, the link between MYC deregulation and MM prognosis was studied. MYC rearrangements were found to be associated with poor outcomes in MM. Prognosis differences among the nine identified MYC SV subtypes were further studied. Sharma et al. conducted a retrospective study on 140 cases from the Mayo Clinic cohort and 658 cases from the Clinical Outcomes in Multiple Myeloma to Personal Assessment (MMRF CoMMpass) cohort to compare the prognostic significance of different MYC SVs. The study revealed an association between inferior outcomes and MYC's partnership with IgL. Together, MYC deregulations are highly important feature in the genetic landscape of MM, and therefore an appealing therapeutic target.

Chapter II

The proto-oncogene MYC

5. The proto-oncogene MYC

(v-myc myelocytomatosis viral oncogene homolog, *c-Myc*) proto-oncogene is one of the most studied genes in the last decades. MYC was first described in 1982 as a cellular homolog of the avian retroviral oncogene v-myc present in the genome of the MC29 avian virus and actively involved in tumor formation in chicken. [32,33]. Watson et al., isolated and cloned the *c-MYC* gene in humans. *c-MYC* gene is located at chromosome 8q24.21 and contains three exons. The first exon is a non-coding exon, while exons 2 and 3 encode the *MYC* transcription factor. Four distinct promoters were described: P0, P1, P2, and P3. P0 is in the untranslated region, P1 and P2 are located in the 5' region of the first exon, while P3 is in the intronic region. More than 75% of *MYC* transcripts originate from P2, followed by 10-25% originating from P1. Both P1 and P2 transcripts can encode two products due to the presence of two major translation initiation sites (CTG and ATG) upstream of CTG at the end of exon 1 and the beginning of exon 2, respectively [34,35]. Two isoforms are driven from the two alternative initiation sites in mature c-myc mRNA encoding 67 kDa or 64 kDa proteins consisting of 439 and additional 14 amino acid residues added to the N-terminal region [36,37] (Figure 4).

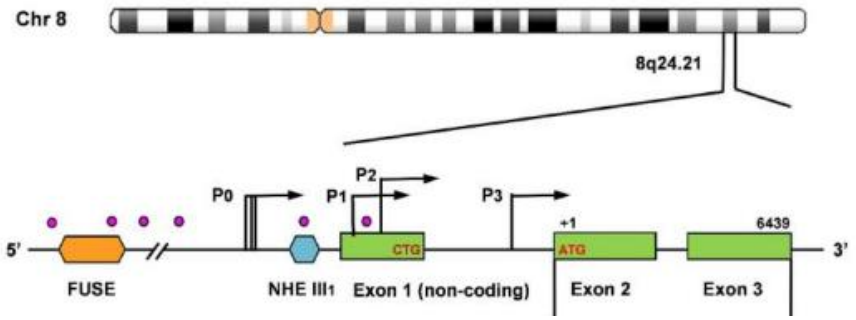

Figure 4| Localization and organization of the *c-MYC* human gene. Upper schema represents *MYC* localization on Chr 8. Lower schema represents the structure of the MYC gene. Three exons represented in rectangles with intronic regions as lines in between. FUSE (Far Upstream Sequence Element) and NHEIII1 (Nuclease Hypersensitivity Element III 1) are two cis-elements that form non-canonical DNA structures controlling c-MYC transcription (modified (Carabet, Rennie, and Cherkasov 2018)).

Myc has two homologous proteins, N-Myc and L-Myc, two transcription factors encoded by two genes first identified in human neuroblastoma and small-cell lung carcinoma, respectively. The *N-MYC* gene, located at chromosome 2p24.1, encodes two proteins of 456 and 464 amino acids with two different translation initiation sites. These two N-Myc proteins are 58 and 64

kDa, respectively. The *L-MYC* gene located at chromosome 1p34.2 encodes two protein isoforms of 364 and 206 amino acids, respectively. Myc protein has several functionally distinct structural domains [38].

5.1 Structure of MYC proteins

Generally, Myc protein consists of three domains and five subregions made up of highly conserved regions. The N-terminal part corresponds to the transactivation domain between residues 1 and 43, which is involved in the transcriptional activation of *MYC* target genes. Within the structure, four main Myc Box (MB) are distinguished with different functional properties, three of them in the N-terminal, while the last motif is in the C-terminal part. MBI is between the residues 44 and 63, and MBII is between the residues 129 and 143. Both MB I and II are located within the transactivation domain and are involved in the regulation of transcriptional activity. MB III is divided into IIIa and IIIb between residues 188-199 and 259-270, respectively. Then, MB IV is located between 304 and 324 amino acid residues. The C-terminal part of Myc contains a bHLH-LZ superdomain composed of three domains: a basic amino acid-rich region (b), responsible for the specific binding to the DNA at the E-box sites (CACGTG), a helix-loop-helix (HLH) domain and a leucine zipper (LZ) motif. bHLH-LZ domain is a conserved sequence found in many other transcription factors involved interacting with other obligatory partners [39–42] .(Figure 5).

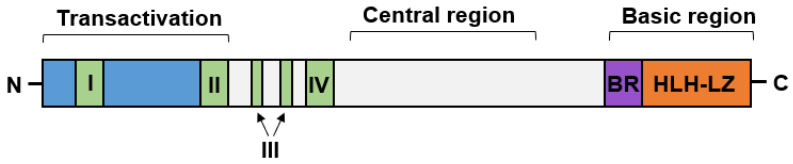

Figure 5| Representation of the structural domains and subregions of Myc proteins. A structural representation of the Myc protein showing the transcriptional activation domain, central region and the basic region involved in DNA binding after heterodimerization with Max. The five conserved subregions indicated by I, II, III a/b, and IV are also indicated.

Myc transcriptional activity requires prior hetero dimerization with Myc-Associated factor-X (MAX), a 151 amino acid protein with a bHLH-LZ region, which is an obligate partner of Myc. Myc heterodimerizes with its partner protein Max, and functions as a sequence-specific DNA-binding transcription factor [43,44]. The c-Myc/Max complex recognizes a preferential DNA sequence known as canonical MYC E-box, and in a concentration-dependent manner, c-

Myc/Max can bind with low affinity to additional non-canonical binding sites, such as E-Box sequence variants (CATGTG) or the E-box-free AACGTT sequence [45]. More than 25,000 E-boxes have been identified within the human genome [46]. Given that a gene can have several E-boxes, Myc/Max complexes can regulate the expression of over 11% of human genes [47]. Max itself can homodimerize and bind DNA or heterodimerize with another protein known as Mad [48].

5.2 MYC function

in vivo models have provided substantial knowledge regarding Myc function. *L-MYC* deficient mice are viable and show no congenital abnormalities, with normal reproductively competent, suggesting the possibility of complementation of L-Myc deficiency by other Myc oncoproteins [49]. Other investigations carried an inactivation of both *c-MYC* alleles suppressed c-Myc expression without a compensatory increase in N- or L-Myc; this inactivation casued a prolongation of the G1 and G2 phases while the S phase duration remains unchanged [50]. Several studies have demonstrated reciprocal control of *c-Myc* and *N-Myc* expression [51,52]. N-Myc is functionally complementary to c-Myc and can replace it throughout development, leading to viable, fertile adult mice N-Myc overcoming c-MYC absence, while *c-MYC* Knockout mouse models show lethality at the embryonic stage due to placental defect [53,54].

The *c-MYC* gene produces a highly conserved nuclear transcription factor that directly or indirectly regulates the expression of numerous genes involved in a handful of critical biological functions, including cell proliferation [55], apoptosis [56] transcription, translation, and cell metabolism [57] (Figure 6).

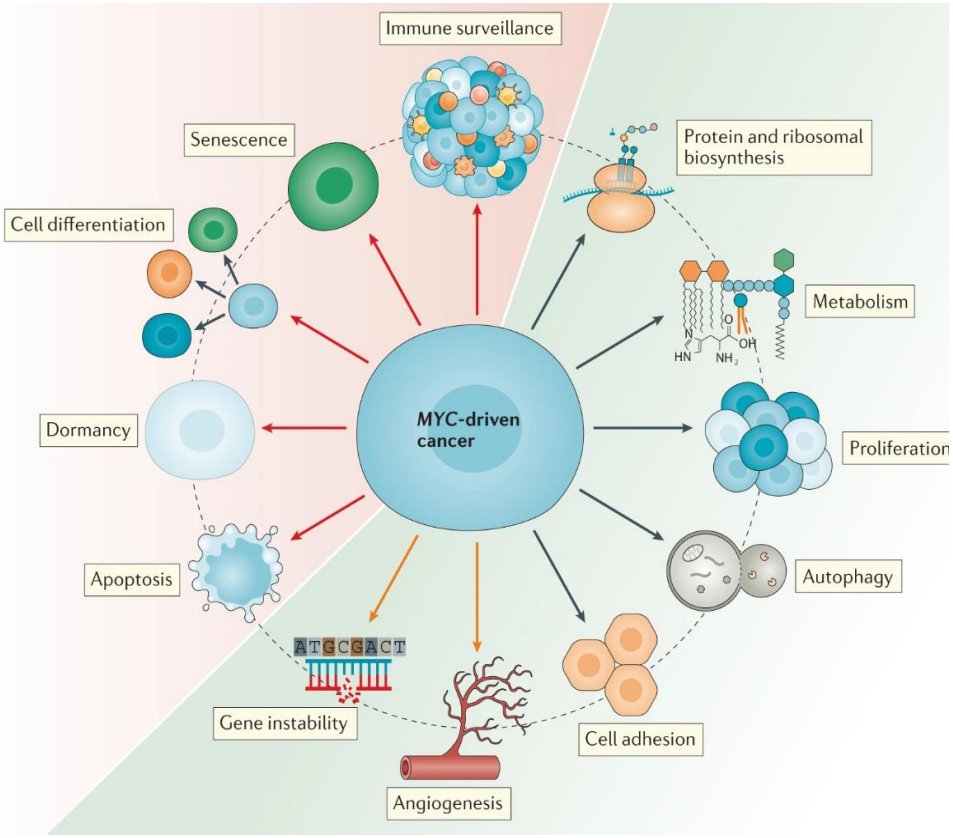

Figure 6| Summary of the main cellular functions regulated by MYC. MYC positively regulates the expression of a wide range of genes involved in proliferation, protein biosynthesis and metabolism (Green area). On the other hand, MYC blocks other cellular functions (red area) involved in differentiation and senescence hereby promoting cancer progression. (Dhanasekaran et al., 2022).

5.2.1 Cell cycle and proliferation

One of the primary functions of *MYC* is to promote the cell cycle [58]. c-Myc is involved in the cell cycle's various phase transitions, importantly the G1-S transition of the cell cycle [59,60]. It was found that the vast majority of positive cell cycle regulators are targets of c-Myc [61]. *MYC* induces the expression of cyclins (D, E, A and B1) and cyclin-dependent kinases (CDKs) 1,2,4 and 6. The *MYC*-induced expression of *CDK4* and *cyclin D2* is responsible for sequestering the CDK inhibitor KIP1 (p27) and thus enables the release and activation of the cyclin E-CDK2 complexes, essential for cell cycle progression [62,63]. In 2011, Bretones et al., found that MYC induces cyclin A and B, which activates CDK1 to phosphorylate P27 at Thr-187 and, therefore, recognized by SKP2, which induces P27 proteasome-dependent degradation [61,64]. MYC also induces the expression of E2 Promotor Binding Factor (*E2F*) to promote progression to S-phase [65]. Together with E2F, MYC activates the minichromosome maintenance protein complex (MCM), a helicase essential for DNA replication to initiate and sustain DNA replication. c-Myc

also represses the transcription of certain genes with the help of Miz1. Miz1 is a zinc finger protein that interacts with the Myc/Max complex to target promoters close to the transcription start site. Among these targeted genes the cell-cycle inhibitors INK4B and p21Cip1/Waf1 [66,67].

5.2.2 Ribosomes and protein synthesis

MYC regulates the expression of many genes involved in protein synthesis and ribosome biogenesis. MYC controls multiple components of ribosome biogenesis by stimulating the transcription of ribosomal RNA gene (rDNA) clusters that encode the 5.8S, 18S, and 28S rRNAs. MYC enhances the transcription of rRNA through chromatin remodeling of rDNA loci and interacting with cofactors such as upstream binding transcription factor (*UBF*) and selectivity factor 1 (*SL1*) that are required for RNA pol I recruitment. MYC-MAX is also responsible for stimulating RNA pol II-dependent transcription by stimulating the transcription of large ribosomal subunit (*RPL*), small ribosomal subunit (*RPS*), nucleophosmin (*NPM1*), and nucleolin (*NCL*) involved in rRNA processing and assembly [68–70]. MYC also interferes with protein synthesis by regulating translation initiation and elongation factors. It modulates the activity of the initiation factors eIF4E, eIF2α, eIF4AI, and eIF4GI, which are involved in mRNA cap regulation and translation initiation [71].

5.2.3 Myc and metabolism

Besides proliferation and protein synthesis, c-Myc regulates numerous metabolic pathways to support a high rate of division and cover the cells' increased need for energy and building blocks to increase its cell mass and replicate its DNA. In the MYC-mediated bioenergetic context, c-Myc promotes glycolysis by stimulating the expression of genes involved in glucose entry and metabolism through binding the classical E-box sequence. Among these genes are the glucose membrane transporters *GLUT1* (*SLC2A1*) and glutamine transporter *ASCT2* (*SLC1A5*) [72,73]. Besides inducing the glycolysis genes expression level, MYC favors specific splice variants, such as favoring pyruvate kinase type M2 (*PKM2*) over (*PKM1*), which we will further discuss in the next chapter. Moreover, *MYC* was found to be linked to the *GLS1* expression level through miRNA. MYC transcriptionally represses miR-23a/b. This repression correlated with enhanced glutamine metabolism through increased mitochondrial *GLS1* expression [74]. Lipid metabolism is another MYC target. MYC promotes citrate production driven by glucose and glutamine and upregulates of several genes related to fatty acid synthesis, such as ATP citrate lase (*ACLY*) and fatty acid synthesis (*FASN*) [75].

MYC regulatory network in metabolism is extended to nucleotide synthesis. MYC induces both purine and pyrimidine biosynthesis-related genes, such as phosphoribosyl pyrophosphate synthetase (*PRPS*) and carbamoyl-phosphate synthetase (*CAD*) [76]. MYC is also involved in the metabolism of amino acids, both essential and non-essential amino acids (EAAs and NEAAs). MYC upregulates critical EAAs transporters such as *SLC7A5* and *SLC43A1*, enabling the cells to maximize the EAAs uptake, which in turn enhances the MYC translation [77]. *MYC* upregulates the expression of enzymes involved in serine and glycine biosynthesis, such as 3-phosphoglycerate dehydrogenase (*PHGDH*), phosphoserine aminotransferase (*PSAT1*), phosphoserine phosphatase (*PSPH*), and serine hydroxymethyltransferase 2 (*SHMT2*) [78,79].

5.2.4 Genomic instability

MYC deregulation and sustained activation can lead to replication stress and errors during replication as it triggers many types of genomic damage, including DNA breaks, chromosomal translocations, losses or gains, aneuploidy, and polyploidy [80]. MYC affects the copy number of several genes involved in genomic instability such as dihydrofolate reductase (*DHFR*) [81,82]. MYC also plays a role in DNA damage response (DDR). *MYC* has been found to regulate the expression of ataxia telangiectasia mutated (*ATM*) and Rad3-related (*ATR*). Both serine/threonine kinases are critical in sensing DNA damage and initiating appropriate repair mechanisms. ATR responds to single-stranded DNA (ssBS) generated by replication stress while ATM responds to double-strand breaks (DSBs) [83,84]. (Poly ADP-ribose polymerase (PARP) is another key factor in the DDR pathway involved in DNA single-strand breaks (SSBs) repair. MYC was showed also to have interconnections with PARP and can predict the sensitivity to PARP inhibitors [85].

5.2.5 Angiogenesis

Angiogenesis is essential for cancer cells, facilitating the delivery of nutrients into the cells and allowing metastasis. MYC promotes vascularization by inducing the expression level of vascular endothelial growth factor (*VEGF*). Two other proteins involved in angiogenesis are regulated by MYC. MYC suppresses Thrombospondin-1 (*TSP-1*), while angiopoietin 1 and 2 are induced by MYC [86]. MYC upregulation in stromal cells, namely cancer-associated fibroblasts (CAFs), which can promote angiogenesis by cytokines and through recruiting endothelial cells [87].

5.2.6 MicroRNAs

MYC gene regulates the expression of numerous genes by different mechanisms. Various studies have shown that the MYC genes could regulate the expression of various miRNAs. MYC induces the expression of miR-17~92 cluster involved in the regulation of apoptosis by repressing the expression of the pro-apoptotic gene known as Bcl-2 Interacting Mediator Of Cell Death (BIM) [88–90]. Other studies showed that MYC also represses the expression of tumor suppressor miRNAs, such as let-7, miR-29, miR-34, miR-15/16 or miR23a/b [72,91,92]. Let-7 family regulates MYC expression through a regulatory feedback loop. let-7 family of miRNA represses the expression of MYC through binding to its 5′-untranslated region (UTR) and activating the RNA-induced silencing complex (RISC) [93,94].

Altogether, MYC regulates critical cellular functions. This positions MYC as a pivotal player in maintaining cellular growth and proliferation. While MYC targeting holds promise in the fight against cancer, its essentiality to normal cells underscores a big challenge in developing therapeutic strategies that selectively affect cancer cells and spare normal cells.

5.3 MYC in cancer

MYC upregulation has been detected and reported in 50-60% of all tumors, ranking MYC as one of the tumor-related genes. *MYC* overexpression can be achieved through different mechanisms, including *MYC* translocations, duplications, activation of MYC translation through PI3K/AKT/mTOR pathway, or various somatic mutations that increase MYC stability, Figure (7).

In MM and Burkitt lymphoma, *MYC* translocations have been identified, t(8;14) making MYC under the control of the immunoglobulin (Ig) heavy chain enhancer which results in overexpression of *MYC*. To study the role of *MYC* translocations in the progression of MM, a MYC-driven MM transgenic mouse model known as (Vk*MYC) was established and convincingly recreated the MYC translocation to the Ig loci [29]. In this mouse model, *MYC* expression is driven in specific cell types or at a particular time in cellular development. *MYC* coding sequence is under the control of the kappa light chain gene regulatory element (Vk). The third exon in the Vk codon contains an engineered stop codon that generates a DGYW motif, a motif preferentially targeted by somatic hyper-mutation machinery (SHM) that can revert the stop codon and promote MYC translation. In this way, *MYC* expression is conditional to Activation-induced cytidine deaminase (*AID*)-dependent SHM in germinal center B cells

[61,93,95]. MYC copy-number gain is another deregulation present in various cancers, including MM, breast, lung and colorectal cancers [71,96,97]. Perturbation of upstream signaling pathways is another mechanism of MYC dysregulation that affects protein stability. Two phosphorylation sites, threonine 58 (Thr58) and serine 62 (Ser62), located within the N-terminal MBI box, are involved in controlling the protein's stability. Studies have shown that Ser62 phosphorylation stabilizes c-Myc, while Thr58 phosphorylation destabilizes the protein. The Raf-MEK-ERK Mitogen-activated protein kinase (MAPK) pathway is involved in Ser62 phosphorylation, thus preventing proteasome-mediated degradation of Myc and increasing the half-life of newly translated Myc protein [98]. Ras/Raf/MAPK activation due to mutations in NRAS and KRAS was found in approximately 40% of MM patients [99]. As seen before, Let-7 microRNA regulates MYC expression, too. The overexpression of the RNA-binding protein (Lin28B) depletes the level of the Let-7 family of microRNA, thus increases the MYC translation [94,99]. Interferon regulatory factor (IRF4) is a key transcription factor and a central mediator of lymphoid and myeloid cell development. Genome-wide chromatin immunoprecipitation showed that MYC is a direct target of IRF4 and that IRF4 binds to the MYC promoter region to increase its activation [100].

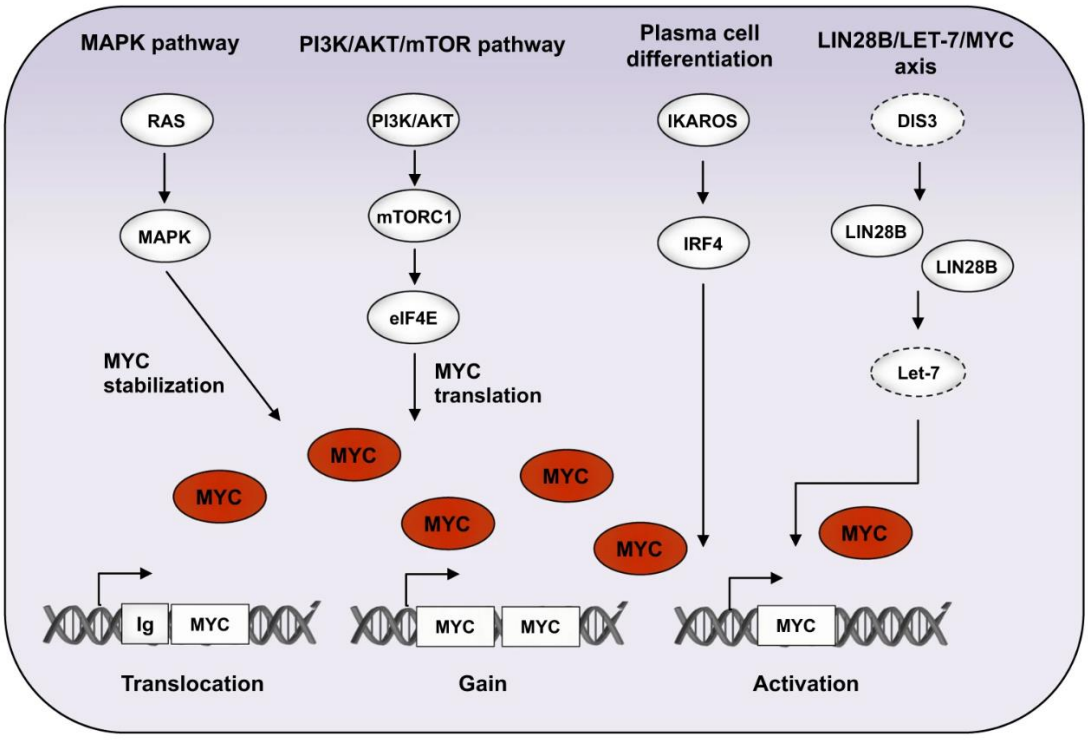

Figure 7| Summary of the main MYC deregulation in cancer (Jovanović et al., 2018)

5.4 Targeting MYC

MYC has emerged as a significant focus in cancer research due to its critical role in tumorigeneses and progression, as discussed earlier. Yet, targeting MYC remains a challenge. Myc lacks enzymatic activity, the intrinsically disordered location of its main functional domains, protein localization inside the nucleus, and the short half-life of the protein (20–30 minutes) made the available approaches to target MYC suffer from low potency, high toxicity, and poor pharmacokinetics properties. Different strategies have been established, including targeting *MYC* transcription, translation, protein stability, and interactions (Figure 8).

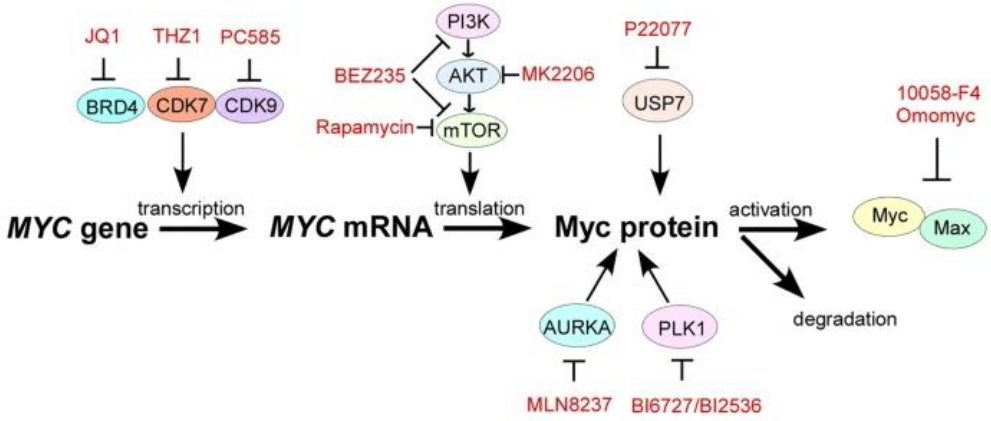

Figure 8| The different available strategies to target MYC (Chen et al.,2018)

5.4.1 Inhibiting MYC transcription

Inhibiting the transcriptional regulator (BRD4) has been shown to modulate the transcription of *MYC*. BRD4 is a member of the BET (bromodomain and extra terminal domain) family of transcriptional regulators that regulates *MYC* transcription. BRD4 binds to acetylated lysine residues in H3 and H4 within the promoter region and recruits the positive transcription elongation factor b (P-TEFb), which phosphorylates the negative elongation factors, allowing RNA polymerase II (pol II) to proceed with transcriptional elongation. This mechanism is known as Pause Release and Transcriptional Elongation [101–103]. BRD4 inhibitors, such as thieno-triazolo-1,4-diazepine known as JQ1 have been shown to compete with BRD4 in binding to acetylated lysine [104]. JQ1 resulted in significant anti-tumoral effects both *in vitro* and *in vivo* in various cancer types such as Burkitt's lymphoma, acute myeloid leukemia, multiple myeloma, and pancreatic ductal adenocarcinoma [105–107]. Other than BRD4 inhibition, other strategies to target BRD4 degradation were also developed to achieve more potent suppression

of *MYC* transcription. The proteolysis targeting chimeras (PROTACs) engineered bifunctional small molecules that induce selective degradation of the protein of interest by recruiting ubiquitin-proteasome system (UPS). The PROTAC molecule consists of two essential parts: a ligand that binds to the protein of interest and a ligand that recruits the E3 ubiquitin ligase. Different PROTAC molecules are available to target BRD4, such as ARV-825, dBET, and MZ1 which have been studied in pre-clinical models [108,109]. Other ways to modulate *MYC* transcription are through Cyclin-dependent kinases 7 and 9 (CDK7 and CDK9); uniquely among CDKs with critical roles in transcription initiation and elongation. CDK7 functions as a part of the CDK-activating kinase complex (CAK), which activates other cyclin-dependent kinases, such as CDK9 through T-loop phosphorylation. CDK9 forms a complex with P-TEFb to stimulate transcriptional elongation by phosphorylating serine 2 residue within the C-terminal domain of Pol II [110]. Several molecules have been developed to target CDK7, such as THZ1, a potent and selective CDK7 inhibitor and demonstrated efficacy in inhibiting *MYC* transcription in MYC-driven cancers. Moreover, SNS-032 and PC585 are inhibitors of CDK9 and suppress *MYC* transcription by blocking CDK-9 mediated phosphorylation of Pol II [111(p9)].

5.4.2 Inhibiting MYC translation

MYC translation is dependent on translation initiation factor 4F (eIF4F). The eIF4F consists of eIF4E, eIF4A, and eIF4G subunits. mRNA translation initiation can be blocked by 4E-BP1, which was reported to sequester the eIF4E subunit. mTOR was found to phosphorylate 4E-BP1, resulting in a release of the eIF4E subunit and eventually the assembly of the eIF4F complex and mRNA translation. Thus, the PI3K/AKT/mTOR inhibitors rose as potential therapeutics to target MYC translation. Among these inhibitors are TGR1202 a PI3Kd inhibitor also known as Umbralisib, and the mTOR inhibitor rapamycin [112,113].

The rocaglate family is another translation inhibitors that inhibits the eIF4A subunit [114]. CMLD010509 is a member of the rocaglate family, which proved its efficacy to block the translation program of a specific set of oncoproteins in MM including MYC, MDM2, CCND1, MCL-1, and MAF [115]. Another compound used to inhibit MYC translation is CX-5461, a cell-permeable benzothiazole compound that selectively inhibits RNA polymerase I -mediated pre-rRNA transcription which consequently reduce the level of ribosome biogenesis and impaired protein synthesis. Therefore, CX-5461 intervenes with the enhanced translational levels of MYC-driven cells. MM cells overexpressing MYC showed an enhanced sensitivity to CX-5461 [116].

5.4.3 Targeting MYC stability

Under physiological conditions, MYC has a relatively short life, and it is tightly regulated by the ubiquitin-proteasome system (UPS) [117,118]. FBW7 ubiquitin E3 ligase targets the Thr58 phosphorylated MYC to trigger proteasomal degradation. Several deubiquitinating enzymes, such as the multi-substrate ubiquitinating enzyme USP7, are involved in MYC stabilization. USP7 binds to c-MYC and N-MYC preventing proteolysis [119]. P22077 is a USP7 inhibitor, which was identified through an activity-based chemical proteomics approach. P22077 promotes MYC ubiquitination and degradation and showed promising results on the xenograft models of MYC-driven neuroblastoma and hepatocellular carcinoma [120–122]. Other USP7 inhibitors have been identified such as GNE-6640, GNE6776 and XL177A

5.4.4 Targeting MYC-MAX heterodimer

The obligatory functional partnership between MYC and MAX raised the question of the efficacy of disrupting MYC-MAX heterodimerization to suppress MYC-dependent cellular function. Small molecules have been identified to block the interaction between the two proteins, such as MYCMI-6 and 10058-F4 [123,124]. Other molecules modulate the MYC-MAX heterodimerization through stabilizing the MAX-MAX homodimer, thus sequestering MAX from MYC, such as KI-MS2-008 [125]. Other strategies focused on finding molecules to block the MYC-MAX complex binding to DNA. KSI-3716 effectively blocks the heterodimer from binding to target gene promoters [126,127]. A compound called OMO-103 (Omomyc) is another widely known synthetic peptide-based inhibitor that forms omomyc homodimers which can compete with MYC-MAX and interfere with its ability to bind DNA [128]. Omomyc also promotes MYC instability through proteasomal degradation [129].

Despite the recent advances, targeting MYC clinically remains a challenge. For this reason, collective efforts have focused on finding innovative therapeutic strategies to target MYC that can provide both selectivity and low toxicity. In this regard, the cancer dependency map is receiving greater interest to uncovering cancer vulnerabilities.

Chapter III

Gene Dependency

6. Cancer Dependency map (DepMap)

DepMap is an ongoing systematic effort to identify genomic vulnerabilities and potential therapeutic targets in various cancer types. It employs large-scale functional genomics profiling, including shRNA and CRISPR-Cas9 knockout screen, which systematically identifies the essentiality of individual genes in cancer cells or in a context-specific cancer cell. The aim is to further exploit these conditionally essential genes to develop targeted-therapies that can spare normal cells [130,131]. DepMap has empowered and accelerated precision cancer treatment research. Through this tool, G.V Kryukov et al. discovered that the loss of methylthioadenosine (*MTAP*) triggers a selective dependency on protein arginine methyltransferase 5 (*PRMT5*) and its binding partner *WDR77* [132]. Similarly, the Cancer dependency map was used to identify vulnerabilities in chromatin remodeling subunits SWI/SNF-mutant cancer cells. Kim et al., revealed a selective dependency on *EZH2*, the catalytic subunit of the Polycomb repressive complex 2 (*PRC2*) an essential transcriptional regulator [133]. Achilles database is one of the Cancer dependency map projects that was developed in Broad Institute.

6.1 Achilles database

This project aimed to identify the link between a specific genomic feature and the "Achilles heel" across various cancer types. Briefly, these screens consist of hundreds of cell lines of diverse human cancers infected with pooled shRNA plasmid library targeting around 9000 genes with an average of five shRNA per gene, delivered to the cells by lentiviruses as vectors at low Multiplicity of infection (MOI) so that each cell got transduced by one shRNA. Next, the transduced cells were passed up to 40 days for at least 16 doublings. The abundance of shRNAs after propagation was measured by illlumina-based sequencing with respect to the initial shRNA refernce to assess the cellular dependency on each shRNA's targeted gene. At last, the most depleted shRNA belong to the most essential genes for cellular proliferation and viability [131,134] (Figure 9).

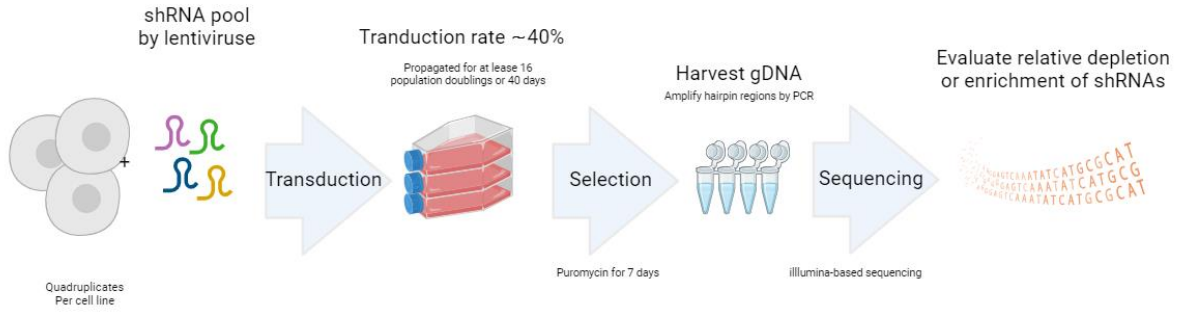

Figure 9| Schematic representation of the pooled shRNA screen

6.2 Analytic Technique for Assessment of RNAi Similarity (ATARiS)

It is essential to give a numeric value to the gene essentiality to better discriminate the genes that can decrease cell growth without killing the cell. Besides, inconsistent phenotypes can be resulted from different shRNAs which are designed to target the same gene. This phenotypic difference can be primarily reasoned to different degrees of on-target gene suppression and potential perturbation of off-target transcripts (variable degree of suppression of their intended gene) thus ATARiS score is calculated as the numeric outcome for each shRNA to assess the dependency. Briefly, ATARiS is a computational method that is designed to analyze the phenotypic patterns from large-scale screens in which each gene is targeted by at least two RNAi or shRNA. ATARiS score therefore summarize the RNAi or shRNA reagents designed to target the same gene and behave similarly (consistent phenotypic readouts) across screened samples to conclude an effect that is likely due to the suppression of the intended gene rather than off-target suppression. The algorithm will create two types of results to create the shRNA knock down score [135]:

Gene solution when the algorithm observes phenotypic readout produced by on-target reagent, it will transform this to quantitative value. High gene solution indicates effective targeting. After generating all gene solutions for each gene, the algorithm computes: *RNAi or shRNA consistency score* This score represents the confidence that the observed phenotype is the result of on-target suppression. A high consistence score implies that the phenotypic readout of a reagent in every screened sample has strong correlation to a large number of reagent profiles within the same gene solution. Consistency score may be interpreted as *p*-value to evaluate the confidence in each reagent.

Chapter IV

Cancer Metabolism

7. Metabolism

Metabolism is life-sustaining chemical and enzymatic reactions within living cells to maintain growth, division, and other biological processes. Metabolism is divided into catabolism and anabolism reactions. Catabolism refers to the breakdown of macromolecules such as proteins, glucose, and fat to produce energy. In contrast, anabolism is the energy-consuming biosynthesis of bigger molecules, including carbohydrates, proteins, lipids, and nucleic acids. These two biochemical processes coordinate to form a complex network called metabolic pathways. This network is essential to maintain the survival and functionality of the cells and is tightly regulated by hormones and enzymes.

7.1 Glycolysis

Glycolysis biochemical reactions occur in the cytoplasm, which is responsible for converting glucose to pyruvate generating ATP and NADH. Glucose transporter GLUT is responsible for the glucose entry. In the cytoplasm, glucose is phosphorylated into glucose-6-phosphate (G6P) by hexokinase in an irreversible reaction consuming ATP. G6P is then converted to fructose-6-phosphate (F6P) via the isomerization activity of glucose-6-phosphate isomerase (GPI). Another phosphorylation reaction is mediated by phosphofructokinase (PFK) producing fructose-1,6-biphosphate (F1,6P), which is then cleaved into two three-carbon molecules called glyceraldehyde 3-phosphate (G3P) via aldolase. G3P is then metabolized into 1,3-bisphosphoglycerate (1,3PG) and NADH by the oxidoreductase enzyme glyceraldehyde 3-phosphate dehydrogenase. Thereafter, the high-energy intermediate 1,3PG release phosphate group to convert ADP to ATP and produce 3-phosphoglycerate (3PG); this reaction is catalyzed by phosphoglycerate kinase (PGK). 3PG is then converted into 2- phosphoglycerate (2PG) by phosphoglycerate mutase (PGM), whose activity requires the presence of Mg^{+2}. Afterwards, the dehydration and phosphorylation step take place via enolase (ENO) and pyruvate kinase (PK) to form phosphoenolpyruvate, pyruvate, and ATP, respectively. Two molecules of ATP and 2 NADH are produced in total through this pathway. In the last step of glycolysis, pyruvate is degraded to lactate by the enzyme lactate dehydrogenase (LDH), a ubiquitous enzyme that couples the reduction of pyruvate to lactate with the oxidation of NADH to NAD+. Lactate then exits the cell via a monocarboxylate transporter (MCT) transporter. This is known as anaerobic glycolysis. The conversion between pyruvate and lactate is reversible and is essential to maintain a balanced NAD+ /NADH ratio. Pyruvate can have another fate; in normoxia conditions, pyruvate is transported into the mitochondria through mitochondrial pyruvate

carrier transporters (MPC) and undergo further metabolism via pyruvate dehydrogenase (PDH) to form acetyl-CoA. Acetyl-CoA then enters the TCA cycle to fulfill its role in energy production. Another fate of pyruvate is to form oxaloacetate via pyruvate carboxylase (PC) [136] (Figure 10).

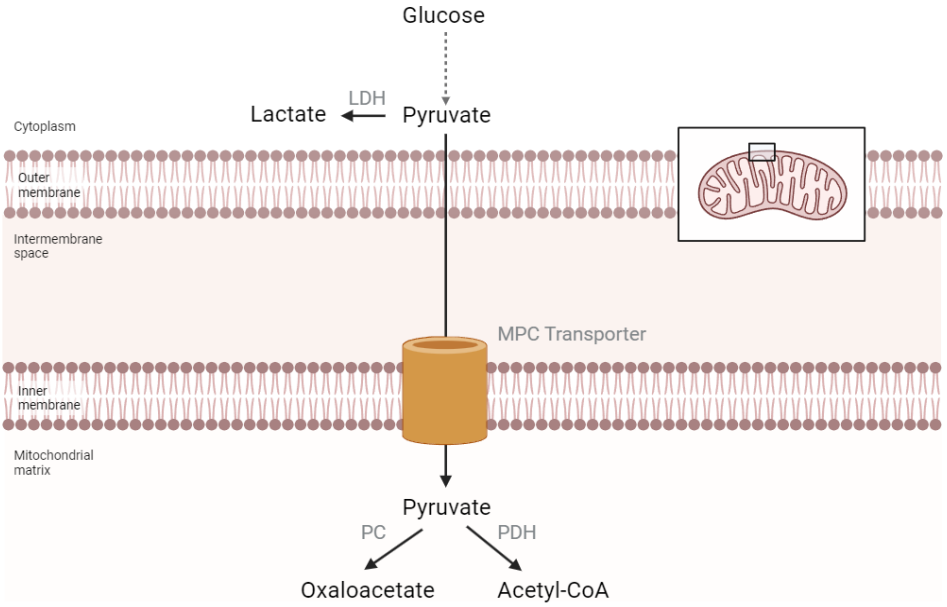

Figure 10| The metabolic fates of pyruvate. LDH: lactate dehydrogenase; MPC: mitochondrial pyruvate carrier; PC: pyruvate carboxylase; PDH: pyruvate dehydrogenase.

7.2 Citric acid cycle or Tricarboxylic acid cycle (TCA) cycle

Besides glycolysis, the citric acid cycle is another essential pathway for cellular bioenergy, discovered by the German biochemist Hans Krebs. The first reaction of the cycle is mediated by citrate synthase (CS) in the mitochondria, combining acetyl-CoA with oxaloacetate to produce citrate. Produced citrate can then have two fates, either the flow of the citric cycle or exportation out of the mitochondria via its specific transporter (SLC25A1) and use for fatty acids and amino acid synthesis. The second reaction of the cycle is the conversion of citrate to its isomer isocitrate by the enzyme aconitase (ACO). Next, isocitrate is oxidized to alpha-ketoglutarate a-KG via isocitrate dehydrogenase (IDH1), generating NADH and CO_2. IDH1 then converts a-KG to succinyl-CoA and produces NADH. Succinyl-CoA is then converted into succinate through a reaction catalyzed by succinyl-CoA synthetase (SCS) and produces GTP. Afterwards, succinate is oxidized to fumarate by succinate dehydrogenase, which also generates $FADH_2$. Malate is then produced from fumarate in a fumarase-mediated reaction. Thereafter, malate is oxidized to oxaloacetate by malate dehydrogenase (MDH1), generating

the third NADH in the process (Figure 14B). The following reaction can summarize the TCA cycle.

Acetyl-CoA +3 NAD^++ GDP +GDP +Pi +2 H_2O+ FAD → CoA-SH + 3 $NADH_2$+ $FADH_2$+ GTP +2 CO_2 + H^+.

7.3 Fatty acid metabolism

Mitochondrial citrate is an essential intermediate for de novo fatty acid formation, produced from glycolysis metabolism coupled to the TCA cycle or glutamine influx into the TCA cycle. Citrate is exported to the cytoplasm to be metabolised to oxaloacetate and Acetyl-CoA by ATPcitrate lyase (ACLY) [137]. The acetyl-CoA produced can be further metabolized into HMG-CoA (3-hydroxy-3-methylglutaryl-coenzyme A) and mevalonate via hydroxy-3-methylglutary-CoA reductase (HMGCR) and hydroxy-3-methylglutary-CoA synthase (HMGCS) to produce cholesterol. Citrate can also participate in fatty acid synthesis through its metabolism to malonyl-CoA and palmitate via acetyl-CoA carboxylase (ACC) and fatty acid synthase (FASN), respectively. Production of each palmitate molecule requires 14 NADPH and 7 ATP molecules. The produced fatty acid can further be stored as triglyceride or transformed into phospholipids to build cell membranes.

On the contrary, the process of breaking down fatty acid is carried out in the mitochondria and known as β-oxidation. Long chain fatty acids can be transferred to mitochondrial via carnitine palmitoyltransferase-I (CPTI) to undergo β-oxidation. CPTI catalyse the conversion of fatty acids to acyl-carnitines at the outer mitochondrial membrane. Next, the acyl-carnitine is transported across the inner mitochondrial membrane by carnitine translocase (CAT). Inside the matrix, the acyl-carnitine is converted back to acyl-CoA via CPTII. Then, Acyl-CoA starts the β-oxidation and degrades to acetyl-CoA in four steps. The first step, is dehydrogenation to form trans-2-enoyl CoA, followed by a hydration reaction forming 3-hydroxyacyl CoA, further oxidized to 3-ketoacyl CoA. Ketothiolase then catalyses the thiolysis reaction of 3-ketoacyl CoA to produce a shorter acyl CoA and acetyl CoA Which can then be integrated into the TCA cycle to produce NADH and $FADH_2$ to be used for oxidative phosphorylation and energy production. The two-carbon shortened acyl-CoA then re-enters the beta-oxidation process (Figure 11).

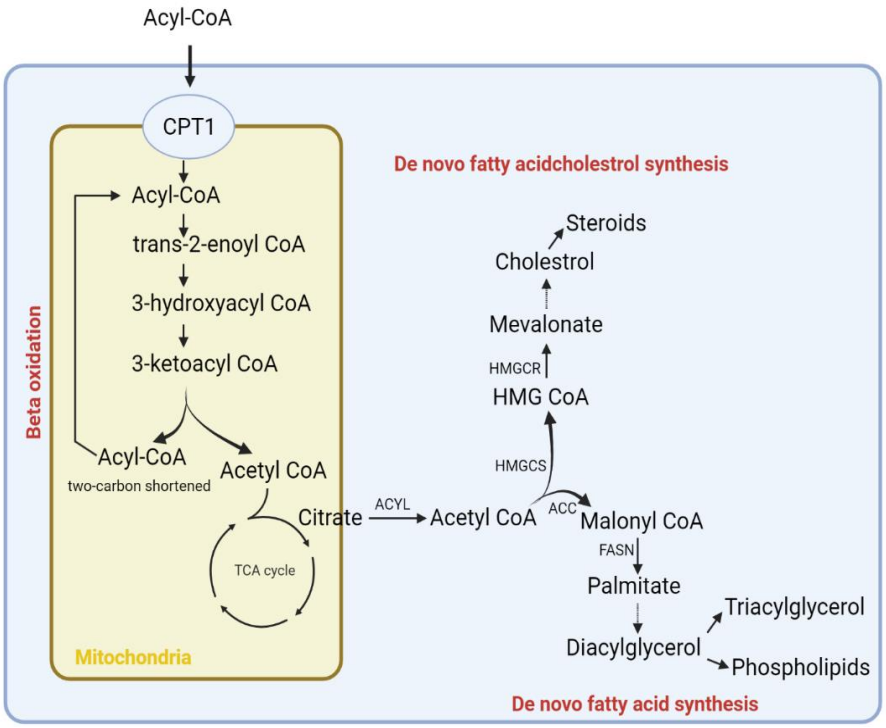

Figure 11| Overview of cellular fatty acid metabolism. Lipid metabolism consists of two distinct arms, namely, fatty acid oxidation (β-oxidation) and lipid synthesis that consists of fatty acids and cholesterol De novo synthesis.

7.4 Oxidative phosphorylation (OXPHOS)

Tremendous amount of energy is produced by mitochondria, which is defined as the "powerhouse" of the cell [138]. This energy is produced in the form of a high-energy molecule, ATP. The coenzymes produced by glycolysis and the TCA cycle, which are NADH and $FADH_2$, serve as high-energy electron carriers used in a mitochondrial metabolic pathway named oxidative phosphorylation through the electron transport chain (ETC). Electrons are removed from the electron donor (NADH and $FADH_2$) to the electron acceptor (O_2) in one direction through a series of redox reactions. The coupling between electron transport along the respiratory chain and the exit of protons to be used by F0F1 ATP-synthase produces ATP. These reactions take place through enzymes embedded within the mitochondrial inner membrane complex (I-IV) as well as two mobile electron carriers, coenzyme Q and cytochrome c (Figure 15C).

7.4.1 The respiratory chain: composition

Complex I (NADH dehydrogenase)

The first and the largest enzyme of the respiratory chain, NADH donates electron to ubiquinone also known as coenzyme Q (CoQ). As electrons pass to coenzyme Q, four protons (H+) are pumped simultaneously from the mitochondrial matrix to the mitochondrial intermembrane space, creating a proton gradient. Complex I consists of two domains, hydrophobic intermembrane domain and matrix hydrophilic domain. The electron transfer between NADH and CoQ occurs in the hydrophilic domain via a set of iron/sulfur Fe-S centers while the four protons are expelled from the membrane domain.

$$NADH + 4H^{+}(matrix) + \ CoQ \ \rightarrow NAD^{+} + CoQH2 + 4H^{+}(intermembrane)$$

Different molecules inhibit complex I; the most commonly used is Rotenone, a lipophilic natural compound derived from *Lonchocarpus* and *Derris* roots and stems. Rotenone blocks the electron transfer from the Fe-S centers in complex I to CoQ. Piericidin A, another natural compound, inhibits complex I [139].

Complex II (Succinate dehydrogenase)

Complex II has four subunits (SDHA, SDHB, SDHC, SDHD). $FADH_2$ donates electrons to complex II and transfers them to coenzyme Q, causing its reduction to CoQH2. However, this complex does not lead to pumping any protons across the inner mitochondrial membrane. Instead, it is coupled with the conversion of succinate to fumarate in a three-step reaction which uses the FAD and two Fe-S clusters as redox factors.

$$Succinate + \ FADH^{2} + \ CoQ \ \rightarrow FAD + CoQH2 + Fumarate$$

Complex II can be inhibited using molecules, such as Thenoyltrifluoroacetone (TTFA), which binds to the ubiquinone-binding site to block the electron flow. Like TTFA, Carboxin is another chemical compound that inhibits complex II by binding to its ubiquinone-binding site and, therefore, inhibits the transfer of electrons from succinate to ubiquinone [140,141].

Complex III (Ubiquinone: cytochrome c oxidoreductase)

The reaction at this complex occurs in two steps. Ubiquinol is oxidized and two cytochrome c molecules are reduced. Every electron transferred to cytochrome c translocate 2 protons (H^{+}) into the mitochondrial intermembrane space. Cytochrome c then transports the electrons to complex IV.

$$2CytFe^{3+} + CoQH_2 + 2H^+(matrix) \rightarrow CoQ + 2CytCFe^{2+} + 4H^+(intermembrane)$$

In addition to its role in the ETC, complex III is involved in ROS generation as it can release superoxides into the mitochondrial intermembrane space, which subsequently reach the cytosol and stabilize the HIF-1α protein [142]. Complex III can be inhibited by antimycin A, a chemical compound produced by *Streptomyces Kitazawensis.* Antimycine binds specifically to the quinone reduction site (Qi) to inhibit the ubiquinol oxidation in the ETC [143].

Complex IV (Cytochrome c oxidase)

Cytochrome c oxidase (COX) belongs to the heme-copper oxidase family. Complex IV is composed of 14 subunits, three of them encoded by nuclear DNA (COX1-3). The electrons given up by cytochrome c enter this complex in the COX2 subunits and enter the binuclear copper center, termed CuA. The electrons are then transferred to the heme α group in COX1 and then to heme α3, which is associated with another copper iron CuB that is essential for its function and finally, oxygen acts as a terminal acceptor in the chain due to its high electronegativity. Oxygen reduction to water is coupled with pumping two protons (H^+) across the inner mitochondrial membrane.

$$4CytFe^{2+} + O_2 + 8H^+(matrix) \rightarrow 4CytCFe^{3+} + 2H_2O + 4H^+(intermembrane)$$

Complex IV can be inhibited by cyanid (CN-) compounds such as cyanid potassium (KCN) which binds to heme α3. Other compounds such as sodium azide (NaN3) and arsenic trioxide (ATO) are also known to inhibit the ETC through inhibiting complex IV [144,145].

7.4.2 ATP synthase complex

ETC generated a proton gradient across the inner mitochondrial membrane. This gradient drives the hydrogen proton back to the mitochondrial matrix through ATP synthase. ATP synthase is the final enzyme of the ETC and is coupled to the production of ATP from ADP. ATP synthase contains two distinct protein components: F0 and F1. F0 resides in the inner mitochondrial membrane and has the pore through which the protons flow to the matrix. The F1 faces the mitochondrial matrix, carries the metabolic center of ATPase, and has multiple subunits, three α, three β, one γ, one ε and one δ and form a knob-like structure. Conformational changes in F1 subunits catalyze the formation of ATP from ADP and Pi.

$$ADP + 4H^+(intermembrane) + Pi \rightarrow ATP + 4H^+(matrix)$$

Oligomycin A was discovered to inhibit the ATP synthase in 1958 by Henry Lardy et al. [146]. The binding of oligomycin to the c-ring subunit in the F0 resides causes conformational changes that block the proton translocations thus ATP synthase [147].

The ATP produced by the respiratory chain must be exported outside the mitochondria to meet the dynamic energy demands of the cell. An energy transfer system located in the mitochondrial inner membrane is responsible for transferring ATP from the mitochondrial to the cytoplasm and other cellular locales. The system consists of dedicated proteins; the most well-known is the ADP/ATP translocase or adenine nucleotide translocase (ANT).

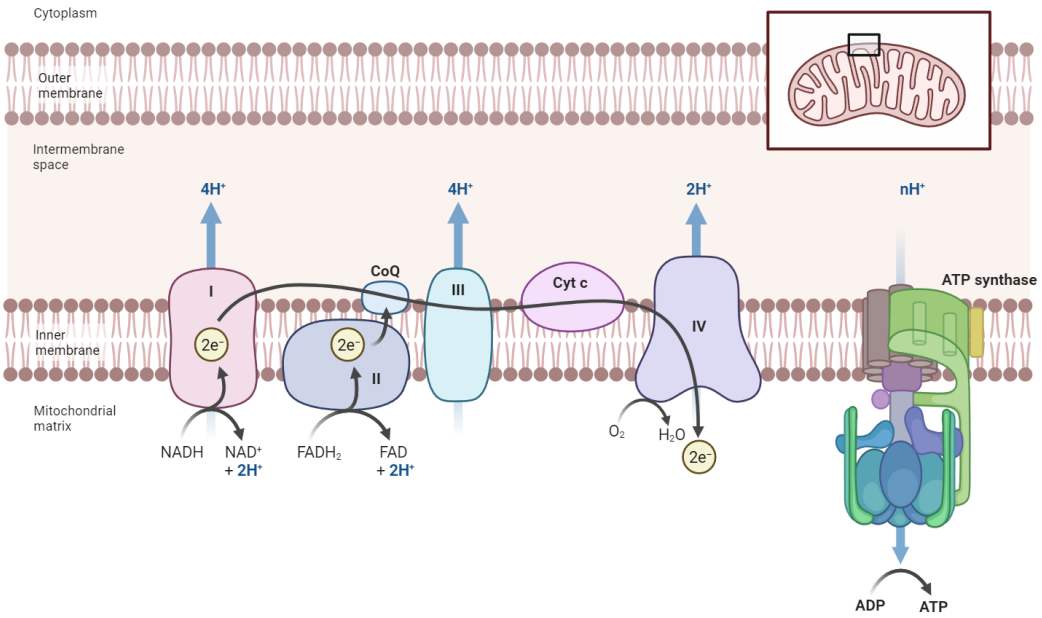

Figure 12| Electron transport chain (ETC). Electrons are transferred through complex I to IV to form proton gradient that drives the production of ATP to fuel other cellular functions.

7.4.3 Regulation of oxidative phosphorylation

I. Allosteric regulation

Fine-tuning of ATP production is necessary for rapid adaptation to various energetic states. This regulation is done by regulating different molecules produced or used by the ETC. First, the phosphorylation of ADP by ATP synthase depends on the proton gradient generated at the level of respiratory chain complexes. Part of this proton gradient returns to the matrix by simple diffusion, known as basal proton leakage. ANT is involved in basal proton leakage and therefore plays a critical role regulating oxidative phosphorylation.

The ATP/ADP ratio is an indicator of the cellular energy state. An increase in the cytosolic ATP/ADP ratio will stimulate the mitochondrial respiration, stimulating the substrate metabolism to supply the oxidative pathways [148,149]. Moreover, NADH/NAD+ ratio is a key factor in regulating the rate of catabolism and energy production. NAD+ regulates the activity of three Krebs cycle enzymes: isocitrate dehydrogenase, α-ketoglutarate dehydrogenase, and malate dehydrogenase. An elevated NADH/NAD+ ratio signifies an abundance of reducing equivalents and energy surplus this downregulates OXPHOS activity to maintain energy homeostasis. In contrast, a low NADH/NAD+ ratio can signal energy stress such as nutrient deprivation or exercise, thus requiring the maintenance of high OXPHOS activity to increase ATP production [150].

Furthermore, the PDH complex that converts pyruvate and NAD+ to acetyl-CoA and NADH is tightly regulated by four pyruvate dehydrogenase kinases (PDK 1-4) and two pyruvate dehydrogenase phosphatases (PDP1 and PDP2). PDH complex is allosterically regulated by its products, it is inhibited by NADH, acetyl-COA and ATP In the presence of high concentrations of NADH and/or acetyl-CoA, phosphorylation by PDK of the pyruvate dehydrogenase complex inhibits pyruvate entry into the mitochondria and thus mitochondrial respiration [151,152].

II. Transcriptional regulation

As explained earlier, it is essential for the cells to adapt their energy metabolism to their energy demands. Previous studies showed that cells can increase their mitochondrial mass in response to increased energy requirements. This is known as mitochondrial biogenesis and therefore defined as the process required for the development and division of pre-existing mitochondria, to increase mitochondrial mass in response to changes in energy demands. Many factors are required to regulate mitochondrial biogenesis such as peroxisome proliferator-activated receptor)-γ coactivator-1α (PGC-1α). PGC-1α induces mitochondrial biogenesis through

activating other transcription factors such as nuclear respiratory factors (NRF1 and NRF2), this leads to an increase in the transcription of mitochondrial genes encoded by the nuclear genome. In parallel, mitochondrial transcription factor A; also known as mtTFA or Tfam is another key regulator in the mitochondrial biogenesis which drives the transcription and replication of mitochondrial genome [153,154].

III. Post translational regulation.

Subunits of the respiratory chain are controlled by phosphorylation. Phosphorylation of complex I on the NDUFS4 subunit by cAMP-dependent kinase (PKA) increases the assembly and function of the complex, thus the mitochondrial respiration[155,156]. Complex IV is also a subject of PKA. Phosphorylation of the subunit COX4I1 on Ser58 increases the activity of Complex IV. Other kinases are also involved in the phosphorylation of various respiratory subunits, such as cyclin B1–CDK1 phosphorylate several complex I subunits, including NDUFA12 and NDUFS2 and NDUFS6 [157]. Acetylation is another essential PTM to regulate mitochondrial respiration activity. Around 20% of mitochondrial protein possesses putative acetyllysine sites. Lysine-acetylated proteins were found among different mitochondrial energetic pathways. Six proteins in the TCA cycle can be subject to this modification including fumarate dehydrogenase, malate dehydrogenase, isocitrate dehydrogenase and succinate dehydrogenase. Furthermore, 26 proteins involved in OXPHOS undergo acetylation including nine subunits of complex I (NUDFV1, NDUFS1, NDUFS6, NDUFA1, NDUFA4, NDUFA5, NDUFA9, NDUFA10, NDUFB3) and 27 other proteins involved in lipid metabolism and beta-oxidation [158]. Acetylation is a reversible reaction thus deacetylation enzymes are also key regulators in mitochondrial activity including the mitochondrial NAD-dependent deacetylase (SIRT3). Sirt3−/− mice result in NDUFA9 hyperacetylation that correlates with reduced mitochondrial activity due to the inhibition of Complex I activity [159].

7.5 Amino acid metabolism

7.5.1 Glutamine

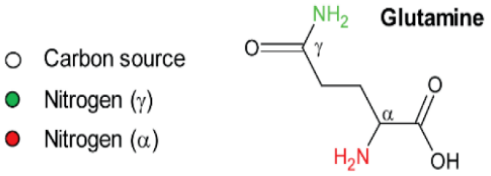

Figure 13| Illustration of the chemical structure of glutamine.

Glutamine is the most abundant amino acid in the bloodstream and plays a vital role in cellular metabolism. Glutamine has two nitrogen atoms at the α and γ positions (Figure 13). Glutamine-derived glutamate has different fates providing carbon and nitrogen sources for growing cells. Glutamate is then deaminated via glutamate dehydrogenase (GDH or GLUD) or transaminated by aspartate aminotransferase or alanine aminotransferase to produce α-ketoglutarate, which can directly enter the TCA cycle to serve as a carbon source. As a nitrogen donor and carrier, the γ-nitrogen (amide group) of glutamine is essential for nucleotide production when the nitrogen of the amide group is incorporated into the purine and pyrimidine rings. Glutamine α-nitrogen is also a substrate for non-essential amino acid synthesis through transamination and deamination reactions [160].

- Glutamine transporters

Glutamine influx is mediated by numerous transporters belonging to several protein families with different systems. Some of these transporters are shared by other neutral or cationic amino acids. These transporters were classified based on substrate specificity, pH and ion dependence, and regulatory properties. Broadly, we classified transporters into Na^+ dependent and Na^+ independent, each category includes different systems [161–163] (Table 4). Glutamine mainly enters the cell through the Solute linked carrier family 1-member A5 (SLC1A5) or ASCT2. SLC1A5 gene is located on chromosome 19. It encodes a protein of 541 amino acid residues with nine transmembrane domains and expressed in many healthy tissues: brain, kidney, lung, intestine, muscle, placenta and pancreas [164]. In addition, SLC1A5 is often expressed together with other glutamine transporters including SLC7A5/3A2 that enable amino acid exchange to allow leucine entry and consequently mTORC1 activation.

Class	System			
Na+ dependent transporters	System ASC	Specific for alanine, serine, and cysteine		SLC1A5
	System N	Narrow specificity to substrates containing *N*itrogen in their side chain, such as glutamine, histidine, and asparagine		SLC38A3, SLC38A5, SLC38A7
	System B_0	Specificity to neutral amino acids	$B^{(0,+)}$	SLC6A14, SLC3A2
			B^0AT1	SLC6A19
	System A	Alanine-preferring transporters		SLC38A1, SLC38A2
Na^+ independent transporters	System L	Leucine-preferring transporters		SLC7A5, SLC7A8, SLC7A6

Table 4| The basic characteristics of the glutamine transporters

- Glutaminase

The first step of glutamine metabolism is the hydrolysis of the glutamine amide to produce glutamate. This reaction is catalyzed by glutaminase (GLS), the gatekeeper enzyme for glutaminolysis. Glutaminase was first described by Krebs in 1935. Two types of glutaminase, each comprising several isoforms were identified: the kidney-type (KGA or GLS or GLS1) and the liver-type (LGA, also called GLS2), encoded by two different genes. Glutamine is responsible for 70% of glutamate synthesis at neurons levels thus GLS1 is highly important for glutamatergic synaptic transmission. The GLS $^{(-/-)}$ mice show behavioral disorders leading to the failure to feed that can be explained by deficits in the organization of goal-directed behavior associated with respiratory disorders such as hypoventilation, leading to their death within the first postnatal day (36 hours). The heterozygous mice (+/−) survived beyond 36 hours and had only moderate disorders [165].

GLS1 is encoded by a gene of chromosome 2 and exists in different splice variants [166]. The three main splice variances are KGA, which is the longest form. Glutaminase C (GAC) which

is identical to (KGA) except the C-terminal region and the (GAM) which is a shorter variant with no catalytic activity [167]. KGA and GAC are 669 and 598 amino acid residues with a predicted molecular mass of 73.5 kDa and 65.5 kDa, respectively. While GAM has a sequence of 169 amino acids only. KGA and GAC isoforms are active as tetramers, formed as dimers of inactive dimers in the presence of inorganic phosphate. The interaction sites to form the dimers and tetramers are in the catalytic part. The activated GAC then forms a polymeric superstructure composed of multiple tetramers [168,169]. Cassago et al. showed that KGA has a cytoplasmic location in breast, lung, and prostate cancer lines, whereas GAC has a mitochondrial location. The authors hypothesize that the prediction of ankyrin repeat domains presence in the C-terminal of KGA could explain the retention of this isoform outside the mitochondrial boundaries, as these domains are known to promote protein-protein interactions and participate in transcriptional regulation [170] (Figure 14).

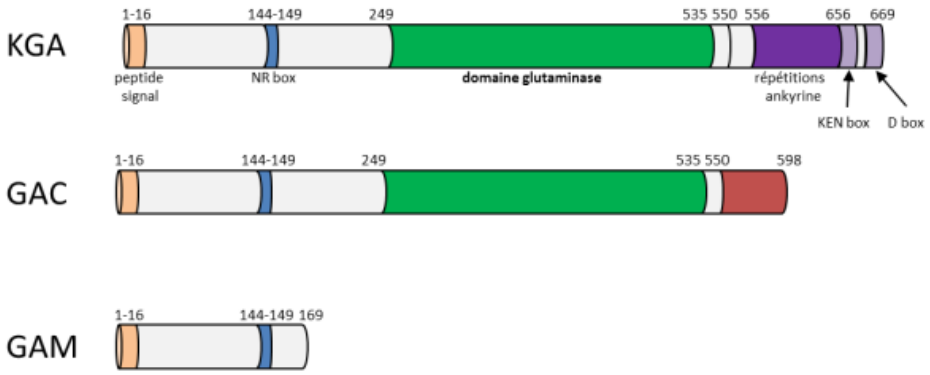

Figure 14| Structures of the glutaminase isoforms

7.5.2 Other amino acids

Other amino acids play a pivotal role in cellular bioenergy and biosynthesis. Aspartate is another important non-essential amino acid, a precursor for nucleotide and protein synthesis [171]. Patel et al. Showed that exogenous aspartate rescues the cell cycle arrest induced by glutamine deprivation in KRas-driven cancer cells [172]. Methionine metabolism is also essential and participates in the DNA methylation and epigenetic regulations [173]. Interestingly, unlike normal cells, cancer cells cannot proliferate when deprived of exogenous methionine or when it is replaced by its metabolic precursor, homocysteine [174,175]. Besides glutamate, cysteine and glycine are required for glutathione synthesis and antioxidant defence [176].

7.6 Pentose phosphate pathway

The Pentose phosphate pathway (PPP) is another essential metabolic pathway linked to glycolysis through G6P. The pathway is divided into oxidative (irreversible) and nonoxidative (reversible) reactions. The first step of the pathway is the conversion of G6P to 6-phosphogluconolactone by glucose-6-phosphate dehydrogenase (G6PD), generatinga NADPH. The 6-phosphogluconolactone is then hydrolysed into 6-phosphogluconate by 6-phosphogluconolactonase, which will undergo a redox reaction and a decarboxylation mediated by 6- phosphogluconate-dehydrogenase to form ribulose-5-phosphate and NADPH. During the non-oxidative phase, ribulose-5-phosphate is metabolised into ribose-5-phosphate or xylulose-5-phosphate by ribulose-5-phosphate isomerase or ribulose-5-phosphate-3-epimerase, respectively. These two molecules can then be transformed into glyceraldehyde-3-phosphate (G3P) and sedoheptulose-7-phosphate by transketolase, then further metabolized by transaldolase into fructose-6-phosphate (F6P) to re-join the glycolysis, erythrose-4-phosphate (E4P) and xylulose-5-phosphate which undergo another reaction by transketolase to produce glyceraldehyde-3-phosphate and fructose-6-phosphate which in turn re-join glycolysis too. The role of the PP pathway can be divided too. The NADPH produced by the oxidative part of the PP pathway is an essential cofactor for glutathione reductase (GR) to maintain reduced glutathione (GSH), which has a key role in redox homeostasis, besides the role of NADPH in cholesterol and fatty acid synthesis. Secondly, the nonoxidative PPP generates ribose-5-phosphate (R5P), the precursor of nucleic acid anderythrose-4-phosphate the precursor for aromatic amino acid synthesis such as phenylalanine, tyrosine, and tryptophan (Figure 15D).

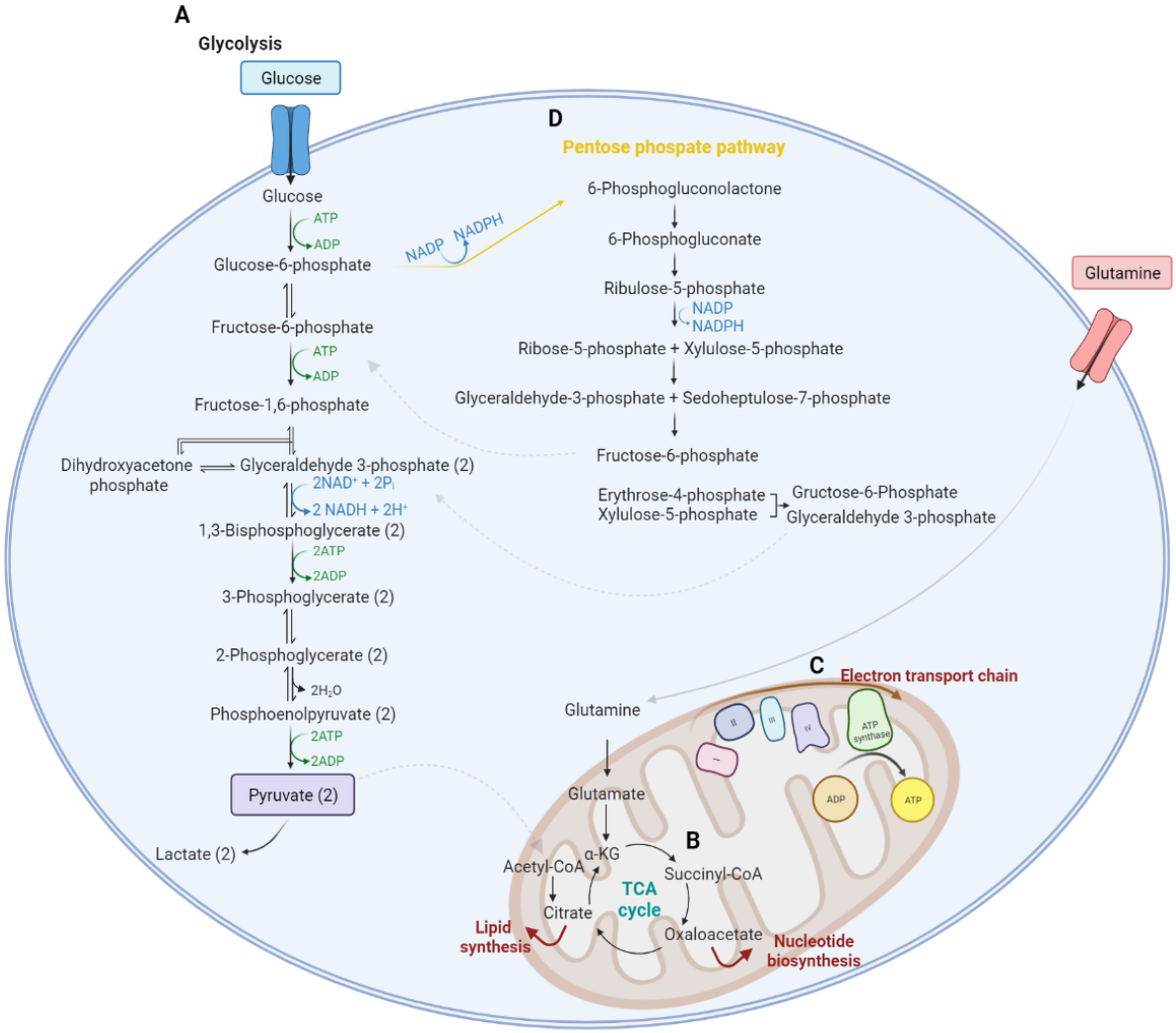

Figure 15| General scheme of the main cellular metabolic pathways. (A) Glycolysis**. (B)** TCA cycle**. (C)** Electron transport chain ETC. **(D)** Pentose phosphate pathway**.**

7.7 NAD metabolism

As we have discussed earlier, NAD is essential for the activity of the main metabolic pathways in the cell, such as TCA cycle, ATP production and redox balance. Beyond energy production, NAD is essential for DNA repair through the action of poly-ADP-ribose polymerases (PARP) to maintain genomic integrity. Furthermore, as described earlier, NAD serves as a co-substrate for sirtuin enzymes, orchestrating the deacetylation reactions that modulate gene expression of various mitochondrial proteins to maintain energy homeostasis.

Two NAD+ synthesis pathways are known, Firstly, NAD de novo synthesis that is initiated by tryptophane obtained from diet or alternatively nicotinic acid (a form of vitamin B3). Both nicotinic acid and quinolinic acid derived from tryptophan are converted to nicotinic acid

mononucleotide (NAMN). Then, the nicotinic acid-specific mononucleotide adenylyltransferase (NMNAT) converts NAMN to nicotinic acid dinucleotide (NAAD), which is then converted into NAD through a series of enzymatic reactions including phosphorylation and adenylation catalyzed by NAD synthase (NADS). [177,178]. Secondly, the NAD salvage pathway starts with nicotinamide (NAM), which mammal cells predominantly use, or nicotinamide riboside (NR). These are both converted to nicotinamide mononucleotide (NMN) by the specific nicotinamide phosphoryltransferase (NAMPT) or NR-specific kinase (NRK). Nicotinamide mononucleotide-specific adenylyltransferase (NMNAT) generates NAD+ from NMN (Houtkooper et al., 2010; Okabe et al., 2019) (Figure 16).

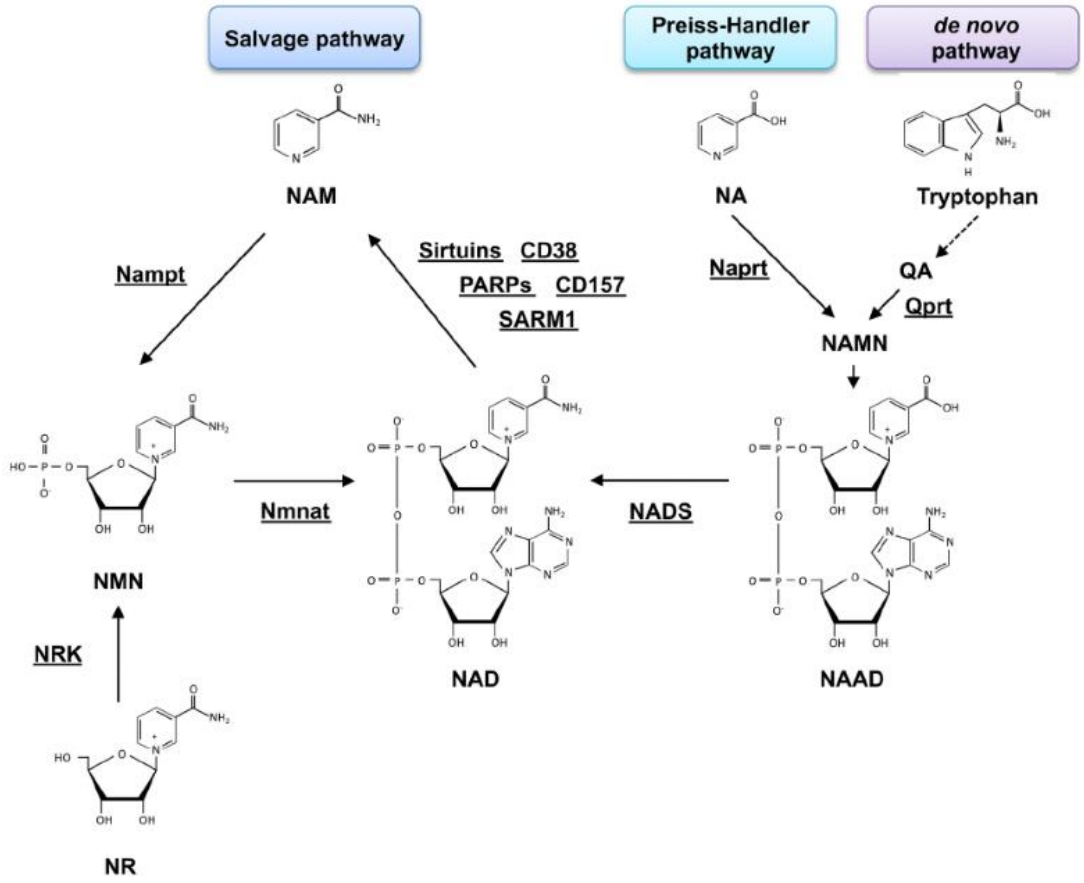

Figure 16| NAD synthesis pathways via salvage pathway using NAM or NR and de novo pathway using tryptophan and preiss-handler pathway using NA as precursors (Okabe et al., 2019).

In addition to its major function in energy metabolism, NAD is also a precursor of nicotinamide adenine dinucleotide phosphate (NADP) by NAD kinase in the cytosol or by NAD(P) transhydrogenase (NNT) localized to the inner mitochondrial membrane that converts NADP and NADH to NADPH and NAD [181,182]. NADP and its reduced form (NADPH), an essential

coenzyme of the signaling pathways involved in the detoxification of reactive oxygen species, such as glutathione and thioredoxin reductase system and pentose phosphate pathway.

NAD metabolism regulation

Due to the NAD pivotal role, a balance between NAD synthesis and consumption is essential to maintain NAD+ homeostasis that copes with energy supplies and demands. Increased NAD+ levels in the cell result from three main strategies, including stimulating the activity of NAD+ synthesis enzymes, providing NAD+ precursors, or, on the contrary, inhibiting the pathways that are highly consuming in NAD+.

The NAD homeostasis is maintained at different subcellular compartments, which are regulated by subcellular-specific NAD+-consuming enzymes and transporters. One of the key enzymes in NAD regulation is NAMPT. It exists as monomers and functions as homodimers [183]. NAMPT monomers subcellularly localized as extra and intracellular eNAMPT and iNAMPT, respectively. Intracellular NAMPT (iNAMPT) is mainly responsible for the synthesis of the NAD intermediate NMN, while the extracellular NAMPT (eNAMPT) acts as a cytokine named PBEF (pre-B cell colony-enhancing factor) or an insulin-mimetic hormone and is involved in various cellular processes [184]. The activity of iNAMPT is regulated through post-translational modifications including phosphorylation and acetylation. Phosphorylation of NAMPT at Ser314 by AMP-activated protein kinase (AMPK) can enhance the NAMPT activity [185]. Moreover, NAMPT acetylation affects enzyme's stability and activity. Sirtuin-1, a NAD-dependent deacetylase is more active upon increased NAD+ level. Activated sirtuin-1 then deacetylase NAMPT and potentially increase its activity [186]. Moreover, the activity of NAMPT is affected by the NADH/NAD+ ratio. A decrease in the *NAMPT* expression is associated with an increase in the NADH/NAD+ ratio and is overexpressed upon a decrease in the ratio NADH/NAD+ [187,188]. Another key NAD biosynthesis enzyme is NMNAT. Three isoforms of NMNAT were currently known in human, : NMNAT-1, specific to the nucleus, NMNAT-2 specific for the Golgi apparatus while NMNAT-3 is specific for the mitochondria [189].

The NAD/NADH ration in different cellular compartments are linked such as the link between the mitochondrial and cytosolic NAD/NADH ration through Malate-aspartate and glycerol-3-phosphate shuttles as NADH and NAD cannot cross the mitochondrial membrane [190] (Figure 17).

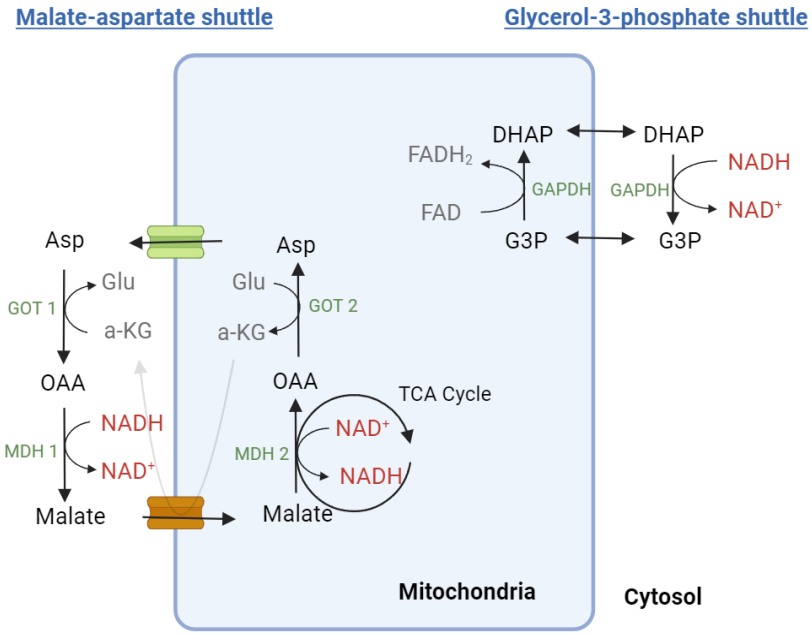

Figure 17| Cytosolic/mitochondrial NADH shuttles. Cytosolic and mitochondrial NADH are exchanged through two shuttle systems: Malate–aspartate shuttle and glycerol-3-phosphate shuttle.

In the Malate-aspartate shuttle (MAS), cytosolic malate dehydrogenase (MDH1) generates malate and replenishes cytosolic NAD from NADH generated by glycolysis. Malate is then transported across the mitochondrial inner membrane which exports a-KG from the mitochondrial to the cytosol simultaneously. Next, malate is converted to oxaloacetate (OAA) in a reaction catalyzed by mitochondrial malate dehydrogenase (MDH2) and coupled with the interconversion of NAD to NADH. OAA is transaminated into aspartate by mitochondrial aspartate aminotransferase (GOT2). This reaction uses glutamate as a nitrogen donor, which is converted to a-KG. Aspartate is then exported to the cytosol. Lastly, aspartate is converted into OAA by (GOT1) to maintain MAS activity. In addition to the MAS shuttle, the glycerol-3-phosphate shuttle is highly important. The cytosolic glycerol 3-phosphate dehydrogenase (GAPDH) converts DHAP generated by glycolysis into glycerol-3 phosphate (G3P) and simultaneously oxidizes NADH to NAD+ in the cytosol. The mitochondrial GAPDH catalyzes the reversed reaction converting G3P into DHAP while FAD is reduced to $FADH_2$ [191].

8. Hallmarks of cancer

The evolutionary process of normal cells transforming into cancer cells is a complex and heterotypic process known as tumorigenesis that involves genetic and epigenetic changes affecting multiple cellular processes and signaling pathways leading to uncontrolled cell proliferation. The hallmarks of cancer are a set of acquired functional capabilities that define the cancer phenotype and contribute to the tumor progression. Cancer hallmarks include sustained proliferation, insensitivity to growth-inhibitory signals, evasion of cell death, replicative immortality, angiogenesis, invasion, and metastasis [192]. Later in 2011, two enabling hallmarks were incorporated. Enabling hallmarks are crucial to enable cells to acquire the hallmarks of cancer and have a significant role in disease progression. These traits include tumor-promoting inflammation and genome instability. Furthermore, this model was extended, and two emerging traits were added to the original six, including abnormal energy metabolism and evasion of immune destruction [193] (Figure 18).

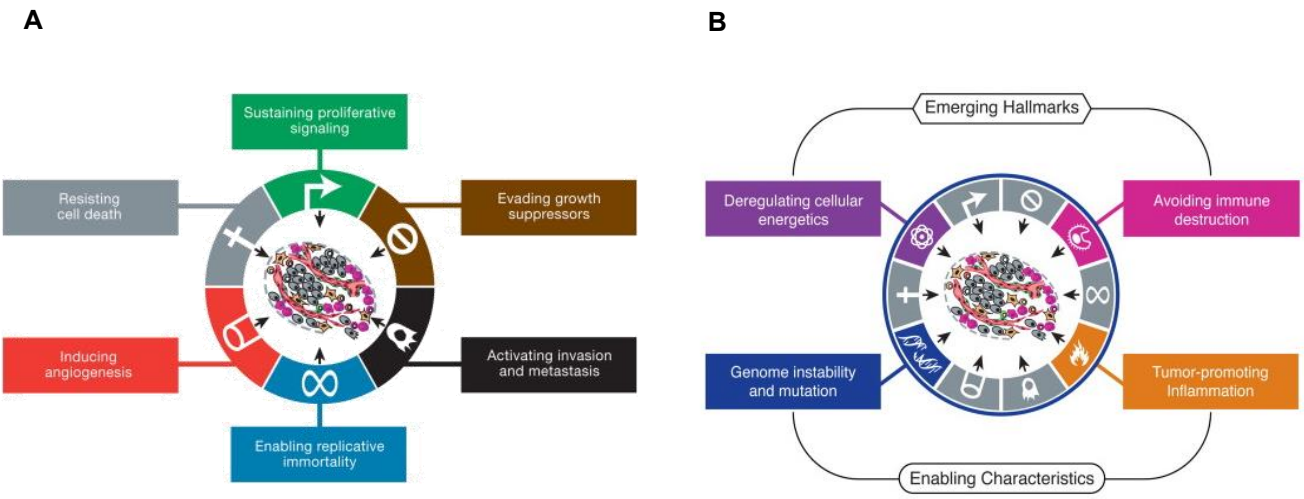

Figure 18| Hallmarks of Cancer. (A) Primary illustration of cancer hallmarks as described by Hanahan and Weinberg in 2000 **(B)** Updated illustration of cancer hallmark with the inclusion of emerging and enabling factors (Hanahan D et Weinberg RA, 2011)

9. Tumor metabolism

This deregulated control of cellular proliferation demands adjustments of metabolism to ramp up cellular bioenergetic and biosynthesis. Therefore, cancer metabolism has emerged as a promising field for discovering novel cancer therapies.

9.1 Glycolysis in cancer

In the presence of oxygen, normal cells use mitochondria to produce energy from oxidizing glucose, while lactate production is favored in hypoxic conditions (< 2% O_2). In the 1920s, Otto Warburg was the first to describe that, unlike normal cells, tumor cells have a higher need for glucose and a higher rate of lactate production, invariant in the presence of oxygen [194–196]. However, this pathway is less efficient, producing 2 ATP molecules for one glucose molecule, whereas oxidative phosphorylation produces 36 molecules. Thereby, Warburg hypothesized that cancer cells' irreversible defects in mitochondrial respiration led to favoring the fermentation of glucose into lactate to maintain energy requirements. This phenomenon was later found not to be linked to respiration damage but to the imbalance between glycolysis and respiration [197,198]. ATP production from glucose flux may exceed the rate of ATP production by oxidative phosphorylation, depending on an abundance of precursors. This metabolic adaptation is essential to maintain the overflow metabolism and ATP production in cancer cells. This upregulation in glycolysis demands an increase in the uptake and metabolism of glucose. As we have discussed earlier, MYC is a key regulator for various cellular function. MYC deregulations are mirrored on aerobic glycolysis as almost all glycolytic genes were found to be downstream effectors of MYC, such as glucose transporter *SLC2A1* (*GLUT-1*) that was found to be stimulated by MYC in various tumors [199]. Nearly all glycolytic enzymes such as *hexokinase II* (*HK2*), *enolase 1* (*ENO1*) and *lactate dehydrogenase A* (*LDHA*). This ability of MYC to stimulate glycolytic genes was explained by its binding to conserved E-boxes (5'-CACGTG-3') [200]. HK2 was reported to mediate metabolic reprogramming in EGFR VIII-mutated glioblastoma. EGFR VIII promotes the expression of an alternative splicing variant of MAX known as delta MAX which enhances MYC-dependant transformation thus HK2 expression and aerobic glycolysis [201]. In addition, MYC-LDHA signalling promotes tumor progression through promoting aerobic glycolysis in pancreatic cancer [202]. In MM the expression of HK2 and LDHA is associated with poor clinical outcome [203,204]. MYC does not affect glycolytic genes only at transcriptional level but also through alternative splicing, elevating the expression of pyruvate kinase type M2 (PKM2) over (PKM1). PKM2 is

documented to switch metabolism to aerobic glycolysis [205]. PKM2 exists in a high activity tetramer with high affinity for PEP or low activity dimer with low PEP affinity and is nearly inactive under physiological conditions. The presence of PKM2 in tetramer pushes pyruvate to the normal respiratory chain while the dimer form of PKM2 shifts the cells to lactate production. The ratio between these forms is regulated by the availability of some metabolic intermediates such as F1,6P and serine that induce the highly active tetramer formation. Low-activity dimer form of PKM2 is favorable in cancer cells which triggers glycolysis reprogramming thus increases the abundance of glycolytic intermediates resulting in the increase of the activity of other metabolic pathways such as pentose phosphate pathway to promote tumor growth [206]. AKT signaling is another major driver of glucose metabolism over OXPHOS in cancer cells [207]. Lately, Bloedjes et al. highlighted the role of AKT signaling to maintain both glycolysis and OXPHOS in MM cells by restricting the forkhead box O (FOXO) transcription factor [208].

Additionally, hypoxia-inducible factor (HIF)-1α is another transcription factor which has a critical effect on glucose transporters and glycolysis genes and favors aerobic glycolysis [209]. In cancer cells, *HIF-1* is frequently overexpressed due to intratumoral hypoxia or genetic alterations [210–212] This overexpression is associated with adverse clinical outcome in various cancers including lung, ovarian, breast and gastrointestinal cancers [213–216]Moreover, hypoxia-driven drug resistance was reported in MM, this resistance is a consequence of increased glycolysis [203].

9.1.1 Glycolysis inhibitors

Enzymes involved in the glycolysis pathways have been potential targets for inhibitors looking for powerful anticancer therapeutic approaches used as a single agent or in combination with other agents. The glucose analog 2-deoxyglucose phosphate (2-DG) compound with the most advanced clinical development. Upon cellular uptake, 2-DG is phosphorylated by HK2. However, this phosphorylated form of 2-DG cannot be further metabolized leading to its accumulation inside the cells and glycolysis, PPP, and glycosylation pathways inhibition. 2-DG was also found to significantly enhance the anticancer activity of other therapeutic modalities. Glycolysis inhibition with 2-DG was shown to improve the efficacy of trastuzumab in Her2+ breast cancer and paclitaxel in NSCLC and osteosarcoma in vivo models [217,218]. Other HK inhibitors such as 3-bromopyruvate (3-BrPA) or lonidamine were in clinical and pre-clinical studies, respectively. Furthermore, inhibitors of the glucose transporters GLUT have also been investigated to target the first rate-limiting of glycolysis. GLUT isoforms have unique tissue distribution. Among the isoforms, GLUT 1-4 were the most investigated, with a particular focus

on GLUT1. GLUT1 inhibitors have been tested only in preclinical studies such as STF-31 which was found to inhibit renal cell carcinoma growth and WZB117 which showed significant growth inhibition in lung cancer [219,220]. Moreover, several small molecule activators such as TEPP-46 exist to stabilize PKM2 in the active tetramer by enhancing the association of PKM2 subunits, which allows the reprogramming of the cell towards glucose oxidation and inhibit the lactate formation [221]. PDK inhibitors are among the studied compounds including an analog of the PDC known as Dichloroacetate (DCA), which has been used since 1970s and its antitumor effects were investigated in lung, breast, glioblastoma cancers [222]. However, its clinical trials were stopped due to its low potency and toxicity [223]. The formation and efflux of lactate as a last step of glycolysis is also studied as a pharmacological target. The MCT1 transporter inhibitor, AZD3965 delays tumor growth in vivo and is currently in Phase I/II trial in solid tumor and lymphoma [224,225].

9.2 Glutaminolysis in cancer

Alongside with altered glycolysis, cancer cells have shown extensive flexibility to metabolically fit the increased demands of proliferation and biomass. This flexibility is demonstrated by altered mitochondrial metabolism, lipid metabolism, and amino acid metabolism [226–228]. Glutamine metabolism alterations in cancer were reported in 1955 [229], since then studying glutamine metabolism and its attribution in tumor progression received interest. As previously stated, SLC1A5 is one of the main glutamine transporters thus its expression has been often found increased in many human cancers, such as breast, ovarian, prostate, kidney, hepatocarcinoma and stomach cancers to increase glutamine influx [230]. Furthermore, the glutamine influx via SLC1A5 is essential to maintain the mTOR function [231]. Likewise, GLS is another key actor glutaminolytic gene in cancer cells. GLS1 level was found to be increased in response to various oncogene including MYC as we have detailed earlier as well as TGF-ß, Rho-GTPases and the Raf-Mek-Erk pathway [232]. In MM, a rely on extracellular glutamine and the lack of sizable expression of glutamine synthesis (GS) was reported. The expression level of glutaminolysis-related genes and the neoplastic phenotype of plasma cells are coherent, as it has been documented by several contributions. Analyses of MM patient samples have also reported decreased levels of Gln and hyperammonemia suggesting high gln catabolism rate [233,234]. However, other studies reported GS-positive MM cells and relative resistance to gln-deprivation [235,236].

9.2.1 Glutaminase regulation

Several oncogenes and tumor suppressors have been linked to the regulation of glutamine metabolism. Glutamine uptake is the first step of glutamine catabolism. This uptake is mediated by different transporters that were subject to expression alteration during tumor progression. MYC is surmised to enhance the metabolic capacity of the growing cells, as we previously described in the case of many genes involved in glycolysis and nucleotide biosynthesis. MYC also stimulates glutamine metabolism at both transcriptional and posttranscriptional levels. *MYC* gene was found to transcriptionally activate transporters, including main glutamine transporters *SLC1A5*, *SLC38A1/2* and *SLC7A5* [73,237,238]. *MYC* also regulates other glutaminolysis-related genes such as *glutaminase*, *glutamate dehydrogenase* (*GDH*), *aspartate aminotransferase* (*GOT*) and *alanine aminotransferase* (*GPT*). *MYC* can also increase *GLS1* expression through suppressing miRNAs miR-23a/b which targets the 3'UTR region of the GLS1 mRNA [72]. Several studies reported that lymphoid and prostate cancer lines that overexpress MYC are more sensitive to glutamine deprivation than glucose [72].

In addition, mutated or amplified Ras family oncogenes were also found to be involved in glutamine metabolism reprogramming in many cancers. *KRAS* mutation promotes glutaminolysis by up-regulating *GOT* and reducing the expression of *GLUD1* in Pancreatic ductal adenocarcinoma (PDAC) therefore *KRAS* mutations decrease glutamine oxidative towards the glutamine utilization in different biosynthetic pathways. Furthermore, Glutamine deprivation in *KRAS*-transformed fibroblast led to cell cycle arrest in the S-phase and this effect was rescued by the addition of deoxyribonucleotides highlighting the role of glutamine in nucleotide biosynthesis [239–241]. PI3K/Akt/mTOR pathway plays a key role in metabolic regulation. mTOR is activated by nutrients availability; this activation contributes to the GDH inhibition in proliferating cells to support non-essential amino acid synthesis [242,243]. Conversely, Csibi et al., concluded that mTOR stimulates glutamine anaplerosis by activating GDH via SIRT4 inhibition [244]. On the other hand, mTORC1, via S6K1, drives the translation of MYC through phosphorylation of eIF4B, which increases GLS1 expression [245].

9.2.2 Glutaminolysis inhibitors

Glutamine metabolism has been an important research topic to develop new therapeutic targets in cancer. Inhibitors were developed to target and block different steps of the glutamine catabolism pathways.

9.2.2.1 Glutamine transporters inhibitors

Several studies tried to identify glutamine transporter inhibitors, hypothesizing that blocking this early step of glutamine import can have a greater effect than inhibiting other downstream steps of glutamine metabolism. In cancer cells, the import of glutamine from the extracellular environment is mainly mediated by SLC1A5. L-γ-Glutamyl-p-nitroanilide (GPNA) competitively binds to the SLC1A5 substrate-binding site and prevents glutamine uptake [246]. In 2018, another SLC1A5 inhibitor was discovered, (2S)-2-amino-4-[bis[[2-[(3-methylphenyl)methoxy]phenyl]methyl]amino]-butanoic acid also known as (V-9302) showing improved potency and selectivity over GPNA. V-9302 is a small molecule that acts as a competitive inhibitor of SLC1A5 [247]. Interestingly, V-9302 was shown to block glutamine uptake in triple-negative breast cancer (TNBC) cells but not effector T-cells resulting in a superior T-cell response while diminishing tumor growth [248]. As a single agent, V-9302 demonstrated an anti-tumor effect against non-small cell lung cancer (NSCLC) besides its synergistic effect that was observed combined with Almonertinib [248]. SLC38A2 is another main glutamine transporter in cancer, which was also the subject of different studies. While there may not be well-established inhibitors that can selectively target SLC38A2, some compounds such as N-methyl-aminoisobutyric acid (MeAIB) inhibit SLC38A1 and SLC38A2 due to their structural and functional similarities. MeAIB was reported to reduce melanoma cell growth, invasion and migration [249].

Moreover, several inhibitors of the SLC7A5 co-transporter have been studied, mainly in vitro. The 2-aminobicyclo-(2,2,1)-heptane-2-carboxylic acid (BCH) was synthesized to inhibit L system transporters. BCH demonstrated anti-tumor activity in lung, ovary, and breast cancer [171,250,251].

9.2.2.2 GLS inhibitors

Being the rate-limiting enzyme of glutaminolysis, several inhibitors have been identified or synthesized in recent years to target GLS. Bis-2-[5-(phenylacetamido)- 1,3,4-thiadiazol-2-yl]ethyl sulfide (BPTES) is one of the well-studied GLS inhibitors and from which most of the other patent GLS inhibitors were derived. Elan Pharmaceuticals, Inc. patented BPTES in 2002 (US6451828B1) as a selective and potent inhibitor of GLS. However, BPTES antitumor activity had not been reported until 2010, when Seltzer MJ et al. studied its effects on glioblastoma tumors [252]. The mechanism of action of BPTES was revealed in 2011 by Thangavelu K et al. They revealed that BPTES binds to the KGA's allosteric regulation site to stabilize its inactive

tetrameric form, it inhibits KGA over GLS2 and γ-glutamyl transpeptidase [232,253]. Compound 968 is another glutaminase inhibitor that was discovered in 2015. It preferentially binds to the monomeric state of GAC and prevents it from undergoing activating conformational changes, but it has no effect on the GAC that reaches the activation state before 968 binding [254].

2-Pyridineacetamide,N-[5-[4-[6-[[2-[3-(trifluoromethoxy)phenyl]acetyl]amino]-3 pyridazinyl]butyl]-1,3,4-thiadiazol-2-yl] known as (CB-839) is another allosteric inhibitor of GLS that was patented by Calithera Biosciences, Inc (WO2018039442). CB-839 did not show only good potency but good permeability and solubility too, thus preferred over BPTES. Similar to BPTES, binds to the allosteric site of glutaminase leading to the formation of inactive tetramer[255]. The tetramer formed is then unable to bind Pi or form the active superstructure. CB-839 is now in phase I/II clinical trials since 2014 against many cancer types as a single agent but in combination with other clinical drugs (Table 5).

Phase	Disease	Treatment	Status	NCT number
I	Acute Myeloid Leukemia (AML), Acute Lymphocytic Leukemia (ALL)	CB-839 in combination with azacitidine.	Complete	NCT02071927
I/II	Colorectal, Colon, Rectal cancers	CB-839 in combination with capecitabine	Active	NCT02861300
I	Non-Hodgkin's Lymphoma (NHL), Multiple Myeloma, Waldenstorm's Macroglobulinemia (WM), Other B-cell NHL, T-cell NHL	CB-839 in combination with standard-dose pomalidomide and low-dose dexamethasone	Complete	NCT02071888
I	Leptomeningeal Neoplasm, Metastatic Lung-Non-Small Cell Carcinoma, Metastatic Malignant Neoplasm in the Brain, Lung Non-Small Cell Carcinoma	CB-839 HCL in combination with sapanisertib	Recruiting	NCT04250545
II	Triple Negative Breast Cancer	CB-839 in combination with Paclitaxel	Complete	NCT03057600
II	Clear Cell Renal Cell Carcinoma	CB-839 in Combination with Everolimus	Complete	NCT03163667
II	Recurrent Plasma Cell Myeloma	CB-839 HCl in Combination with Carfilzomib and Dexamethasone	Active	NCT03798678

Table 5| Current clinical trials for CB-839

9.2.2.3 Glutamine analogues

DON (6-diazo-5-oxo-L-norleucine) -the earliest compound verified as a glutaminase inhibitor- is a glutamine analog originally isolated from fermentation broth of a Streptomyces in the 1950s. DON was found to irreversibly inhibit KGA and its isoforms by binding to the enzyme active site and covalently modifying the catalytic serine Ser286. However, it is not specific as it broadly inhibits other glutamine-utilizing enzymes such as glutamine synthetase and amidotransferase. DON showed initial clinical benefit, but the clinical trials were stopped later due to toxicity [256]. Other glutamine analogs were identified as irreversible inhibitors such as O-diazoacetyl-DL-serine known as Azaserine and Acivicin that inhibits y-glutamyl transpeptidase (GGT) [257,258].

9.2.2.4 L-asparaginase

The discovery of L-asparaginase (L-ases) can be traced back to the early 1960s when Kidd demonstrated the efficacy of guinea pig serum in rat lymphoma tumor regression [259]. A few years later and in several studies, Broome discovered that asparaginase is responsible for the previously observed anti-lymphoma effect [259]. Asparaginase catalyzes the hydrolysis of asparagine (Asn) to aspartate (Asp). Asparagine is a non-essential amino acid that can be synthesized by the cells by the enzyme asparagine synthase (ASNS) from Asp and Gln or obtained from diet. Lymphoblastic leukemia cells do not express *ASNS* and rely on extracellular Asn to fuel cell growth and protein synthesis therefore Asn depletion leads ultimately to leukemic cell death [262].

There are two types of L-ases used clinically and are derived from two different bacteria. *Escherichia coli* asparaginase, available in pegylated (Oncaspar) and non-pegylated (Kidrolase) forms. Pegylated forms improved the pharmacodynamics and pharmacokinetics of native asparaginase. Pegylation was found to prolong half-life and alter the pharmacokinetics and pharmacodynamic properties, allowing for a longer duration of action and lower administration frequency compared to non-pegylated forms. The second type of L-ases is produced in *Erwinia chrysantemii* (Erwinase). This enzyme also influences glutamine metabolism and depletes extracellular glutamine but to a lesser extent than asparagine [263]. Initially glutaminase activity of L-ases was considered to be responsible for the side effects of L-ase. Later in 2014 Chan et al. demonstrated that the L-ases glutaminase activity is essential for its anti-tumor activity in ASNS expressing cells [264,265,262].

9.2.2.5 Other inhibitors

The second step of glutaminolysis and the formation of αKG from glutamate, can also be inhibited. Epigallocatechin gallate (EGCG), is a natural compound in green tea that can inhibit GDH [266,267]. Another way to inhibit this step is to use a transaminase, such as amino oxyacetate (AOA) [268]. Another step of glutamine metabolism that can be also inhibited is the ATP-dependent conversion of glutamate to glutamine catalyzed by glutamine synthesis and known as the only enzyme that allows the formation of glutamine. GS is encoded by GLUL (glutamate ammonia ligase) gene located on Chromosome 1q23 [269]. GLUL inhibitors were also studied including methionine sulfoximine (MSO), and phosphinothricin (PPT) [270].

9.3 Fatty acid metabolism in cancer

Being the main component of cellular membranes, highly proliferating cancer cells continually synthesis fatty acids [137].Unlike normal cells, cancer cells favors de novo fatty acid synthesis over exogenous sources [271]. Alteration in lipid metabolism was observed in several cancers. Yet, some cancers scavenge lipids from surrounding adipocytes, such as ovarian tumors in which fatty acid binding protein 4 (FABP4) is upregulated to provide fatty acids for rapid tumor growth [272]. Upregulation of various crucial genes along the fatty acid metabolism pathway was discovered. CD38, transmembrane glycoprotein, known as *fatty acid translocase* (*FAT*) is upregulated in breast, ovarian, and prostate cancers [273–275]. Another enzyme implicated in cancer is FASN, which is overexpressed in multiple cancers and linked to poor prognosis such as in prostate, colon, and lung cancer [276–278].

9.3.1 Fatty acid metabolism inhibitors

Targeting lipid synthesis is receiving increased recognition for cancer treatment. Several FASN inhibitors have been tested in vitro and in vivo such as cerulenin, C75 and orlistat demonstrated significant antitumor activity (Lupu and Menendez, 2006). TVB2640 is another FASN inhibitor currently in Phase II trials for HER2+ Metastatic Breast Cancer. Chemically inhibiting ACLY by (SB-204990) is another approach to block fatty acid synthesis. Notably, this approach is limited by potential toxicity due to its effects on the acetyl-CoA level that is involved in other essential pathways such as the acetylation of proteins and nucleic acids [279]. Furthermore, ACC inhibitors such as ND-646 was used to inhibit fatty acid synthesis and therefore compromise cellular growth and viability of non-small cell lung cancer (NSCLC) [280].

9.4 NAD metabolism in cancer

As described earlier, NAD promotes different cellular functions to maintain cellular survival and proliferation thus it has an elevated importance in the fast-dividing cancer cells. Genetic and epigenetic modifications alter NAD metabolism in cancer cells. Overexpression of *NAMPT* was observed in various cancer types including ovarian, colorectal, breast, gastric, prostate and malignant lymphomas [281–286]. High *NAMPT* levels result in a high NAD level to sustain rapid metabolism and proliferation. Several miRNAs were found to mediate *NAMPT* expression such as miR26b which was reported to suppress *NAMPT* expression through binding to the 3'-UTR. miR26b was found to be downregulated in colorectal cancer [287]. Similarly, miR206 was found to be downregulated in breast and pancreatic cancer [288,289].

NAMPT is regulated epigenetically through long non-coding RNA (lncRNA) in triple-negative breast cancer (TNBC). Nicotinamide phosphoribosyltransferase antisense RNA (NAMPT-AS) is a lncRNA that is known to regulate *NAMPT* expression through various mechanisms. At the transcriptional level, NAMPT-AS was shown to recruit POU2F2 (a member of the POU transcription factor family) to bind to the *NAMPT* promoter, leading to induced NAMPT expression. Additionally, at the posttranscriptional level, NAMPT-AS functions as a competing endogenous RNA that competitively binds to miR-548b-3p to protect *NAMPT* from degradation and consequently increase the NAMPT mRNA pool [290].

Besides *NAMPT*, *NAPRT* expression was found to be upregulated in ovarian, prostate, and pancreatic cancers. Interestingly, other cancer types including glioblastoma, gastric and colorectal cancers showed that *NAPRT* expression levels were significantly reduced, mainly due to promoter hypermethylation [291–293]. This reported downregulation of *NAPRT* lead to

increased reliance on NAMPT and salvage pathway to meet the demands for NAD+ thus rendering the cells more sensitive to NAMPT inhibitors [294,295].

Furthermore, NMNAT is a central enzyme in NAD biosynthesis and exhibits a role in cancer cell survival. The first interest of NMNAT in cancer was its function to activate the anticancer prodrug Tiazofurin (NAD analog) through adenylation. Tiazofurin resistance was reported in some cancers and was found to be associated with the low NMNAT activity in the cell [296,297]. NMNAT was also found to be able to suppress rRNA transcription. Thus, inhibiting NMNAT was reported to induce high levels of ribosomal biogenesis, facilitating tumor development [298]. On the other hand, reduced NMNAT1 expression was found to correlate with better overall survival in patients with various cancers including bladder, liver and breast cancer [299].

9.4.1 NAD metabolism inhibitors

In recent years, interfering with NAD metabolism has emerged as an attractive therapeutic strategy to modulate cellular functions for treating malignant disease.

Synthetic "C" nucleosides such as 2-beta-D-ribofuranosylthiazole-4-carboxamide (Tiazofurin) and 2-beta-D-ribofuranosylselenazole-4-carboxamide (Selenazofurin) were known to interfere with NAD metabolism. Tiazofurin (Taz) and Selenazofurin (Sel) yield structural analogs of NAD after their intracellular metabolism known as TAD and Sad, respectively. Consequently, these analogs block NAD coenzyme functions. The antitumor activity of TAD and SAD was reasoned to be linked to inhibiting the NAD-dependent enzyme, Inosine 5-monophosphate (IMP) dehydrogenase, thus blocking the conversion of IMP into guanosine 5-monophosphate (GMP). An effect that was reversible by providing extracellular guanosine nucleotides. Taz and Sel also were reported to affect NAD metabolism, by reducing the use of nicotinamide and therefore decreasing the NAD pool. Some cell lines demonstrated a resistance to Taz due to their inability to metabolize it, such as P388 cell line [300]. Notably, Taz and Sel showed general cytotoxicity translated in clinic with poor outcome.

Furthermore, NAD-producing enzymes present a set of targets that can be used to combat proliferating cancer cells. Being the rate-limiting enzyme in the NAD salvage pathway, NAMPT rose as a promising target with encouraging preclinical results. Ten NAMPT inhibitors have been assessed in clinic and CHS828 was among the initial NAMPT inhibitors trials. CHS828 antitumor effects were tested on patients with solid tumors (NCT00003979). Notably, the study reported dose-limiting critical toxicity shown as frequent gastrointestinal symptoms

and mild hematological toxicity dominated by transient thrombocytopenia and lymphocytopenia [301,302].

Through high-throughput screening, Max Hasmann and Isabel Schemainda reported (E)-N-[4-(1-benzoylpiperidin-4-yl) butyl]-3-(pyridin-3-yl) acrylamide (FK866 or APO866) as a selective noncompetitive NAMPT inhibitor. FK866 gradually depletes NAD and eventually induces apoptosis [303]. The crystallographic studies of the FK866-NAMPT showed that FK866 inhibits NAMPT through binding to an allosteric regulatory site. Various clinical trials reported FK866 activity against B-cell Chronic Lymphocytic Leukemia, melanoma and Cutaneous T-cell Lymphoma (NCT00435084, NCT00432107 and NCT00431912).

NAMPT inhibitors have been commonly hindered in clinical trials by poor response and dose-limiting toxicity. Numerous studies aimed to increase the clinical response rate mainly through two approaches. Firstly, by targeting NAPRT-deficient tumors, as discussed earlier, and secondly, by applying a rescue strategy. A rescue strategy that was developed is the FK866 co-administration with nicotinamide to boost the NAD metabolism in normal cells while fully depriving tumor cells; therefore, this strategy can allow an NAMPT inhibitor to be dosed higher than what was used in the early clinical trial [304].

Other NAMPT inhibitors were also developed over the years including OT-82 which was discovered by chemical library screen followed by hit to lead optimization by OncoTaris OT-82 showed higher potency and more favorable toxicity profile compared to early-generation NAMPT inhibitors [305,306]. While NAMPT inhibitors are the only NAD metabolic inhibitors in clinic, few compounds that displayed NAPRT inhibitory activity were identified. 2-hydroxynicotinic acid (2-HNA) as a competitive inhibitor and several non-steroid anti-inflammatory drugs including mefenamic, flufenamic acid and phenylbutazone. While only 2-HNA was reported to have antitumoral activity [307,308]. Recently, Ghanem et al. identified two compounds through virtual screening that function as NAPRT inhibitors [309].

NMNAT inhibitors also exist, on the top of the list gallotannin, a polyphenolic plant metabolite is the most potent inhibitor of the three NMNAT isoforms with a slight selectivity for NMNAT3, followed by NMNAT1 and finally NAMNT2. Additionally, other studies identified Vacor, a substrate metabolized by NAMPT and NMNAT2 to produce a NAD analog known as Vacor adenine dinucleotide (VAD), which leads to the inhibition of both enzymes, as well as NAD-dependent hydrogenases [310–312].

10. Research Problem and hypothesis

MM remains an incurable malignancy in which MYC emerges as a central player in the disease progression from precursor stages to symptomatic MM. Increased *MYC* expression due to *MYC* structural variants (SV) are found in 41% of newly diagnosed MM patients and 67% of total MM cases [28]. Among *MYC* SVs, the Ig insertion subtype (specifically IgL) was associated with poor patient outcomes. It is therefore essential to develop clinical approaches to target MYC in MM cells. However, as we have seen earlier, targeting MYC remains an unmet need, raising the question: How to target a vital transcription factor that has proven elusive to direct inhibition?

Given that the survival of cancer cells depends on a multitude of factors that distinguish them from normal cells, these include but are not limited to the oncogenic driver genes. Here, we hypothesized that the proliferative advantages induced by *MYC* overexpression in MM creates dependencies of these cells on specific pathways for their survival. These conditionally essential genes constitute a druggable dependency. Consequently, this work aimed to identify these vulnerabilities in *MYC* OE cells and further investigate these dependencies as a therapeutic intervention with minimal toxicity. Towards this goal, we employ a large-scale loss of function screen and a drug screen to characterize and target the genomic vulnerabilities in the context of *MYC* upregulation (Figure 19).

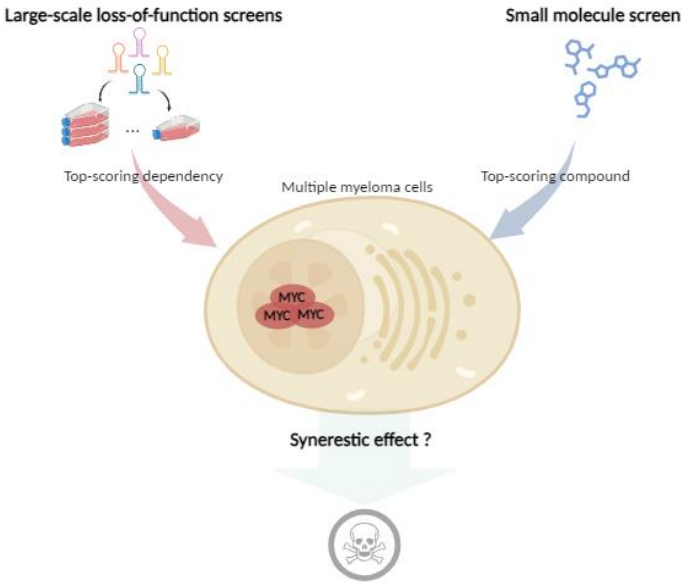

Figure 19| Research design to identify differential genomic dependencies in MYC overexpressing MM cells combining large-scale loss of function and drug screens.

Results

11. Results

Article: MYC dependency in GLS1 and NAMPT is a therapeutic vulnerability in multiple myeloma

(iScience journal)

Lama Hasan Bou Issa[1], Léa Fléchon[1], William Laine[1], Aicha Ouelkdite[1], Silvia Gaggero[1], Adeline Cozzani[1], Remi Tilmont[2], Paul Chauvet[2], Nicolas Gower[2], Romanos Sklavenitis Pistofidis[3], Carine Brinster[1], Xavier Thuru[1], Yasmine Touil[1], Bruno Quesnel[1, 2], Suman Mitra[1], Irene M. Ghobrial[3], Jérôme Kluza[1], Salomon Manier[1, 2 ‡]

[1]Canther, INSERM UMR-S1277 and CNRS UMR9020, Lille University, Lille 59000, France
[2]Department of Hematology, CHU Lille, Lille 59000, France
[3]Dana-Farber Cancer Institute, Harvard Medical School, Boston, MA 02215, USA
‡ Lead Contact

Correspondence: salomon.manier@inserm.fr (S.Ma.)

Summary

Multiple myeloma (MM) is an incurable hematological malignancy in which MYC alterations contribute to the malignant phenotype. Nevertheless, MYC lacks therapeutic drugability. Here, we leveraged large-scale loss-of-function screens and conducted a small molecule screen to identify genes and pathways with enhanced essentiality correlated with MYC expression. We reported a specific gene dependency in glutaminase (GLS1), essential for the viability and proliferation of MYC overexpressing cells. Conversely, the analysis of isogenic models, as well as cell lines dataset (CCLE) and patient datasets, revealed GLS1 as a non-oncogenic dependency in MYC-driven cells. We functionally delineated the differential modulation of glutamine to maintain mitochondrial function and cellular biosynthesis in MYC overexpressing cells. Furthermore, we observed that pharmaceutical inhibition of NAMPT selectively affects MYC upregulated cells. We demonstrate the effectiveness of a novel synergistic combination of GLS1 and NAMPT inhibitors, suggesting that targeting glutaminolysis and NAD synthesis may be a promising strategy to target MYC-driven MM.

Introduction

Multiple Myeloma (MM) is a plasma cell malignancy characterized by the proliferation of monoclonal plasma cells in the bone marrow. MM accounts for approximately 13% of all hematological cancers [313]. The disease passes through precursor or asymptomatic stages, with monoclonal gammopathy of undetermined significance (MGUS) and smoldering multiple myeloma (SMM) [314,315]. While MM oncogenesis is initiated by primary genetic events, mainly hyperdiploidy and immunoglobulin heavy chains (IgH) translocations, secondary genetic events play a major part in the disease progression [316–318]. *MYC* translocations are among the most recurrent secondary aberrations in newly diagnosed MM patients. Mainly translocation t(8;14), in which the *MYC* (8q24) juxtaposes the IgH enhancer on the derivative chromosome 14 leading to *MYC* overexpression [317,319–321]. MYC protein dimerizes with its obligatory partner MAX to bind to the E-box element (CACGTG) and function as a sequence-specific DNA-binding transcription factor[322]. *MYC* is a master regulator of numerous key biological activities, including cell growth, cell cycle, and metabolism. *MYC* expression being a common property of all proliferating cells, the intrinsically disordered location of its main functional domains in addition to the protein localization inside the nucleus and its short half-life, collectively these properties raise the challenge to find innovative ways to target MYC without causing unacceptable toxicities [323,324].

Certain pathways in cancer cells have increased importance compared to normal cells in the interest of buffering different stress levels, such as replication stress, or DNA damage. These pathway dependencies also provide exploitable vulnerabilities to cancer cells, which can be targeted for therapeutic interventions. This approach can result in stress overload and apoptosis of cancer cells while sparing normal cells. In this regard, cancer dependencies are receiving greater interest to uncover genes with enhanced essentiality in a specific cellular context. Here, we hypothesized that the proliferative advantage promoted by *MYC* overexpression induces differential genomic dependencies on particular signaling pathways, thus creating vulnerabilities with potential therapeutic relevance.

To test this hypothesis, we applied large-scale, unbiased approaches to identify vulnerabilities in MYC overexpressing MM cells by exploiting cancer dependency map and conducting small molecule screening. We report specific dependencies of MYC overexpressing cells on Glutaminase (GLS1) and Nicotinamide phosphoribosyltransferase (NAMPT) in MM. GLS1 is

pivotal in glutamine metabolism, which catalyzes the conversion of glutamine into glutamate and ammonia[325,326]. NAMPT is a key enzyme in the NAD salvage pathway, which recycles nicotinamide (NAM) back into NAD[327]. The fate of glutamine and NAD are tightly interconnected, involved in various aspects of cellular bioenergetics and adaptation to hypoxic conditions. We further observed a synergistic activity of the dual inhibition of GLS1 and NAMPT in MM. Together, our data demonstrated that combinatorial treatment of CB-839 and FK-866 constitutes a potential novel therapeutic strategy against MM in the context of MYC upregulation.

Results

MYC overexpression in MM growth is dependent on GLS1 activity. We searched for genomic vulnerabilities associated with MYC overexpression by leveraging genome-scale pooled shRNA screening data in a panel of 236 cancer cell lines from Project Achilles to identify the genes essential for proliferation and survival of high *MYC*-expressing cell lines. *MYC* expression level for each cell line was determined using expression profile data from the Cancer Cell Line Encyclopedia (CCLE). We correlated 54,393 shRNA sensitivity profiles with *MYC* expression level identified four shRNAs that strongly correlated with reduced viability in *MYC*-high but not *MYC*-low cells: *MAX* (r = -0.51, $p < 0.001$), an obligate partner of MYC representing an internal validation of our method, followed by *GLS1* (r = -0.48, $p < 0.001$) and *SLC1A1* (r = -0.42, $p < 0.001$), encode the rate-limiting enzyme in glutamine metabolism (glutaminase) and cytoplasmic glutamine transporter, respectively (Figure 1A; Table S1). This correlation between the sensitivity to shGLS1, shSLC1A1 and *MYC* expression level demonstrated a selective dependency on glutamine metabolism in the context of MYC overexpression. Since *MYC* is a powerful driver gene that modulates the expression of numerous genes, we defined *MYC* gene signature score (Z-score) derived from the expression of hallmark MYC target v2 (58 genes) [328]. We correlated Z-score to the shRNA sensitivity profiles from Project Achilles to identify differential genomic dependencies that correlate with *MYC* signature. Our analysis revealed that the higher score of MYC target v2 is associated with higher GLS1 dependency (Figure 1B; Table S2). Due to the rarity of MM cell lines with low MYC expression level, we generated an MM isogeneic model overexpressing *MYC* in U266 cell line transduced with EF1A-C-MYC lentiviral vector (Figure S1A and S1B). For validation, we introduced two distinct doxycycline-inducible shGLS1 in order to induce depletion of GLS1. Both shGLS1#1 and shGLS1#2 caused a selective reduction in proliferation of U266/MYC cells over U266/Ctrl cells (Figure 1C; Figure S1C). We also observed a higher sensitivity to glutamine-deprived conditions of MYC-high cells as compared to MYC-low cells (Figure S1D). We used pharmacological inhibition of the glutamine metabolism pathway for further validation. CB-839, a potent non-competitive inhibitor of GLS1, on a wide spectrum of cancer cell lines including MM, breast, colon, and lung cancer. Notable we observed a strong negative correlation between CB-839 response and *MYC* expression level (Figure 1D; Figure S1E). We also tested V-9302, a competitive antagonist of transmembrane glutamine transporter SLC1A5. Similarly, we observed a higher sensitivity of MYC-high cell to SLC1A5 inhibition

(Figure 1E; Figure S1F). Taken together, these results indicate that *MYC* overexpression confers higher dependency on glutamine metabolism pathway and confers enhanced sensitivity to pharmacological inhibition of GLS1.

GLS1 function as a non-oncogenic dependency. To further examine the relationship between MYC oncogenic signaling and glutamine dependency, we analyzed the transcriptome and translational profiles of the U266 isogenic model *via* RNA-seq and TMT mass tag, respectively. At the transcriptomic level, we identified 119 and 829 genes significantly up-or down-regulated with a fold change higher than 2 and a *P* value < 0.05. Among the top-upregulated genes were genes related to cell cycle, including (*CDK6*; FC = 3.7, p < 0.001), (*ERCC6L*; FC = 2.17, p < 0.001), (*GEM*; FC= 2.87, p <0.001), (*MYB*; FC =2.68, p <0.001) and glycolysis (*HK2*; FC = 5.4, p < .001), whereas several zinc finger transcription factors were among the most significantly downregulated genes (Figure 2A; Table S3). On the protein level, our proteomics analysis identified 29 and 15 proteins significantly up or downregulated with a fold change higher or lower than 2, respectively, and a *P* value < 0.05 showed significant down-regulation in the interferon type I signaling pathway (Figure 2B; Table S4). We next sought to test whether the enhanced dependency on GLS1 is due to an upregulation of glutamine metabolism-related genes. Interestingly, those genes were not significantly upregulated on either RNA or protein level (Figure 2C and 2D). Likewise, expression data from CCLE database derived from data for 169 hem cell lines indicated no significant upregulation of the glutamine metabolism-related genes (Figure 2E). To obtain further insights into the core enriched pathways in *MYC* overexpressing cells, we compared their enrichment in our isogenic model, in 169 hematological cell lines from CCLE, and in two independent patient datasets (GSE4452 - MMRF-CoMMpass). All datasets were grouped by *MYC* expression level. Gene set enrichment analysis (GSEA) consistently showed a correlation pattern with significant enrichment of ribosomal biogenesis and translational activity pathway, while no significant enrichment in the glutamine metabolism-related gene sets (Figure 2F-2I; Table S5). This is in line with the higher translational activity induced by *MYC* [329–332]. Collectively, we show that MYC does not transcriptionally nor translationally upregulate glutamine metabolism pathway. These findings likely reflect a non-oncogenic dependency in *MYC* overexpressing cells on GLS1.

GLS1 inhibition selectively compromises the metabolic fitness of MYC OE cells. Initially, glutamine metabolism in the mitochondria and its conversion to CO_2 and H_2O is an oxygen-consuming process. This process is a major metabolic fate of glutamine and a primary source

of bioenergy. Using the seahorse XF analyzer we measured the kinetic oxygen consumption rate (OCR) response in U266/Ctrl and U266/MYC under glutamine supplement. U266/MYC cells possess the ability to oxidize glutamine at a higher rate compared to U266/Ctrl. Injecting CB-839 at 5 μM was able to abolish the glutamine-induced OCR in U266/MYC demonstrating the incapability of MYC OE cells to maintain sufficiently high level of oxidative phosphorylation under glutamine metabolism disruption (Figure 3A). Additionally, we assessed the effect of CB-839 and GLS1 knockdown on the mitochondrial function of U266/Ctrl and U266/MYC by running a mitochondrial stress test (Figure 3B; Figure S2A). Both knockdown of GLS1 expression and pharmacologic GLS1 inhibition by CB-839 in U266/MYC was accompanied by mitochondrial impairment at basal and the FCCP-induced (maximal) OCR confers impaired mitochondrial function and consequently reduction in the oxidative phosphorylation (OXPHOS) activity (Figure 3C and 3D; Figure S2A). The effect of CB-839 was observed in dose-dependent manner in U266/MYC, while we observed less impact on U266/Ctrl and only at higher concentration of CB-839. To extend this observation, we generated a second isogeneic model overexpressing *MYC* in Loucy cell line; an acute lymphoblastic leukemia (ALL) cell line that has low *MYC* expression level. We transduced Loucy cells with EF1A-C-MYC lentiviral vector (Figure S2B). Next, we assessed the metabolic profile of the Loucy isogenic model and observed similar results to the U266 isogenic model. Loucy/MYC showed a significantly higher energetic profile compared to Loucy/Ctrl represented by higher basal and maximal OCR levels. This higher mitochondrial function was impaired by 5μM CB-839 (Figure S2C-S2E). Due to the tight link between OXPHOS and glycolysis for ATP production, we next analyzed the glycolytic profile of our isogenic models. Increased doses of CB-839 triggered an increase in glycolytic activity to compensate for the OXPHOS deficit in U266 isogenic model. In contrast, we observed a significant decrease in the glycolytic reserve in U266/MYC upon GLS1 inhibition, indicating a disruption of the cellular potentials to increase ATP production through glycolysis to meet energy demand (Figure S3A-S3C). Similarly, inhibiting GLS1 caused more differential effect on Loucy/MYC, demonstrated by an increase in the glycolytic activity and a decrease in the glycolytic reserve upon CB-839 treatment, while no effects were observed on Loucy/Ctrl cells (Figure S3D-S3F). Taken together, these findings revealed the essential role of GLS1 in the MYC OE cells to sustain their mitochondrial function for energy production.

CB-839 selective effect is driven by a decreased glutamine utilization in the context of MYC OE. To further determine the downstream effects of GLS1 inhibition in the context of

high MYC expression, we analyzed the abundance of 116 key metabolites in U266/MYC and U266/Ctrl cell lines (Table S6). U266/MYC showed a higher glycolytic profile combined with elevated TCA cycle metabolites (Figure 4A). We next identified the metabolic changes under GLS1 inhibition. CB-839 showed a significant reduction in the ATP:ADP ratio in U266/MYC and not U266/Ctrl marking an important energy debt (Figure 4B). Moreover, we found that CB-839 caused significant suppression of the TCA cycle in *MYC* high cells (Figure 4C). Accordingly, the co-incubation with the main glutamine derivative (αKG) rescued the proliferation defect caused by CB-839 in U266/MYC (Figure 4D). We have also found a significant depletion in the carnitine level under GLS1 inhibition in U266/MYC; thus, the cells failed to accelerate the fatty acid oxidation (FAO) to rescue the resulting energy depletion (Figure 4E). Besides its role as a carbon donor, the resulting glutamate is an indispensable donor of nitrogen for macromolecule synthesis such as glutathione (GSH). GSH has a major role in mitigating the effects of reactive oxygen species (ROS). Notably we observed a significant increase in the total GSH level in U266/MYC. This observation is in line with other studies that linked MYC expression and GSH level [333,334]. This level was reduced by 54.92 ± 12.1% under GLS1 inhibition (Figure 4F). Furthermore, we observed elevated levels of nonessential amino acids in U266/MYC which indicates a higher translational activity of MYC OE cells, whereas a depletion was observed under GLS1 inhibition (Figure 4G). The above results conclusively show that MYC overexpression results in a preferential metabolic shift to Gln to satisfy the elevated needs for energy, redox regulation, and protein synthesis substrates.

NAMPT inhibition selectively affects MYC OE cells. To identify pharmaceutical agents with which to perturb the proliferation of MM cells in the context of *MYC* overexpression, we performed a small-molecule screen on U266/MYC and U266/Ctrl control cell lines. A total of 1869 well-annotated small molecules were tested, including most of Selleck's inhibitors, FDA-approved compounds, chemotherapeutic agents, as well as some natural products. We determined a differential activity (D-score) for each compound. Among the hits that selectively affected MYC OE cells, we identified five compounds that belong to the PI3K/Akt/mTOR signaling pathway (GSK 1059615, OSU-03012, BIO, AZD 2858, AZD 1080), 5 Aurora kinase inhibitors (MLN8054, VX-680, AMG-900, MLN8237, GSK1059615), (Figure 5A; Table S7). This finding can be reasoned to the enhanced dependency of MYC overexpressing cells on PI3K/Akt/mTOR pathway and Aurora kinase to maintain protein translation and cell division, respectively [335,336]. Interestingly, The Nicotinamide Phosphoribosyl transferase (NAMPT) inhibitor STF-11884 had the highest selectivity inhibition on MYC OE cells (D = 61.05%)

marking our first lead. NAMPT is the rate-limiting enzyme in the nicotinamide adenine dinucleotide (NAD+) synthesis. It catalyzes the first step in the biosynthesis of NAD from nicotinamide (NAM), which is essential for energy production[337]. NAD role is extended to other cellular functions, such as DNA repair through the actions of NAD-consuming enzymes such as PARPs and oxidative stress response [338,339] (Figure 5B). To validate the dependency of MYC OE cells, we used the NAMPT inhibitor FK-866, evaluated in clinical trials (Phase II) for chronic lymphocytic leukemia and cutaneous T-cell lymphoma (NCT00435084 and NCT00431912). We observed a significantly higher sensitivity to FK-866 in MYC overexpressing cells (Figure 5C and 5D; Figure S4A). From these data, we can conclude a potent and differential effect of NAMPT inhibition on MYC OE.

Synergistic activity of CB-839 and FK-866 in MYC OE cells. Considering that Gln and NAD have closely interlinked metabolic networks involving electron transport chain (ETC), TCA and redox regulation [340], we next explored the potential synergy between GLS1 and NAMPT inhibitors. We performed a dose-response matrix to test 9 different combinations of doses ranging from 0 to 20 μM for CB839 and from 0 to 30 nM for FK-866. As hypothesized, FK866 markedly enhanced the anti-multiple myeloma effects of CB-839. The dual inhibition of GLS1 and NAMPT showed a synergistic effect in U266/MYC (ZIP synergy score: 35.896 ± 3.78) or MM1S (ZIP synergy score: 22.3612 ± 11.42), (Figure 6A). In contrast, the combined treatment of CB-839 and FK-866 was mostly additive in U266/Ctrl cells (ZIP synergy score: 4.657 ± 8.29). The lowest combinatorial treatment doses tested achieved on average 37-70% more killing in U266/MYC compared to control cells. This data suggests a selective synergy CB-839 and FK-866 in the context of MYC overexpression in MM. This combination caused a reduction at both basal and maximal respiration of 60-40%, respectively (Figure 6B and 6C). Likewise, combining GLS1 and NAMPT1 inhibitors induced the level of mitochondrial oxygen species and led to a significant mitochondrial depolarization in U266/MYC compared to the effect observed in control cells (Figure 6D and 6E). Taken into consideration the role of NAD supply to maintain the activity of the glycolytic enzyme glyceraldehyde 3-phosphate dehydrogenase (GAPDH), we next set out to measure the glycolytic rate under CB-839 and FK-866 combinatorial treatment. FK-866 effects on the glycolytic rate were observed only after 48 hours of incubation on U266/MYC, while no additional effect was observed by adding CB-839. In comparison, no significant effect was observed on U266/Ctrl (Figure S4B and S4C). Moreover, we investigated if the CB-839 and FK-866 combination affects the drug resistance profile of myeloma cells. We used the dexamethasone-resistant MM cell line (MM1R).

Potently, increased doses of the combination had cytotoxic effect on the MM1R cell line (Figure S5A). Next, we have tested the two proteasome inhibitors that are considered the cornerstone agents in the treatment of MM, Carfilzomib and Bortezomib in increased doses with increased doses of the CB-839 and FK-866 combination. Effectively our combination improved the sensitivity profile of U266/MYC and MM1S to Carfilzomib and Bortezomib. This effect was less potent in U266/Ctrl cells (Figure S5B-5G). Our results align with prior investigations that reported PI sensitizing activity of CB-839 in resistant MM cells [341]. We further assessed the potential synergy of CB-839 and FK-866 *in vivo*. SCID mice were injected with MM1S GFP-Luc^{+} (Figure 7A). After engraftment, mice were randomized into four groups to receive vehicle, CB-839 (200 mg/kg), FK-866 (10 mg/kg) or a combination of both drugs. We observed that the combination of both metabolic inhibitors elicited a strong anti-tumor activity compared to single-CB-839 treatment, as monitored by bioluminescence (BLI) and prolonged overall survival median (OS) of 38 days for the control group, 42 days and 54.5 for single treatment with CB-839 and FK866, respectively and 64.5 days for combination; $p<0.0001$ (Figure 7B and 7C). Taken together, our data indicate that the dual inhibition of GLS1 and NAMPT represents an innovative new therapeutic approach to target gene dependencies in MYC overexpressing MM.

Discussion

Despite the role of *MYC* overexpression in the progression from precursor stages to symptomatic MM, *MYC* remains a long-pursued target due to the short half-life of the protein, the intrinsically disordered location of its main functional domains, the lack of an enzymatically active site, and its nuclear localization [342]. Some strategies to target *MYC* on different axes, such as transcription, translation, and Myc protein stability or interactions have been studied [316,324,343–348]. However, despite the massive efforts, targeting *MYC* on a clinical level remains challenging. Consequently, indirect strategies for targeting *MYC* have arisen as an important approach to effectively and selectively target *MYC*-driven cancer cells.

Here, we report for the first time a differential gene dependency of MYC overexpression on GLS1, an enzyme responsible for converting glutamine to glutamate. Glutamate is then subsequently converted to α-ketoglutarate which feeds into the TCA cycle for ATP production. Previous studies have shown that nutrient such as glutamine can modulate MYC post-transcriptionally [349]. Moreover, MYC interferes with the expression of GLS1 through inhibiting miR-23a/b thus increases the glutamine utilization [350,351]. Here, in the context of MM and

hematological malignancies, we did not observe an enrichment in the glutamine metabolism pathways in *MYC* overexpressing cells. This likely reflects that *MYC* does not induce an overexpression of the glutamine metabolism pathway but is rather dependent on minimal glutaminolysis activity. This suggests a non-oncogenic dependency on *GLS1* driven by *MYC* expression.

We functionally explored these dependencies as a selective targetable vulnerability using CB-839, a potent and selective GLS1 inhibitor currently being used in phase I/II clinical trials in different cancer types (NCT02071927, NCT04250545, NCT03163667). CB-839 exhibited promising preclinical data in several types of solid cancers, such as triple negative cancer[352], lung adenocarcinoma [353], and hematological malignancies, including acute myeloid leukemia (AML) [354,355]. This sensitivity to glutamine inhibition was driven by both redox and bioenergetics stress. In our present study, we demonstrated through different approaches that *MYC* overexpressing cells exhibit heightened sensitivity to perturbation of glutamine metabolism. Our metabolic assays substantiate the essential role of glutamine in maintaining mitochondrial oxidative phosphorylation in *MYC* overexpressing cells. Oxidative phosphorylation (OXHPOS) is an important process that harvests the TCA-generated NADH (Nicotinamide Adenine Dinucleotide) and FADH2 (Flavine Adenine Dinucleotide) to produce ATP. Additionally, integrative analyses of metabolomic profiles revealed that *MYC* overexpression renders MM cells specifically dependent on glutamine to fuel the TCA cycle and maintain high energy production. This observation is in line with previous studies, which reported the important role of glutamine during MM tumorigenesis and an increase in glutamine anaplerosis into the TCA cycle in MM stages compared to pre-malignant stages[233,356]. Prior studies reported a link between cysteine plasma level and sensitivity to GLS1 inhibitors. The increase in cysteine levels was found to increase the intracellular glutamine turnover, which in turn render the cells more sensitive to glutaminolysis inhibitors such as CB-839. It is worth noting that our CE-MS analysis we did not notice any changes in the cysteine level between our U266/Ctrl cells and U266/MYC [357]. Besides energy stress, GLS1 inhibition triggers redox stress and causes a reduction of 60% of the antioxidant glutathione level. This result is in agreement with previous studies in various cancer types [358,359].

Combining CB-839 with other compounds such as mTOR and checkpoint inhibitors held the promise of synergistic effect to enhance the therapeutic activity [360,361]. Thus, we investigated potential synergistic combinations that can exacerbate this metabolic vulnerability. Herein, we demonstrate a pharmacological dependency of MYC-driven cells on NAMPT. FK866 (also known as APO866) is a highly selective non-competitive NAMPT inhibitor firstly presented in

2003 as the first specific nanomolar inhibitor of NAMPT [362]. Preclinically, FK866 exerts potent antitumor activity on various tumor models [363–365]. NAMPT inhibition compromises several cellular processes by depleting NAD levels. NAD is a substrate to numerous enzymes such as sirtuins, and ADP-ribosyl, but most importantly, poly (ADP-ribose) polymerase 1 (PARP1), essential for DNA repair therefore crucial to tumors with high genomic instability [366]. In addition, NAD is a critical cofactor in operating the TCA cycle and glycolysis through oscillating between two redox states (NAD and NADH). Tan et al. showed that FK866 results in the accumulation of glycolytic intermediates and markedly decreases the ATP level [367]. Here we report a selective potency of FK866 in MYC-driven MM to maintain tumor high energy demands through mitochondrial oxidative phosphorylation and not glycolysis.

Due to the tight link between glutamine and NAD biological roles, we examined a novel potential combination between GLS1 and NAMPT1 inhibitors. We observed an exclusive synergy of CB839 and FK866 in MYC overexpressing cells. Collectively, our *in vitro* and *in vivo* results revealed an effective therapeutic combinatory strategy in the context of *MYC* overexpressing MM. Both drugs are currently used in clinical trials, indicating a high translational potential of these findings. With a likelihood of improved clinical outcomes and improved tolerability.

In conclusion, the integration of a genome-scale loss-of-function screen and large drug sensitivity screens provide a powerful approach to identifying therapeutic candidates in specific molecular subsets of MM with a high translational potential. Here, we highlight a combined approach by interfering with glutamine metabolism and NAD production as an effective strategy for targeting *MYC* overexpressing cells in MM. The results of this study will need further validation in different models to be potentially translated in the clinic. Moreover, this approach can be extended to identify other potential synergistic partners as novel strategies to target the undruggable MYC-driven tumor cells.

Limitation of the study

One of the limitations of this study was the unavailability of a multiple myeloma cell line that has low MYC expression levels apart from U266 cell line. While it is theoretically possible to knockdown MYC expression in cell lines to establish two distinct comparison groups within multiple myeloma (MM), previous studies have reported cytotoxicity associated with such manipulations in myeloma cell lines. However, to address this limitation, we generated two isogenic models overexpressing MYC in myeloma and lymphoma. We have also used an array of cell lines derived from diverse cancer types. Additionally, our study relied on publicly

available datasets of expression profiles from both cell lines and patients to further strengthen and validate our conclusions. The other limitation is the lack of another mouse model in which we can further validate this synergy within an immunocompetent environment. Further studies are required to underline the mechanism of this therapeutic synergy in vivo.

Authors contribution

L.H.B.I., J.K., and S.Ma. conceived and designed the study. L.H.B.I. and W.L. performed experiments. L.H.B.I., L.F., W.L., R.S.P., I.G., J.K. and S.Ma. acquired the data. All authors analysed and interpreted the data. L.H.B.I. and S.Ma wrote the manuscript. All authors reviewed, edited, and approved the manuscript.

Acknowledgement

This work was supported by ARC France Foundation grant. We also acknowledge the support from Contrat de Plan Etat-Région CPER Cancer 2015-2020.

Declaration of interests

The authors declare no conflict of interest.

Figure titles and legends

Figure 1. Interrogation of genome-scale pooled short hairpin RNA (shRNA) screening data to identify potential vulnerability in MYC overexpressing cells. **A.** Point biserial correlation coefficients for association with MYC overexpression are blotted against Benjamini-Hochberg corrected P value for 54.393 shRNA. Genes scored as differentially lethal in MYC overexpressing cell lines were highlighted, MAX (r = -0.51, $p < .001$), GLS1 (r = -0.48, $p < .001$), SLC1A1 (r = -0.42, $p < .001$) and E2F6 (r = -0.41, $p < .001$). **B.** Point biserial correlation coefficients for association with MYC signature are blotted against Benjamini-Hochberg corrected *P* value for 54.393 shRNA. **C.** Analysis of proliferation of U266/Ctrl and U266/MYC transduced with a lentiviral vector expressing either an inducible (shGLS1#1) and (shGLS1#2) cultured with or without doxycycline for the indicated time in order to induce depletion of GLS1. * Indicates p values < 0.05, ** indicates p-value < 0.01, *** indicates p-value < 0.001; 1-way ANOVA with tukey's test was used to compare between cell lines. **D-E** Heatmap represents the dose-response effect in 13 human cancer cell lines of various cancers including: Breast cancer, MM, renal cancer, colon cancer and lung cancer. Cell lines were treated with CB-839 (0-200µM for 48 hours) and V-9302 (0-30µM for 48 hours). The percentage survival (expressed as percentage of the DMSO-treated control) is visualized in color format according to their values on a linear scale (0%-100%) and row-ranked by IC_{50} values from lowest to highest. Cell lines with high MYC expression values were highlighted in red. Data in (**C**-**E)** are represented as mean ± SEM of triplicates of three representative experiments.

Figure 2. MYC oncogenic signaling and glutamine dependency. A. Volcano plot of RNA-Seq of U266/MYC versus U266/Ctrl showing 119 and 829 genes significantly up-and down-

regulated, respectively, with a fold change (FC) higher than 2. B. Volcano plot of TMT-MS of U266/MYC versus U266/Ctrl showing 28 and 15 proteins significantly up-and down-regulated, respectively, with a fold change (FC) higher than 2. C. mRNA expression level and D. protein abundance of glutaminolysis-related genes in U266/Ctrl and U266/MYC. E. Expression data of glutaminolysis-related genes in Hem cell lines (n=169) from CCLE database (Affymetrix U133+2 expression array) grouped into *MYC*-high versus *MYC*-low cell lines. F-I Gene set enrichment analysis demonstrating the most significantly up-regulated genes in the context of high *MYC* expression against C5 gene set, in; F. The U266 isogenic model. G. Hem cell lines (n=169) from CCLE database grouped into *MYC*-high versus *MYC*-low cell lines. H and I. The cohort of patient datasets: GSE4452 (Carrasco; n=40), and MMRF RG (CoMMpass; n=40). Selected pathways were shown. Data in (**C**-**E)** are represented as mean ± SEM. * Indicates p values < 0.05, ** indicates p-value < 0.01, *** indicates p-value < 0.001; Student *t* test.

Figure 3. The role of glutamine in maintaining mitochondrial function. A. Kinetic OCR response in U266/Ctrl and U266/MYC cells to glutamine (2mM) followed by CB-839 at (1 or 5 μM). B. Kinetic plot and corresponding bar graphs of normalized OCR obtained during mitochondrial stress test of U266/Ctrl and U266/MYC treated with or without the indicated concentration of CB-839 for 4 hours, cells were exposed sequentially to each mitochondrial modulator of mitochondrial activity at the indicated times to assess C. Basal respiration. D. Maximal respiration. Data are presented as mean ± SEM calculated from 3 technical replicates. * Indicates p values < 0.05, ** indicates p-value < 0.01, *** indicates p-value < 0.001; Student *t* test. DMSO-treated cells were used as a non-treated control (NT).

Figure 4. Enriched metabolic pathways under GLS1 inhibition. **A.** Shown is a metabolic network of glycolysis and TCA cycle, metabolites abundance was colored by their abundance difference in U266/MYC compared to U266/Ctrl (color key). B. ATP:ADP ratio was determined to assess the energy state of U266/Ctrl and U266/MYC treated with 1μM CB-39 for 48 hours. C. Heatmap comparing relative levels of metabolites in U266/Ctrl and U266/MYC treated with 1μM CB-39 for 48 hours. D. The differential effect of αKG (1 mM) on the viability of U266/Ctrl and U266/MYC cultured under the indicated concentration of CB-839 for 48 hours. E. Intracellular Carnitine F. Total Glutathione and G. Non-essential amino acids levels, sum of [Ala], [Arg], [Asn], [Asp], [Gln], [Glu], [Gly], [Pro], [Ser] and [Tyr], measured in U266/ctrl and U266/MYC treated with CB-839 for 48 hours. All data were normalized to cell

count and presented as mean ± SEM. Comparison of more than three groups were performed by one-way ANOVA test. * Indicates p values < 0.05, ** indicates p-value < 0.01, *** indicates p-value < 0.001. DMSO-treated cells were used as a non-treated control (NT).

Figure 5. Differential effect of NAMPT inhibition in MYC OE cells. A. Scatter plot representation of a small-molecule library (~2000 compounds) against U266 isogenic model cells. Each dot represents the inhibition difference between U266/Ctrl and U266/MYC achieved with each compound at a concentration of 10 μM for 48 hours. Hit thresholds were set to >20 (red) or <-20 (blue). Leads were highlighted. **B.** Schematic of the NAD+ salvage production pathway and the site of action of NAMPT inhibitor (FK-866) and the major downstream cellular functions of NAD+. NAM, nicotinamide; NMN, nicotinamide mononucleotide. C. Heatmap represents the dose-response effect on KMS12, WiDr, K562, U266/Ctrl and U266/MYC. Cell lines were treated with FK-866 (0-100nM for 72 hours). The percentage survival (expressed as percentage of the DMSO-treated control) is visualized in color format according to their values on a linear scale (0%-100%) and row-ranked by IC_{50} values from lowest to highest. Cell lines with high MYC expression values were highlighted in red. D. Normalized Basal and Maximal OCR obtained during mitochondrial stress test of U266/Ctrl and U266/MYC with or without the indicated concentration of: FK-866 for 48 hours. Data are presented as mean ± SEM calculated from 3 technical replicates. DMSO-treated cells were used as a non-treated control (NT). * Indicates p values < 0.05, ** indicates p-value < 0.01, *** indicates p-value < 0.001; Student *t* test.

Figure 6. Combining CB-839 and FK-866 is a powerful strategy against MM. A. Synergy maps of U266/Ctrl, U266/MYC and MM1S cell lines treated with indicated concentration of CB-839 and FK-866 for 72 hours. Synergy score was determined by SynergyFinder using Zero Interaction Potency ZIP (N = 3 biologically independent replicates). B and C. Normalized Basal and Maximal OCR obtained during mitochondrial stress test of U266/Ctrl and U266/MYC with or without the indicated concentration of: CB-839 (1μM) for 4 hours, FK-866 (30nM) for 48h and combined treatment. Data are presented as mean ± SEM calculated from 3 technical replicates. DMSO-treated cells were used as a non-treated control (NT). **D.** Mitochondrial superoxide (MitoSOX) and **E.** tetramethylrhodamine, ethyl ester (TMRE) evaluated in U266/Ctrl and U266/MYC cells. Cells were treated with FK866 (30 nM) for 72 hours and/or CB-839 (5 μM) for 24 hours. Data represent the mean ± the standard error of the mean for 3

biologically separate experiments. * Indicates p values < 0.05, ** indicates p-value < 0.01, *** indicates p-value < 0.001.

Figure 7. *In vivo* synergistic effect of combining CB-839 and FK-866 A. Experimental workflow for the in vivo experiments. Female SCID/CB.17 mice were injected with MM.1S-GFP-Luc+ cells. After engraftment mice were randomized to four groups based on bioluminescence (BLI), and CB-839, FK-866, combination or vehicle control was administrated. Tumor growth was assessed by BLI at the indicated times. B. BLI signal versus time of the four groups of Female SCID/CB.17 mice bearing MM.1S-GFP-Luc+ tumor treated with CB-839, FK-866, combinations, and vehicle control (n=6). C. Kaplan-Meier survival curve, survival was evaluated from the first day of engraftment until mice were sacrificed. * Indicates p values < 0.05, ** indicates p-value < 0.01, *** indicates p-value < 0.001.

STAR ★ METHODS

KEY RESOURCES TABLE

REAGENT or RESOURCE	SOURCE	IDENTIFIER
Antibodies		
anti-c-MYC	Cell Signaling Technology	Cat. # 9402s
anti-GLS1	Cell Signaling Technology	Cat. # 88964
anti-GAPDH	Santa Cruz Biotechnology	Cat. # sc-47724
IgG HRP-linked; anti-rabbit	Cell Signaling Technology	Cat. # 7074s
IgG HRP-linked; anti-mouse	Cell Signaling Technology	Cat. # 7076s
Bacterial and virus strains		
EF1A-C-MYC lentivirus	Cellomics Technology	PLV-10010-50
EF1A-Vector Control lentivirus	Cellomics Technology	PLV-10074-50
Chemicals, peptides, and recombinant proteins		
CB-839	MedChemExpress	HY-12248
FK866	MedChemExpress	HY-50876
FCCP	Sigma	C2920
Oligomycin A	Sigma	75351
Antimycin A	Sigma	A8674
Rotenone	Sigma	R8875
Poly-L-lysine solution	Sigma	D8375
Glucose	Gibco	A2494001
2-DG	Sigma	D8375-1g
Dimethyl 2-oxoglutarate	Sigma-Aldrich	349631
Doxycycline	MedChemExpress	HY-N0565,
Hygromycin	InvivoGen	ant-hg-1
Puromycin	InvivoGen	ant-pr-1
Polybrene	Santa Cruz Biotechnology	sc-134220
Phosphatase Inhibitor Cocktail C	Santa Cruz Biotechnology	sc-45065
Phosphatase Inhibitor Cocktail B	Santa Cruz Biotechnology	sc-45045
RIPA lysis buffer	Cell Signaling Technology	Cat. # 9806
BSA	Sigma-Aldrich	Cat. # A2153
Iodoacetamide	Sigma	I1149
Dithiothreitol	Thermo Fisher	P2325
Saline	Aguettant	3400936694132
Citrate	Sigma-Aldrich	PHR1416
Hydroxypropyl-b-cyclodextrin	MedChemExpress	HY-101103
Luciferin	PerkinElmer	122799
MitoSox Red	Thermo Fisher	M36008
Critical commercial assays		
CellTiter-Glo®	Promega	G7571
RNeasy Micro Kit	Qiagen	74104
Pierce™ BCA Protein Assay Kit	Thermo scientific	23225
SuperSignal™ West Femto Maximum Sensitivity Substrate	Thermo scientific	34094
NEBNext® Ultra™ RNA Library Prep Kit	New England BioLabs	NEB #E7770

TMRE-Mitochondrial Membrane Potential Assay Kit	abcam	ab113852
Deposited data		
Data of RNA-seq	This paper	GEO: GSE241948
Proteomics data	This paper	PXD050010
Experimental models: Cell lines		
Human: U266	DMSZ	ACC 9
Human: MM1S	ATCC	CRL-2974
Human: KMS-12	DMSZ	ACC 551
Human: Loucy	ATCC	CRL-2629
Human: MM1S.luc/GFP	Gifts from Dr. Ghobrial (Dana-Farber Cancer Institute)	N/A
Human: MM1R	Gifts from Dr. Ghobrial (Dana-Farber Cancer Institute)	N/A
Human: KMS18	Gifts from Dr. Ghobrial (Dana-Farber Cancer Institute)	N/A
Human: NCI-H929	ATCC	CRL-3580
Human: MDAMB-231	ATCC	CRM-HTB-26
Human: Caki-2	ATCC	HTB-47
Human: WiDr	ATCC	CCL-218
Human: NCIH-23	ATCC	CRL-5800
Human: NCIH-1650	ATCC	CRL-5883
Human: NCIH-1473	ATCC	CRL-5872
Human: K562	ATCC	CCL-243
Experimental models: Organisms/strains		
Mouse: SCID	Charles River	Strain code: 236
Oligonucleotides		
shGLS1-1 (tet,Hyg)	FenicsBIO	HSH-812279-Hyg-2
shGLS1-2 (tet,Hyg)	FenicsBIO	HSH-812279-Hyg-3
shRNA (tet,Hyg)	FenicsBIO	SH-tet-C02
Software and algorithms		
GraphPad Prism 7	GraphPad software	N/A
Living Image 2.5	Living Image 2.5	N/A
GSEA 4.3.1	GSEA software	https://www.gsea-msigdb.org/gsea/doc/GSEAUserGuideFrame.html
SynergyFinder (version 3.0)	Synergy Finder software	https://synergyfinder.fimm.fi/synergy/20230920124710012638/
Wave (version 2.2.0)	XF Software; Agilent	https://www.agilent.com/en/products/cell-analysis/software-download-for-wave-desktop
Kaluza (version 2.2)	Beckman Coulter	https://www.beckman.fr/flow cytometry/software/kaluza/downloads

RESOURCE AVAILABILITY

- Lead contact

Further information and requests for resources and reagents should be directed to and will be fulfilled by the lead contact, Manier.S (salomon.manier@inserm.fr).

- Materials availability

This study did not generate new unique reagents.

- Data and code availability

1. This paper analyzed existing, publicly available data. These accessions numbers and links were listed in methods details.
2. The RNA sequencing row data have been deposited in Gene Expression Omnibus under GEO: GSE241948.
3. Any additional information required to reanalyze the data reported in this work paper is available from the lead contact upon request.

EXPERIMENTAL MODEL AND STUDY PARTICIPANT DETAILS

Cell culture

All the cells used in this study are of human origin and were cultured in a humidified incubator at 37℃ and 5% CO2 atmosphere. U266, Loucy, KMS-12, MM1S, K562, MDAMB-231, NCIH-23, NCIH-1650 and NCIH-1473 were cultured in RPMI 1640 with GlutaMAX (Gibco, 61870010). Caki-2, WiDr cell lines were cultured in Dulbecco's modified Eagle's medium (DMEM) with GlutaMAX (Gibco, 31966021). Both mediums were supplied with 10% fetal bovine serum and 1% penicillin/streptomycin. For glutamine deprivations, all cell lines were cultured in glutamine-free RPMI (Gibco, 21870076) supplemented with 10% fetal bovine serum and 1% penicillin/streptomycin. MM1S luc/GFP cells were gifts from Dr. Ghobrial (Dana-Farber Cancer Institute) and cultured in RPMI 1640 with GlutaMAX (Gibco, 61870010) supplied with 10% fetal bovine serum and 1% penicillin/streptomycin before xenograft.

Mice

Animal experiments were conducted in accordance with the "Ministère de l'enseignement supérieur, de la recherche et de l'innovation" and European Animal Care guidelines (protocol no. 32950-2021060215277693 v9). Female SCID/CB.17 mice (n=6 per group) were obtained from Charles River Laboratories; mice were 6 weeks-old, 17–20 g. Mice were housed 4 per cage, with a 12-hour light/dark cycle and were allowed to access food and water. Mice were allowed to acclimatize for one week prior to the experiment.

Method Details

Small-molecule screen. U266/Ctrl and U266/MYC cells were treated with 1902 compounds purchased from Selleck Chemicals provided by ICCB-Longwood screening facility, Harvard Medical School. A microplate dispenser, Multidrop™ Combi (Thermo Fisher Scientific), was used to dispense 5,000 cells per well into 384-well microplates. Compounds were added using Seiko Compound Transfer Robot (SGM 611) (V&P Scientific, Inc., CA, USA) at 1µM final concentration. 48 hours post-treatment cytotoxicity was measured by CellTiter-Glo® Luminescent Cell Viability Assay (Promega) according to manufacturer's protocol and luminescence signals were read using EnVision (Perkin Elmer) plate reader.

Cell viability assay. Relative cell growth and survival were measured in 96-well microplate format by using CellTiter-Glo® Luminescent Cell Viability Assay or Caspase-Glo (Promega) as the end point. Cells were seeded at a density of 30.000 cell per well for suspension cells and 5.000 cell per well for adherent cells. Luminescence signals were detected using SpectraMAX. Drug sensitivity was then compared by calculating the IC_{50} values of used cell lines.

Protein and RNA isolation. Proteins were extracted from 2 x 10^6 to 3 x 10^6 cells, cells were pelleted at 300 x g for 5 minutes at room temperature. Pellets were washed with ice cold PBS then lysed using RIPA lysis buffer (Cell Signaling) supplemented with Phosphatase Inhibitor Cocktails (Santa Cruz Biotechnology). Lysates were centrifuged at 12000 x g for 15 minutes at 4 °C and supernatant was kept at -80 °C for further uses. Total RNA was isolated from cells using RNeasy Micro Kit (Qiagen) according to the manufacturer's instructions and evaluated for quantity and quality by NanoDrop spectrophotometer.

Western blot analysis. Protein concentration was measured using Pierce™ BCA Protein Assay Kit (Thermo Scientific) according to the manufacture protocol. For Western blot 80 µg of protein was electrophoresed on and subsequently blotted to nitrocellulose membrane. After blocking with 5% BSA (bovine serum albumin, Sigma-Aldrich) in TBST, blots were incubated with primary antibody overnight and subsequently incubated with secondary antibodies conjugated with horseradish peroxidase (HRP) for one hour. Primary antibody: antibody: anti-c-MYC (1:800), anti-GLS1 (1:800) (Cell Signaling Technology) and anti-GAPDH (1:1000, Santa Cruz). IgG HRP-linked; anti-rabbit (1:3000), anti-mouse (1:3000) (Cell Signaling) Signals were detected using SuperSignal™ West Femto Maximum Sensitivity Substrate (ThermoFisher scientific) and detected with LAS 4000 (GE-Healthcare).

Seahorse XF assay. Oxygen consumption rate and extracellular acidification rate (OCR and ECAR) measurements were performed using the XFe24 or XFe96 Extracellular Flux analyzer (Seahorse Bioscience, Billerica, MA, USA) with standard 24-well or 96-well Seahorse microplates. Briefly, XFe24 and XFe96 microplates were coated with poly lysin-D, 35µl (XFe24) or 15µl (XFe96) one day before seeding. At the day of the experiment, cells were treated with CB839 at 1 or 5µM for 4h, then resuspended in OXPHOS medium containing DMEM (D5030, Sigma-Aldrich), 25 mM glucose, 2 mM L-glutamine, and 1mM sodium pyruvate). Cells were seeded at 250.000/100µl.well^{-1} (XFe24 plate) or 75.000/50µl.well^{-1} (XFe96 plate). Cell plates were centrifuged twice at low speed (160g, 1 min) before incubated in a 37 °C/non-CO_2 incubator for at least 30 minutes to allow for temperature and pH equilibration prior to the start of an assay. Next, 400 µl (XFe24) or 100 µl (XFe96) of warm OXPHOS medium was added to each well of the cell plates. Based on the desired redout compounds were prepared at appropriate concentrations. A volume of 75 µl (XFe24) or 20 µl (XFe96) was added to each injection portals. XFe analyzer settings for OXPHOS measurement: Oligomycin (1 µM), FCCP (0.81-1.72), Antimycin A + Rotenone (1 µM). For the Glutamine oxidation, the assay medium was the base medium without any exogenous fuel substrate. 2mM of Glutamine was injected to initiate glutamine oxidation. CB-839 injection was included in this protocol at 1 or 5µM. For ECAR measurement, the assay medium consists of OXPHOS medium-glucose free. 10mM of glucose was injected to initiate glycolysis followed by Oligomycin (2µM) and then 100mM of 2-DG. OCR and ECAR were reported as absolute rates (pmol/min for OCR and mpH/min for ECAR). In all protocols Hoechst 33342 (Thermo Scientific) Fluorescent Stain was added to portal D at final concentration of 35mM. Metabolic rate was normalized to cell count and data was analyzed with the software Wave (version 2.2.0, Seahorse Bioscience) for further visual presence.

Mitochondrial superoxide membrane potential (ΔΨ) measurements. Cells were seeded in 6-well plates at a density of 0.9x106 cells/well; cells were exposed to single or combination drug treatments as indicated. After the indicated time of incubation, Cells were stained with MitoSOX™ Red Mitochondrial Superoxide Indicator (2.5µM) (CAT No: M36008, Thermo Fisher) and SYTOX blue (1µM) (S34857, Thermo Fisher) to measure mitochondrial reactive oxygen species. To measure mitochondrial membrane potential, we used tetramethylrhodamine ethyl ester TMRE (200nM) (ab113852, Abcam). Labeling was done according to the manufacturer's instructions. Fluorescence intensity was measured by flow cytometry. Experiments were performed in triplicate. The results were processed using Kaluza software 2.2 (Beckman Coulter).

CE-MS spectrometry. For the metabolome analysis, U266/Ctrl and U266/MYC cell lines treated with CB-839 1μM for 48h were prepared in triplicates. The absolute concentration of 116 metabolites was measured using capillary electrophoresis mass spectrometry (CE-TOFMS and CE-QqQMS) in the cation and anion analysis modes for analyzing cationic and anionic metabolites, respectively by the metabolome analysis package Carcinoscope provided by Human Metabolome Technologies (HMT). Samples were prepared following HMT's Sample Preparation Protocol. Briefly, (6×10^6 cells/sample) was used for the extraction of intracellular metabolites. Cells were collected from 100mm plate and washed twice using washing solution (5% mannitol). The cells were then treated with 800 μL of methanol and vortex for 30 s in order to inactivate the enzymes. Next, the cell extract was treated with 550 μL of Milli-Q water containing internal standard (H3304-1002, Human Metabolome Technologies, Inc., Tsuruoka, Japan) and vortex for another 30 s. The extract was obtained and centrifuged at 2300 × g and 4 °C for 5 min and then 350 μL of upper aqueous layer was centrifugally filtered through a pre-washed ULTRAFREE MC PLHCC centrifugal filter units (provided by HMT) at 9100 × g and 4 °C for 90 min. Samples were evaporated under vacuum conditions at room temperature 1500 rpm, 1000 Pa, 2–3 h (until no liquid remains in the filter cup).

Lentiviral infection and GLS1 knockdown. To generate cells stably overexpress *MYC*, U266 and Loucy cell lines were transduced with EF1A-C-MYC (PLV-10010-50, Cellomics Technology, LLC) or EF1A-Vector Control lentivirus (PLV-10074-50, Cellomics Technology, LLC). Cells were plated at 50.000 cell per well and transduced over 8 hours at a multiplicity of infection (MOI) 10 in a growth media supplemented with 2 μg/mL Polybrene (Santa Cruz). After 72 hours, cells were selected in medium containing Puromycin (InvivoGen). Inducible lentiviruse short hairpin RNA (shRNA) encoding shRNA targeting GLS1 were purchased from FenicsBIO: shGLS1-1 (tet,Hyg): ATAGGATATTACTTAAAAGAAA; shGLS1-2 (tet,Hyg): TGCTAGACAAAGATCTTTTTAA; control shRNA (tet,Hyg) (SH-tet-C02). After 72 h, cells were selected in medium containing Hygromycin (InvivoGen). Doxycycline (MedChemExpress) was used to induce shRNA expression.

In silico. Searching for vulnerabilities associated with MYC overexpression in MM we performed in silico analyses based on a Genome-scale pooled shRNA screens (Achilles) to identify genes essential for the proliferation of 236 cancer cell lines. These screens were performed using a lentivirally delivered pool of 50,529 shRNAs targeting 9273 genes. We correlated the shRNA sensitivity profile with MYC expression values across the 236 cell lines from CCLE database (Affymetrix U133+2 expression array). Each data point represents the abundance of one shRNA construct within one cell line as compared with the initial abundance

of that shRNA construct in the initial plasmid DNA pool. To define MYC gene signature we used a subgroup of genes regulated by MYC identified as hallmark_MYC_targets_v2 (https://www.gsea-msigdb.org/gsea/msigdb/cards/HALLMARK_MYC_TARGETS_V2).

RNA-Sequencing. Total RNA was isolated from U266/Control and U266/MYC cells using RNeasy Mini Kit (Qiagen) according to manufacturer's protocol and evaluated for quantity and quality by NanoDrop spectrophotometer. A starting amount of 500 ng of RNA was used to prepare poly-A enriched, single barcoded libraries using the NEBNext® Ultra™ RNA Library Prep Kit (New England Biolabs). Quality control of the libraries was evaluated by Bioanalyzer analysis with High Sensitivity chips (Agilent Technologies). Sequencing was performed on a HiSeq 4000 (Illumina, CA, USA) by 2 X 50 bp paired end reads at the Biopolymers Facility of Harvard Medical School. We used Bcbio_nextgen (https://github.com/chapmanb/bcbio-nextgen/) to process the RNA-seq data. Briefly, cutadapt (https://github.com/marcelm/cutadapt/) was used to trim adapters; trimmed reads were aligned to Human reference genome (GRCh37) with tophat2; read count for each gene was calculated by HT-seq. Genes with low expression (TPM < 1 across all samples) were filtered out. The RNA-seq data are available in the Gene Expression Omnibus (GEO) under the accession number GSE241948. Gene set enrichment analysis (GSEA) was used to identify significantly enriched pathways, with false discovery rate (FDR) < 0.25 and p value < 0.05. Gene sets were downloaded from the Broad Institute's MSigDB (http://www.broadinstitute.org/gsea/index.jsp).

TMT spectrometry. Quantitative proteomic analysis was performed by Tandem Mass Tag (TMT) (Thermo Fisher Scientific, MA, USA) as per manufacturer protocol, with mass spectrometry (MS).

In vivo study. Female SCID/CB.17 mice (n=6 per group) (Charles River Laboratories; 6 weeks-old, 17–20 g) implanted with MM.1S-GFP-Luc$^+$ cells (5 x 10^6 cells injected intravenously). After engraftment, the mice were randomly assigned into four groups based on BLI values and treated with vehicle control, 200 mg/kg CB-839 prepared in [25% (w/v) hydroxypropyl-b-cyclodextrin (HPBCD; MedChemExpress) in 10 mmol/L citrate (Sigma-Aldrich), pH 2 (p.o., b.i.d.)]. 10 mg/kg FK-866 prepared in 20% (w/v) hydroxypropyl-b-cyclodextrin (HPBCD; MedChemExpress) in saline (Aguettant) administrated by intraperitoneal injection twice daily for 4 days, repeated for two weeks followed by single IP injection daily for 4 days weekly repeated over the indicated times or a combination of CB-839 and FK-866 in which each compound was administrated at the same dose and scheduled as single agents. For BLI, mice were injected with 150 mg/kg of D-Luciferin (PerkinElmer),

intraperitoneally. After 5 minutes, mice were anesthetized with 2% isoflurane for 5 more minutes; then they were transferred to the chamber of Xenogen IVIS 50 BLI system (Caliper Life Science), placed with their abdomen toward the camera, and imaged on auto exposure. Using Living Image 2.5 software, regions of interest (ROI) were identified around the tumor and relative photon emission (in photons per second per square centimeter per steradian ($p/s/cm^2/sr$)) of the tumor was measured.

QUANTIFICATION AND STATISTICAL ANALYSIS

Data are reported as means ± SEM of at least three independent experiments, and multiple-group comparisons were performed using one-way analysis of variance (ANOVA) with Tukey's correction unless otherwise stated. GraphPad Prism 7 (GraphPad Software Inc.) and Microsoft Excel were used to generate graphs and statistical analysis. $*P < 0.05$, $**P < 0.01$, $***P < 0.001$. Patients' expression profiles from (MMRF-CoMMpass (https://portal.gdc.cancer.gov/projects/MMRF-COMMPASS), (GSE4452)) with the highest and lowest MYC expression were selected. Hem cell lines (n=169) from CCLE were grouped into MYC high and MYC low groups based on the MYC expression above or below the mean value. GSEA was performed as described previously using GSEA 4.3.1 (https://www.gsea-msigdb.org/gsea/doc/GSEAUserGuideFrame.html). Different gene sets were tested for their enrichment in patient datasets, CCLE as well as U266/Ctrl versus U266/MYC. Gene sets with significant enrichment in MYC OE cells or patients by GSEA were selected on the basis of $P < 0.05$ and q value < 0.25. For the generation of synergy maps, SynergyFinder (version 3.0) was used, testing was performed using drug-response matrices. Synergy scores were then calculated using Zero Interaction Potency (ZIP) reference model. Based on the algorithm, synergy scores of >10 were considered synergistic, while scores < -10 were considered antagonistic and scores between -10 and 10 were considered additive. Overall survival was analyzed by Kaplan-Meier curve, and statistical significance was determined by the log-rank test with Bonferroni's correction.

References

1. Palumbo, A., and Anderson, K. (2011). Multiple Myeloma. N. Engl. J. Med. 364, 1046–1060. 10.1056/NEJMra1011442.

2. Landgren, O., Kyle, R.A., Pfeiffer, R.M., Katzmann, J.A., Caporaso, N.E., Hayes, R.B., Dispenzieri, A., Kumar, S., Clark, R.J., Baris, D., et al. (2009). Monoclonal

gammopathy of undetermined significance (MGUS) consistently precedes multiple myeloma: a prospective study. Blood 113, 5412–5417. 10.1182/blood-2008-12-194241.

3. Weiss, B.M., Abadie, J., Verma, P., Howard, R.S., and Kuehl, W.M. (2009). A monoclonal gammopathy precedes multiple myeloma in most patients. Blood 113, 5418–5422. 10.1182/blood-2008-12-195008.

4. Manier, S., Salem, K.Z., Park, J., Landau, D.A., Getz, G., and Ghobrial, I.M. (2017). Genomic complexity of multiple myeloma and its clinical implications. Nat. Rev. Clin. Oncol. 14, 100–113. 10.1038/nrclinonc.2016.122.

5. Kuehl, W.M., and Bergsagel, P.L. (2002). Multiple myeloma: evolving genetic events and host interactions. Nat. Rev. Cancer 2, 175–187. 10.1038/nrc746.

6. Chng, W.-J., Huang, G.F., Chung, T.H., Ng, S.B., Gonzalez-Paz, N., Troska-Price, T., Mulligan, G., Chesi, M., Bergsagel, P.L., and Fonseca, R. (2011). Clinical and biological implications of MYC activation: a common difference between MGUS and newly diagnosed multiple myeloma. Leukemia 25, 1026–1035. 10.1038/leu.2011.53.

7. Hideshima, T., Mitsiades, C., Tonon, G., Richardson, P.G., and Anderson, K.C. (2007). Understanding multiple myeloma pathogenesis in the bone marrow to identify new therapeutic targets. Nat. Rev. Cancer 7, 585–598. 10.1038/nrc2189.

8. Shou, Y., Martelli, M.L., Gabrea, A., Qi, Y., Brents, L.A., Roschke, A., Dewald, G., Kirsch, I.R., Bergsagel, P.L., and Kuehl, W.M. (2000). Diverse karyotypic abnormalities of the c -myc locus associated with c -myc dysregulation and tumor progression in multiple myeloma. Proc. Natl. Acad. Sci. 97, 228–233. 10.1073/pnas.97.1.228.

9. Affer, M., Chesi, M., Chen, W.D., Keats, J.J., Demchenko, Y.N., Tamizhmani, K., Garbitt, V.M., Riggs, D.L., Brents, L.A., Roschke, A.V., et al. (2014). Promiscuous MYC locus rearrangements hijack enhancers but mostly super-enhancers to dysregulate MYC expression in multiple myeloma. Leukemia 28, 1725–1735. 10.1038/leu.2014.70.

10. Allevato, M., Bolotin, E., Grossman, M., Mane-Padros, D., Sladek, F.M., and Martinez, E. (2017). Sequence-specific DNA binding by MYC/MAX to low-affinity non-E-box motifs. PLOS ONE 12, e0180147. 10.1371/journal.pone.0180147.

11. Dang, C.V., O'Donnell, K.A., Zeller, K.I., Nguyen, T., Osthus, R.C., and Li, F. (2006). The c-Myc target gene network. Semin. Cancer Biol. 16, 253–264. 10.1016/j.semcancer.2006.07.014.

12. Chen, H., Liu, H., and Qing, G. (2018). Targeting oncogenic Myc as a strategy for cancer treatment. Signal Transduct. Target. Ther. 3, 5. 10.1038/s41392-018-0008-7.

13. Rajagopalan, K.N., and DeBerardinis, R.J. (2011). Role of Glutamine in Cancer: Therapeutic and Imaging Implications: FIGURE 1. J. Nucl. Med. 52, 1005–1008. 10.2967/jnumed.110.084244.

14. DeBerardinis, R.J., and Cheng, T. (2010). Q's next: the diverse functions of glutamine in metabolism, cell biology and cancer. Oncogene 29, 313–324. 10.1038/onc.2009.358.

15. Revollo, J.R., Grimm, A.A., and Imai, S. (2004). The NAD Biosynthesis Pathway Mediated by Nicotinamide Phosphoribosyltransferase Regulates Sir2 Activity in Mammalian Cells. J. Biol. Chem. 279, 50754–50763. 10.1074/jbc.M408388200.

16. Liberzon, A., Birger, C., Thorvaldsdóttir, H., Ghandi, M., Mesirov, J.P., and Tamayo, P. (2015). The Molecular Signatures Database Hallmark Gene Set Collection. Cell Syst. 1, 417–425. 10.1016/j.cels.2015.12.004.

17. Schlosser, I. (2003). A role for c-Myc in the regulation of ribosomal RNA processing. Nucleic Acids Res. 31, 6148–6156. 10.1093/nar/gkg794.

18. Van Riggelen, J., Yetil, A., and Felsher, D.W. (2010). MYC as a regulator of ribosome biogenesis and protein synthesis. Nat. Rev. Cancer 10, 301–309. 10.1038/nrc2819.

19. Schmidt, E.V. (2004). The role of c-myc in regulation of translation initiation. Oncogene 23, 3217–3221. 10.1038/sj.onc.1207548.

20. Manier, S., Huynh, D., Shen, Y.J., Zhou, J., Yusufzai, T., Salem, K.Z., Ebright, R.Y., Shi, J., Park, J., Glavey, S.V., et al. (2017). Inhibiting the oncogenic translation program is an effective therapeutic strategy in multiple myeloma. Sci. Transl. Med. 9, eaal2668. 10.1126/scitranslmed.aal2668.

21. Tambay, V., Raymond, V.-A., and Bilodeau, M. (2021). MYC Rules: Leading Glutamine Metabolism toward a Distinct Cancer Cell Phenotype. Cancers 13, 4484. 10.3390/cancers13174484.

22. Lu, S.C. (2009). Regulation of glutathione synthesis. Mol. Aspects Med. 30, 42–59. 10.1016/j.mam.2008.05.005.

23. Yang, D., Liu, H., Goga, A., Kim, S., Yuneva, M., and Bishop, J.M. (2010). Therapeutic potential of a synthetic lethal interaction between the MYC proto-oncogene and inhibition of aurora-B kinase. Proc. Natl. Acad. Sci. 107, 13836–13841. 10.1073/pnas.1008366107.

24. Pourdehnad, M., Truitt, M.L., Siddiqi, I.N., Ducker, G.S., Shokat, K.M., and Ruggero, D. (2013). Myc and mTOR converge on a common node in protein synthesis control

that confers synthetic lethality in Myc-driven cancers. Proc. Natl. Acad. Sci. 110, 11988–11993. 10.1073/pnas.1310230110.

25. Stein, L.R., and Imai, S. (2012). The dynamic regulation of NAD metabolism in mitochondria. Trends Endocrinol. Metab. 23, 420–428. 10.1016/j.tem.2012.06.005.

26. Garten, A., Schuster, S., Penke, M., Gorski, T., de Giorgis, T., and Kiess, W. (2015). Physiological and pathophysiological roles of NAMPT and NAD metabolism. Nat. Rev. Endocrinol. 11, 535–546. 10.1038/nrendo.2015.117.

27. Hong, S.M., Park, C.W., Kim, S.W., Nam, Y.J., Yu, J.H., Shin, J.H., Yun, C.H., Im, S.-H., Kim, K.-T., Sung, Y.C., et al. (2016). NAMPT suppresses glucose deprivation-induced oxidative stress by increasing NADPH levels in breast cancer. Oncogene 35, 3544–3554. 10.1038/onc.2015.415.

28. Heske, C.M. (2020). Beyond Energy Metabolism: Exploiting the Additional Roles of NAMPT for Cancer Therapy. Front. Oncol. 9, 1514. 10.3389/fonc.2019.01514.

29. Thompson, R.M., Dytfeld, D., Reyes, L., Robinson, R.M., Smith, B., Manevich, Y., Jakubowiak, A., Komarnicki, M., Przybylowicz-Chalecka, A., Szczepaniak, T., et al. (2017). Glutaminase inhibitor CB-839 synergizes with carfilzomib in resistant multiple myeloma cells. Oncotarget 8, 35863–35876. 10.18632/oncotarget.16262.

30. Llombart, V., and Mansour, M.R. (2022). Therapeutic targeting of "undruggable" MYC. eBioMedicine 75, 103756. 10.1016/j.ebiom.2021.103756.

31. Allen-Petersen, B.L., and Sears, R.C. (2019). Mission Possible: Advances in MYC Therapeutic Targeting in Cancer. BioDrugs 33, 539–553. 10.1007/s40259-019-00370-5.

32. Ba, M., Long, H., Yan, Z., Wang, S., Wu, Y., Tu, Y., Gong, Y., and Cui, S. (2018). BRD4 promotes gastric cancer progression through the transcriptional and epigenetic regulation of c-MYC. J. Cell. Biochem. 119, 973–982. 10.1002/jcb.26264.

33. Constantin, T.A., Greenland, K.K., Varela-Carver, A., and Bevan, C.L. (2022). Transcription associated cyclin-dependent kinases as therapeutic targets for prostate cancer. Oncogene 41, 3303–3315. 10.1038/s41388-022-02347-1.

34. Viswanathan, S.R., Powers, J.T., Einhorn, W., Hoshida, Y., Ng, T.L., Toffanin, S., O'Sullivan, M., Lu, J., Phillips, L.A., Lockhart, V.L., et al. (2009). Lin28 promotes transformation and is associated with advanced human malignancies. Nat. Genet. 41, 843–848. 10.1038/ng.392.

35. Delmore, J.E., Issa, G.C., Lemieux, M.E., Rahl, P.B., Shi, J., Jacobs, H.M., Kastritis, E., Gilpatrick, T., Paranal, R.M., Qi, J., et al. (2011). BET Bromodomain Inhibition as a Therapeutic Strategy to Target c-Myc. Cell 146, 904–917. 10.1016/j.cell.2011.08.017.

36. Mazur, P.K., Herner, A., Mello, S.S., Wirth, M., Hausmann, S., Sánchez-Rivera, F.J., Lofgren, S.M., Kuschma, T., Hahn, S.A., Vangala, D., et al. (2015). Combined inhibition of BET family proteins and histone deacetylases as a potential epigenetics-based therapy for pancreatic ductal adenocarcinoma. Nat. Med. 21, 1163–1171. 10.1038/nm.3952.

37. Effenberger, M., Bommert, K.S., Kunz, V., Kruk, J., Leich, E., Rudelius, M., Bargou, R., and Bommert, K. (2017). Glutaminase inhibition in multiple myeloma induces apoptosis via MYC degradation. Oncotarget 8, 85858–85867. 10.18632/oncotarget.20691.

38. Wise, D.R., DeBerardinis, R.J., Mancuso, A., Sayed, N., Zhang, X.-Y., Pfeiffer, H.K., Nissim, I., Daikhin, E., Yudkoff, M., McMahon, S.B., et al. (2008). Myc regulates a transcriptional program that stimulates mitochondrial glutaminolysis and leads to glutamine addiction. Proc. Natl. Acad. Sci. 105, 18782–18787. 10.1073/pnas.0810199105.

39. Gao, P., Tchernyshyov, I., Chang, T.-C., Lee, Y.-S., Kita, K., Ochi, T., Zeller, K.I., De Marzo, A.M., Van Eyk, J.E., Mendell, J.T., et al. (2009). c-Myc suppression of miR-23a/b enhances mitochondrial glutaminase expression and glutamine metabolism. Nature 458, 762–765. 10.1038/nature07823.

40. Gross, M.I., Demo, S.D., Dennison, J.B., Chen, L., Chernov-Rogan, T., Goyal, B., Janes, J.R., Laidig, G.J., Lewis, E.R., Li, J., et al. (2014). Antitumor Activity of the Glutaminase Inhibitor CB-839 in Triple-Negative Breast Cancer. Mol. Cancer Ther. 13, 890–901. 10.1158/1535-7163.MCT-13-0870.

41. Galan-Cobo, A., Sitthideatphaiboon, P., Qu, X., Poteete, A., Pisegna, M.A., Tong, P., Chen, P.-H., Boroughs, L.K., Rodriguez, M.L.M., Zhang, W., et al. (2019). LKB1 and KEAP1/NRF2 Pathways Cooperatively Promote Metabolic Reprogramming with Enhanced Glutamine Dependence in KRAS -Mutant Lung Adenocarcinoma. Cancer Res. 79, 3251–3267. 10.1158/0008-5472.CAN-18-3527.

42. Jacque, N., Ronchetti, A.M., Larrue, C., Meunier, G., Birsen, R., Willems, L., Saland, E., Decroocq, J., Maciel, T.T., Lambert, M., et al. (2015). Targeting glutaminolysis has antileukemic activity in acute myeloid leukemia and synergizes with BCL-2 inhibition. Blood 126, 1346–1356. 10.1182/blood-2015-01-621870.

43. Matre, P., Velez, J., Jacamo, R., Qi, Y., Su, X., Cai, T., Chan, S.M., Lodi, A., Sweeney, S.R., Ma, H., et al. (2016). Inhibiting glutaminase in acute myeloid leukemia: metabolic dependency of selected AML subtypes. Oncotarget 7, 79722–79735. 10.18632/oncotarget.12944.

44. Gonsalves, W.I., Jang, J.S., Jessen, E., Hitosugi, T., Evans, L.A., Jevremovic, D., Pettersson, X.-M., Bush, A.G., Gransee, J., Anderson, E.I., et al. (2020). In vivo assessment

of glutamine anaplerosis into the TCA cycle in human pre-malignant and malignant clonal plasma cells. Cancer Metab. 8, 29. 10.1186/s40170-020-00235-4.

45. Bolzoni, M., Chiu, M., Accardi, F., Vescovini, R., Airoldi, I., Storti, P., Todoerti, K., Agnelli, L., Missale, G., Andreoli, R., et al. (2016). Dependence on glutamine uptake and glutamine addiction characterize myeloma cells: a new attractive target. Blood 128, 667–679. 10.1182/blood-2016-01-690743.

46. Muir, A., Danai, L.V., Gui, D.Y., Waingarten, C.Y., Lewis, C.A., and Vander Heiden, M.G. (2017). Environmental cystine drives glutamine anaplerosis and sensitizes cancer cells to glutaminase inhibition. eLife 6, e27713. 10.7554/eLife.27713.

47. Jin, H., Wang, S., Zaal, E.A., Wang, C., Wu, H., Bosma, A., Jochems, F., Isima, N., Jin, G., Lieftink, C., et al. (2020). A powerful drug combination strategy targeting glutamine addiction for the treatment of human liver cancer. eLife 9, e56749. 10.7554/eLife.56749.

48. Sayin, V.I., LeBoeuf, S.E., Singh, S.X., Davidson, S.M., Biancur, D., Guzelhan, B.S., Alvarez, S.W., Wu, W.L., Karakousi, T.R., Zavitsanou, A.M., et al. (2017). Activation of the NRF2 antioxidant program generates an imbalance in central carbon metabolism in cancer. eLife 6, e28083. 10.7554/eLife.28083.

49. Varghese, S., Pramanik, S., Williams, L.J., Hodges, H.R., Hudgens, C.W., Fischer, G.M., Luo, C.K., Knighton, B., Tan, L., Lorenzi, P.L., et al. (2021). The Glutaminase Inhibitor CB-839 (Telaglenastat) Enhances the Antimelanoma Activity of T-Cell–Mediated Immunotherapies. Mol. Cancer Ther. 20, 500–511. 10.1158/1535-7163.MCT-20-0430.

50. Momcilovic, M., Bailey, S.T., Lee, J.T., Fishbein, M.C., Braas, D., Go, J., Graeber, T.G., Parlati, F., Demo, S., Li, R., et al. (2018). The GSK3 Signaling Axis Regulates Adaptive Glutamine Metabolism in Lung Squamous Cell Carcinoma. Cancer Cell 33, 905-921.e5. 10.1016/j.ccell.2018.04.002.

51. Hasmann, M., and Schemainda, I. (2003). FK866, a highly specific noncompetitive inhibitor of nicotinamide phosphoribosyltransferase, represents a novel mechanism for induction of tumor cell apoptosis. Cancer Res. 63, 7436–7442.

52. Nahimana, A., Attinger, A., Aubry, D., Greaney, P., Ireson, C., Thougaard, A.V., Tjørnelund, J., Dawson, K.M., Dupuis, M., and Duchosal, M.A. (2009). The NAD biosynthesis inhibitor APO866 has potent antitumor activity against hematologic malignancies. Blood 113, 3276–3286. 10.1182/blood-2008-08-173369.

53. Olesen, U.H., Thougaard, A.V., Jensen, P.B., and Sehested, M. (2010). A Preclinical Study on the Rescue of Normal Tissue by Nicotinic Acid in High-Dose Treatment

with APO866, a Specific Nicotinamide Phosphoribosyltransferase Inhibitor. Mol. Cancer Ther. 9, 1609–1617. 10.1158/1535-7163.MCT-09-1130.

54. Billington, R.A., Genazzani, A.A., Travelli, C., and Condorelli, F. (2008). NAD depletion by FK866 induces autophagy. Autophagy 4, 385–387. 10.4161/auto.5635.

55. Pogrebniak, A., Schemainda, I., Azzam, K., Pelka-Fleischer, R., Nüssler, V., and Hasmann, M. (2006). Chemopotentiating effects of a novel nad biosynthesis inhibitor, fk866, in combination with antineoplastic agents. Eur. J. Med. Res.

56. Tan, B., Young, D.A., Lu, Z.-H., Wang, T., Meier, T.I., Shepard, R.L., Roth, K., Zhai, Y., Huss, K., Kuo, M.-S., et al. (2013). Pharmacological Inhibition of Nicotinamide Phosphoribosyltransferase (NAMPT), an Enzyme Essential for NAD+ Biosynthesis, in Human Cancer Cells. J. Biol. Chem. 288, 3500–3511. 10.1074/jbc.M112.394510.

Figures

Figure 1

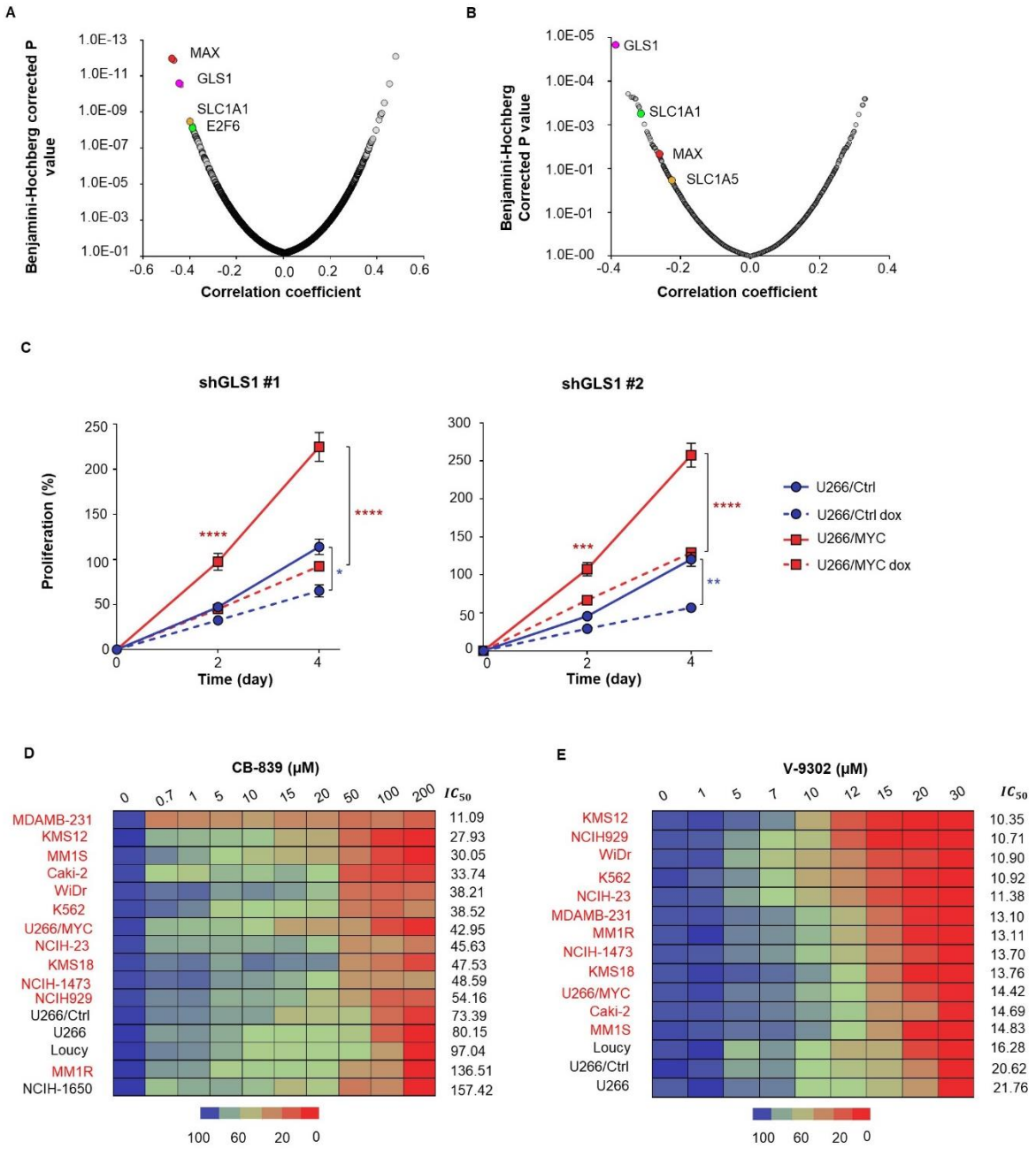

Figure 2

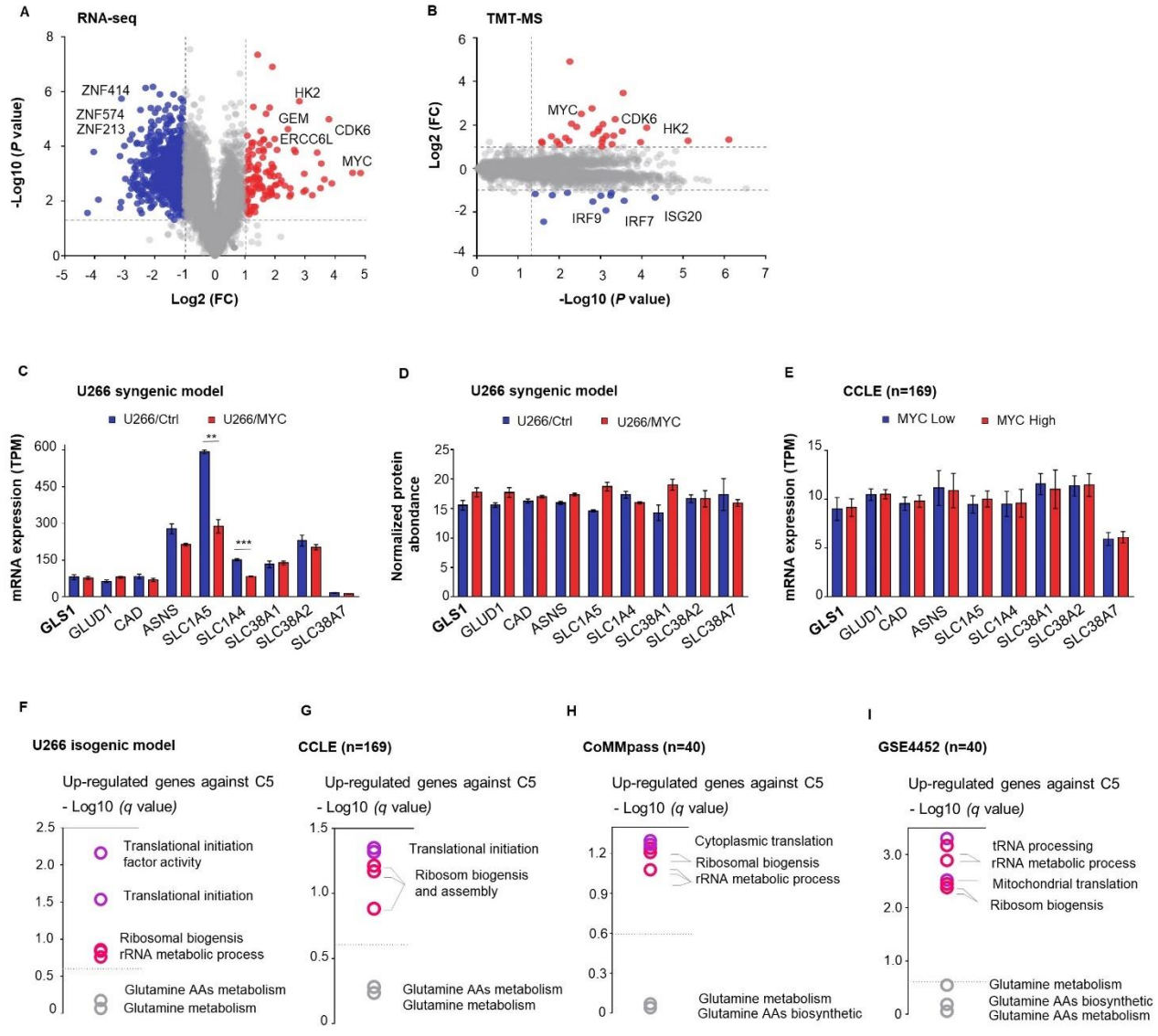
A
RNA-seq
-Log10 (P value)
Log2 (FC)
ZNF414
ZNF574
ZNF213
HK2
GEM
ERCC6L
CDK6
MYC
B
TMT-MS
Log2 (FC)
-Log10 (P value)
MYC
CDK6
HK2
IRF9
IRF7
ISG20
C
U266 syngenic model
U266/Ctrl
U266/MYC
mRNA expression (TPM)
GLS1
GLUD1
CAD
ASNS
SLC1A5
SLC1A4
SLC38A1
SLC38A2
SLC38A7
D
U266 syngenic model
U266/Ctrl
U266/MYC
Normalized protein abondance
E
CCLE (n=169)
MYC Low
MYC High
mRNA expression (TPM)
F
U266 isogenic model
Up-regulated genes against C5
- Log10 (q value)
Translational initiation factor activity
Translational initiation
Ribosomal biogensis rRNA metabolic process
Glutamine AAs metabolism
Glutamine metabolism
G
CCLE (n=169)
Up-regulated genes against C5
- Log10 (q value)
Translational initiation
Ribosom biogensis and assembly
Glutamine AAs metabolism
Glutamine metabolism
H
CoMMpass (n=40)
Up-regulated genes against C5
- Log10 (q value)
Cytoplasmic translation
Ribosomal biogensis
rRNA metabolic process
Glutamine metabolism
Glutamine AAs biosynthetic
I
GSE4452 (n=40)
Up-regulated genes against C5
- Log10 (q value)
tRNA processing
rRNA metabolic process
Mitochondrial translation
Ribosom biogensis
Glutamine metabolism
Glutamine AAs biosynthetic
Glutamine AAs metabolism

Figure 3

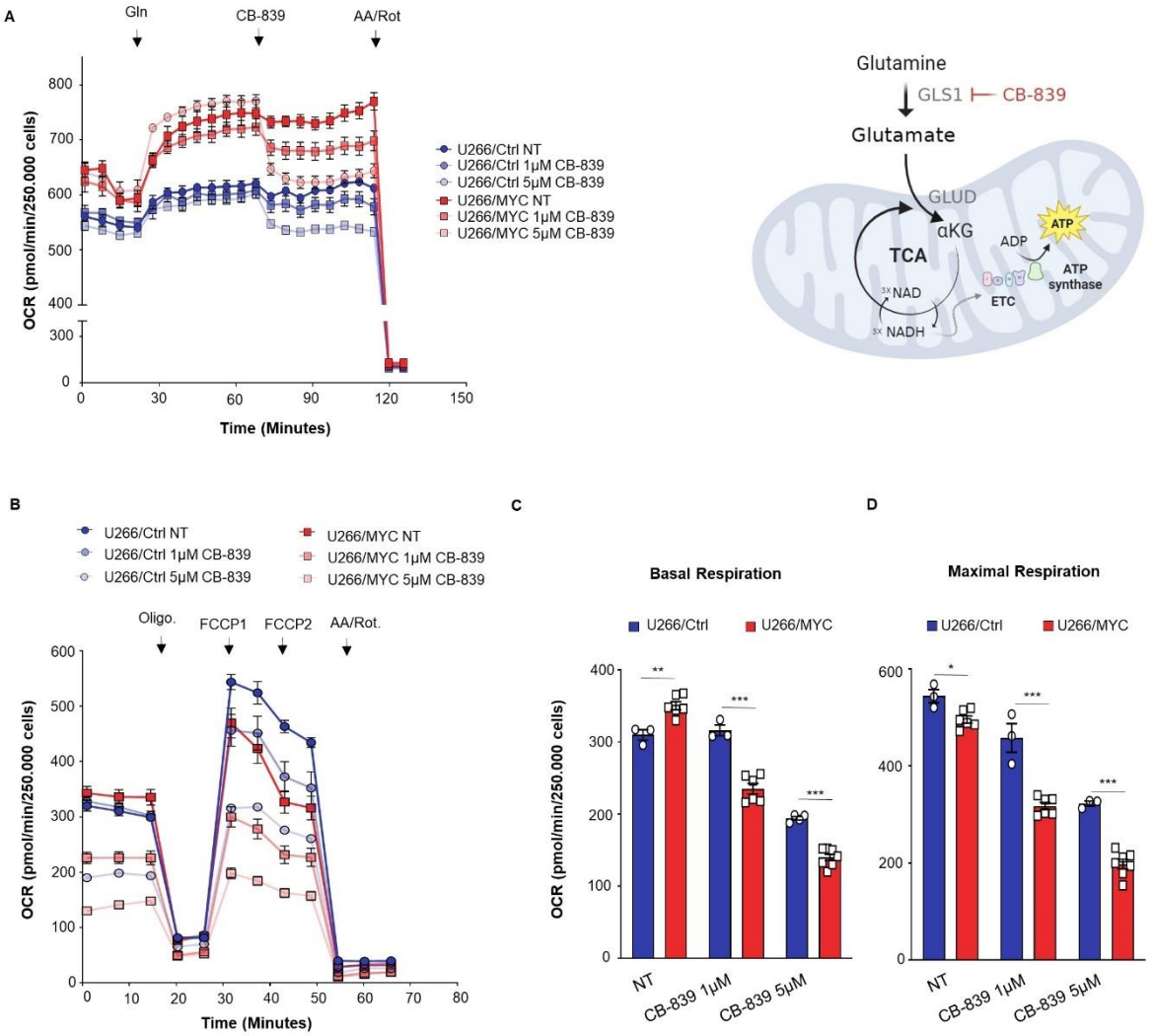
A
Gln
CB-839
AA/Rot
OCR (pmol/min/250.000 cells)
Time (Minutes)
U266/Ctrl NT
U266/Ctrl 1μM CB-839
U266/Ctrl 5μM CB-839
U266/MYC NT
U266/MYC 1μM CB-839
U266/MYC 5μM CB-839
Glutamine
GLS1
CB-839
Glutamate
GLUD
αKG
TCA
ADP
ATP
ATP synthase
ETC
3X NAD
3X NADH
B
Oligo.
FCCP1
FCCP2
AA/Rot.
C
Basal Respiration
D
Maximal Respiration
NT
CB-839 1μM
CB-839 5μM

Figure 4

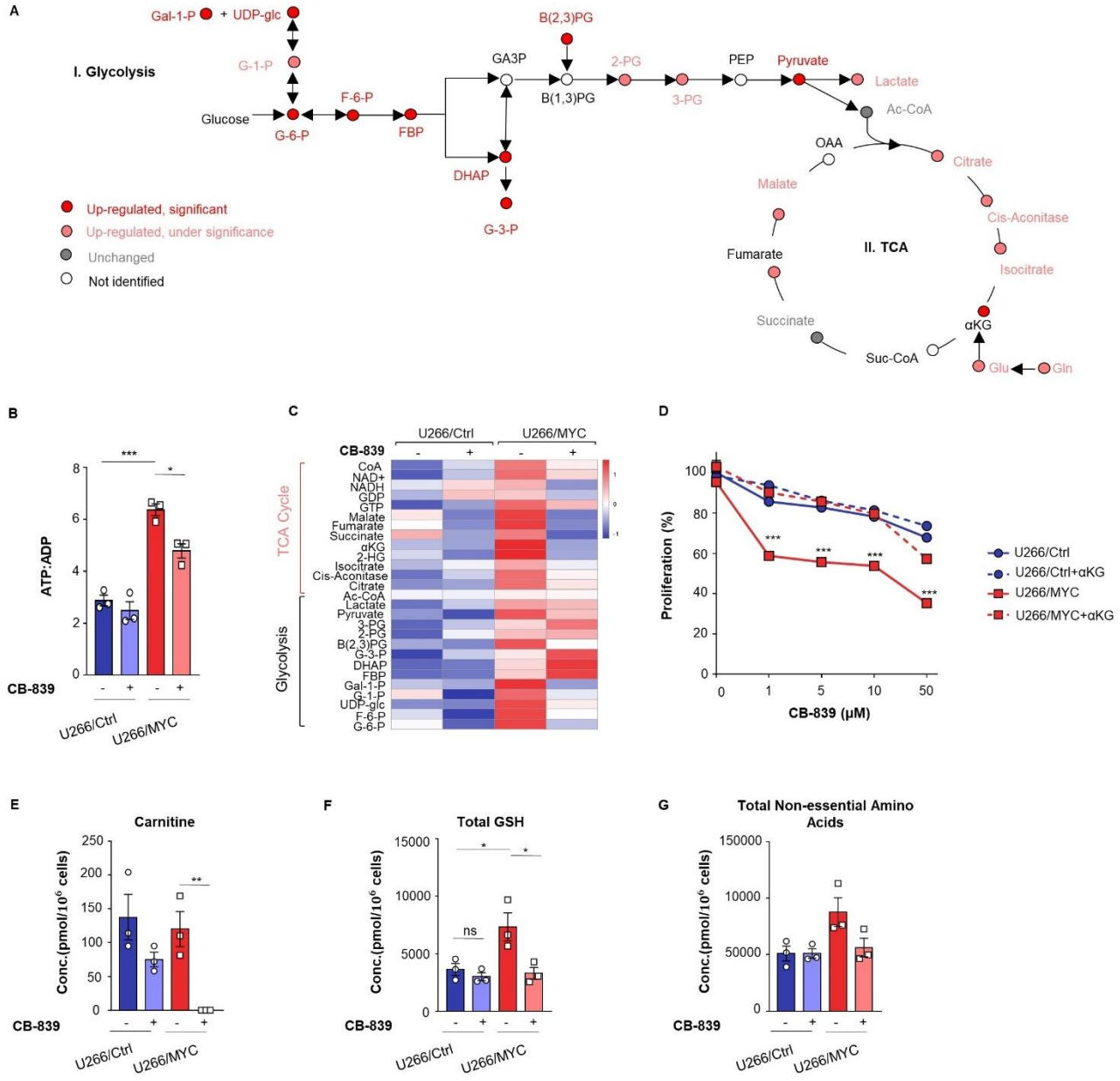
A
Gal-1-P
+ UDP-glc
G-1-P
I. Glycolysis
Glucose
G-6-P
F-6-P
FBP
DHAP
G-3-P
GA3P
B(2,3)PG
B(1,3)PG
2-PG
3-PG
PEP
Pyruvate
Lactate
Ac-CoA
OAA
Citrate
Cis-Aconitase
Isocitrate
αKG
Glu
Gln
Suc-CoA
Succinate
Fumarate
Malate
II. TCA
Up-regulated, significant
Up-regulated, under significance
Unchanged
Not identified
B
ATP:ADP
CB-839
U266/Ctrl
U266/MYC
C
U266/Ctrl
U266/MYC
CB-839
TCA Cycle
Glycolysis
CoA
NAD+
NADH
GDP
GTP
Malate
Fumarate
Succinate
αKG
2-HG
Isocitrate
Cis-Aconitase
Citrate
Ac-CoA
Lactate
Pyruvate
3-PG
2-PG
B(2,3)PG
G-3-P
DHAP
FBP
Gal-1-P
G-1-P
UDP-glc
F-6-P
G-6-P
D
Proliferation (%)
CB-839 (μM)
U266/Ctrl
U266/Ctrl+αKG
U266/MYC
U266/MYC+αKG
E
Carnitine
Conc.(pmol/10^6 cells)
CB-839
U266/Ctrl
U266/MYC
F
Total GSH
Conc.(pmol/10^6 cells)
ns
CB-839
U266/Ctrl
U266/MYC
G
Total Non-essential Amino Acids
Conc.(pmol/10^6 cells)
CB-839
U266/Ctrl
U266/MYC

Figure 5

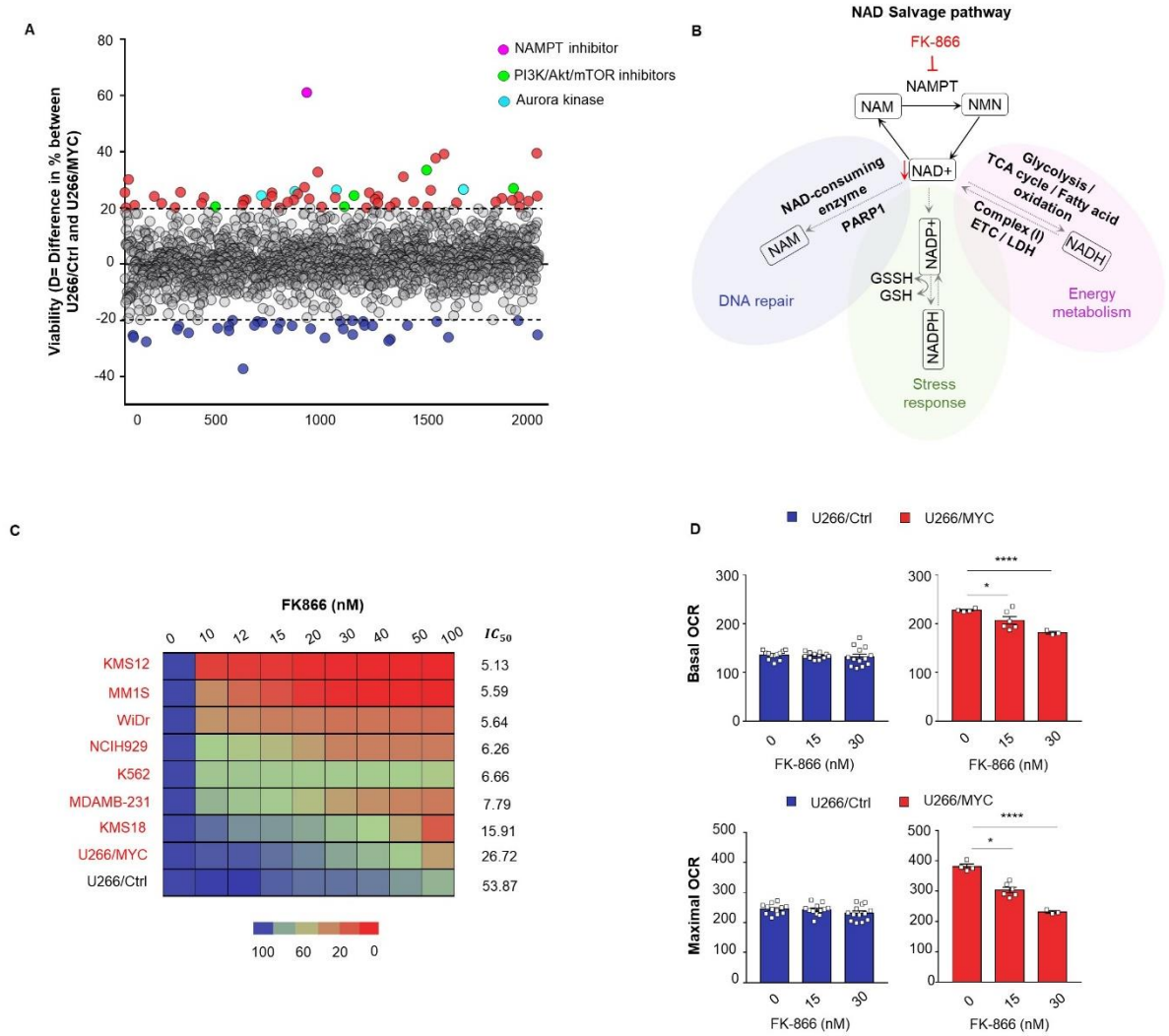
A
Viability (D= Difference in % between U266/Ctrl and U266/MYC)
NAMPT inhibitor
PI3K/Akt/mTOR inhibitors
Aurora kinase
B
NAD Salvage pathway
FK-866
NAMPT
NAM
NMN
NAD+
NAD-consuming enzyme
PARP1
Glycolysis / TCA cycle / Fatty acid oxidation
Complex (I) ETC / LDH
NADH
NADP+
GSSH
GSH
NADPH
DNA repair
Energy metabolism
Stress response
C
FK866 (nM)
IC50
KMS12 5.13
MM1S 5.59
WiDr 5.64
NCIH929 6.26
K562 6.66
MDAMB-231 7.79
KMS18 15.91
U266/MYC 26.72
U266/Ctrl 53.87
D
U266/Ctrl
U266/MYC
Basal OCR
Maximal OCR
FK-866 (nM)

Figure 6

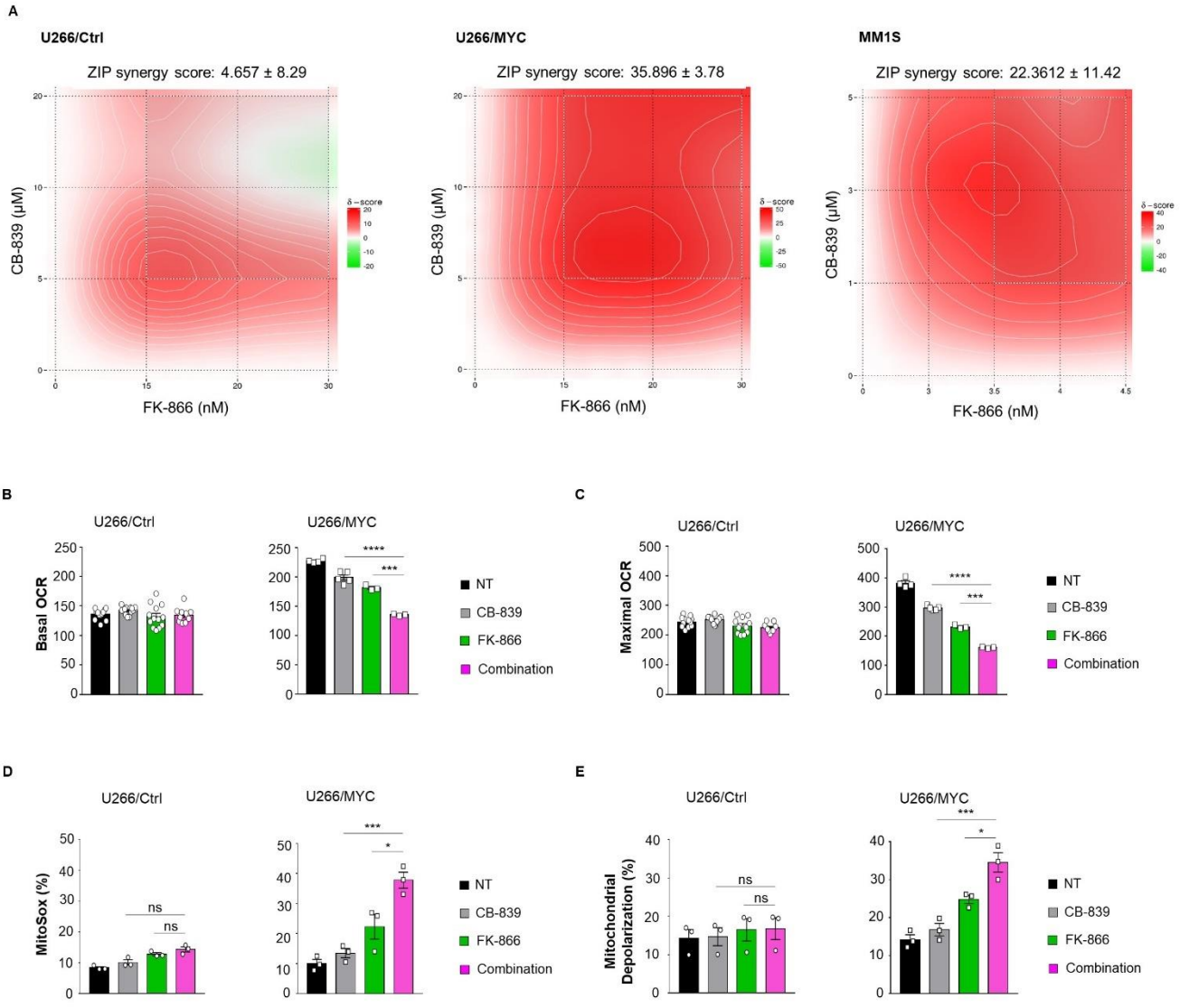

Figure 7

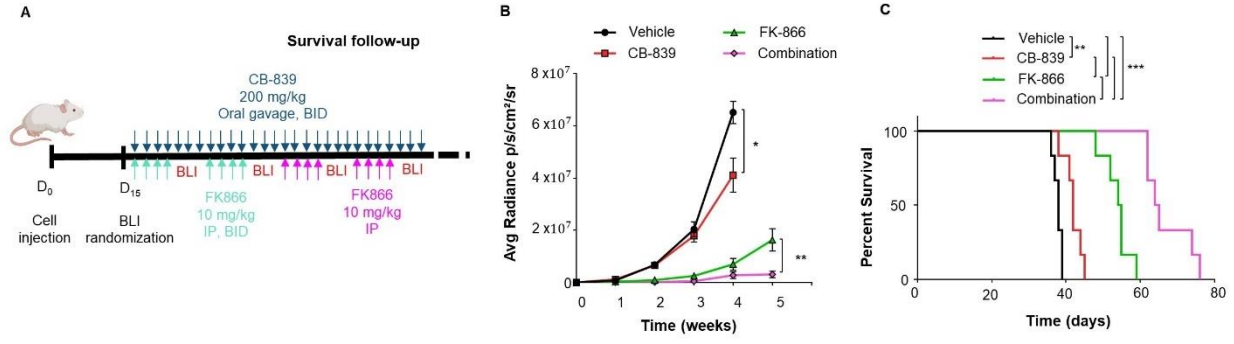

Supplemental Figures and tables

Supplemental figures

Figure S1

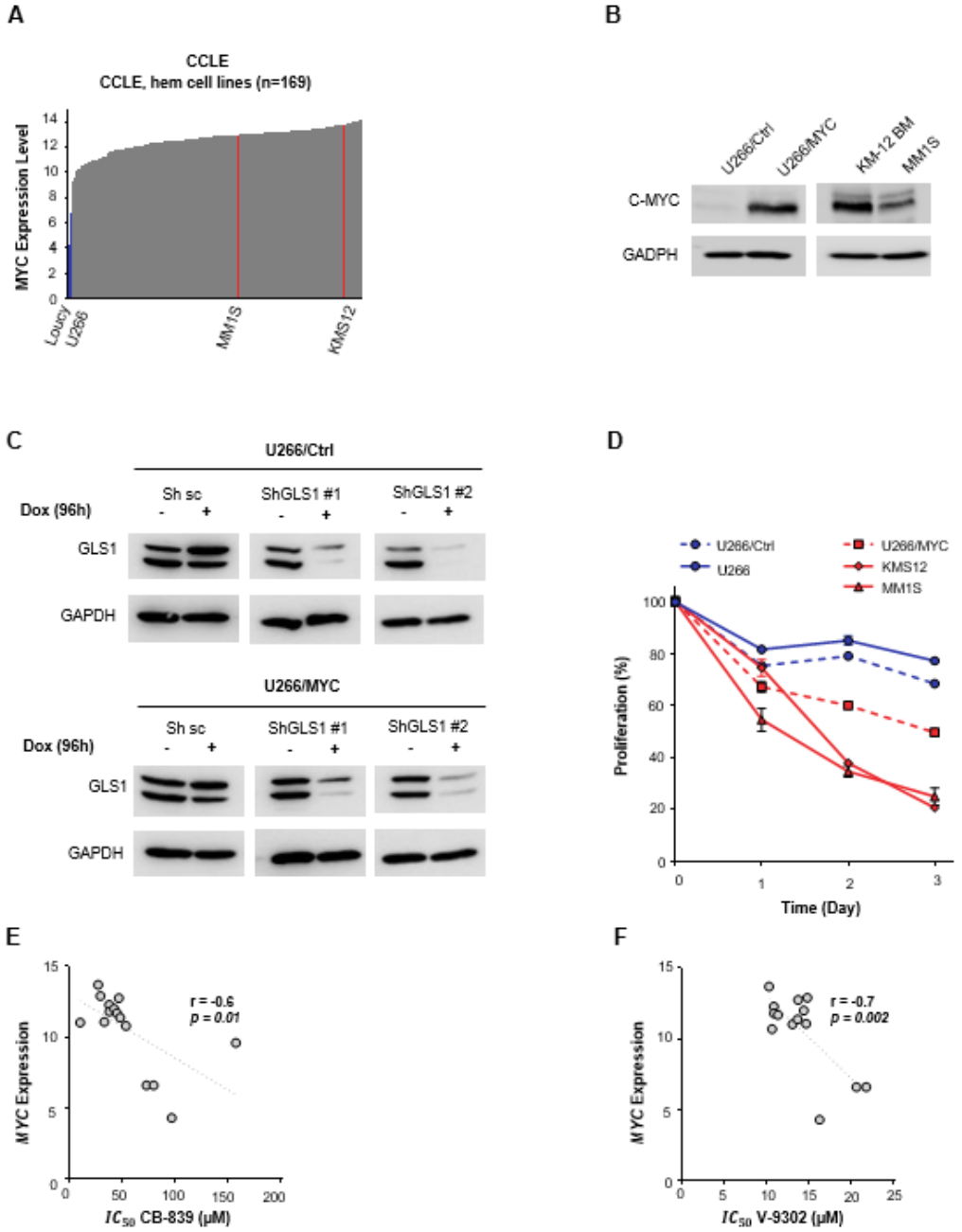

Figure S1. Interrogation of genome-scale pooled short hairpin RNA (shRNA) screening data to identify potential vulnerability in MYC overexpressing cells. Related to Figure 1. A. mRNA expression level of MYC in Hem cell lines (n=169) in CCLE database (Affymetrix U133+2 expression array), cell lines used in our study were highlighted. **B**. MYC expression was assessed by western blot in the indicated cell lines. **C**. GLS1 inducible-knockdown using two independent shRNAs (shGLS1#1) and (shGLS1#2) or a nontargeting control (sh sc) on U266 isogenic model cultured with or without doxycycline for the indicated time. The knock down efficiency was assessed by western blot. **D.** Analysis of proliferation of a panel of MM cell lines under glutamine-free condition. **E-F** Correlation between MYC gene expression levels from CCLE database and the IC50 values of CB-839 and V-9302.

Figure S2

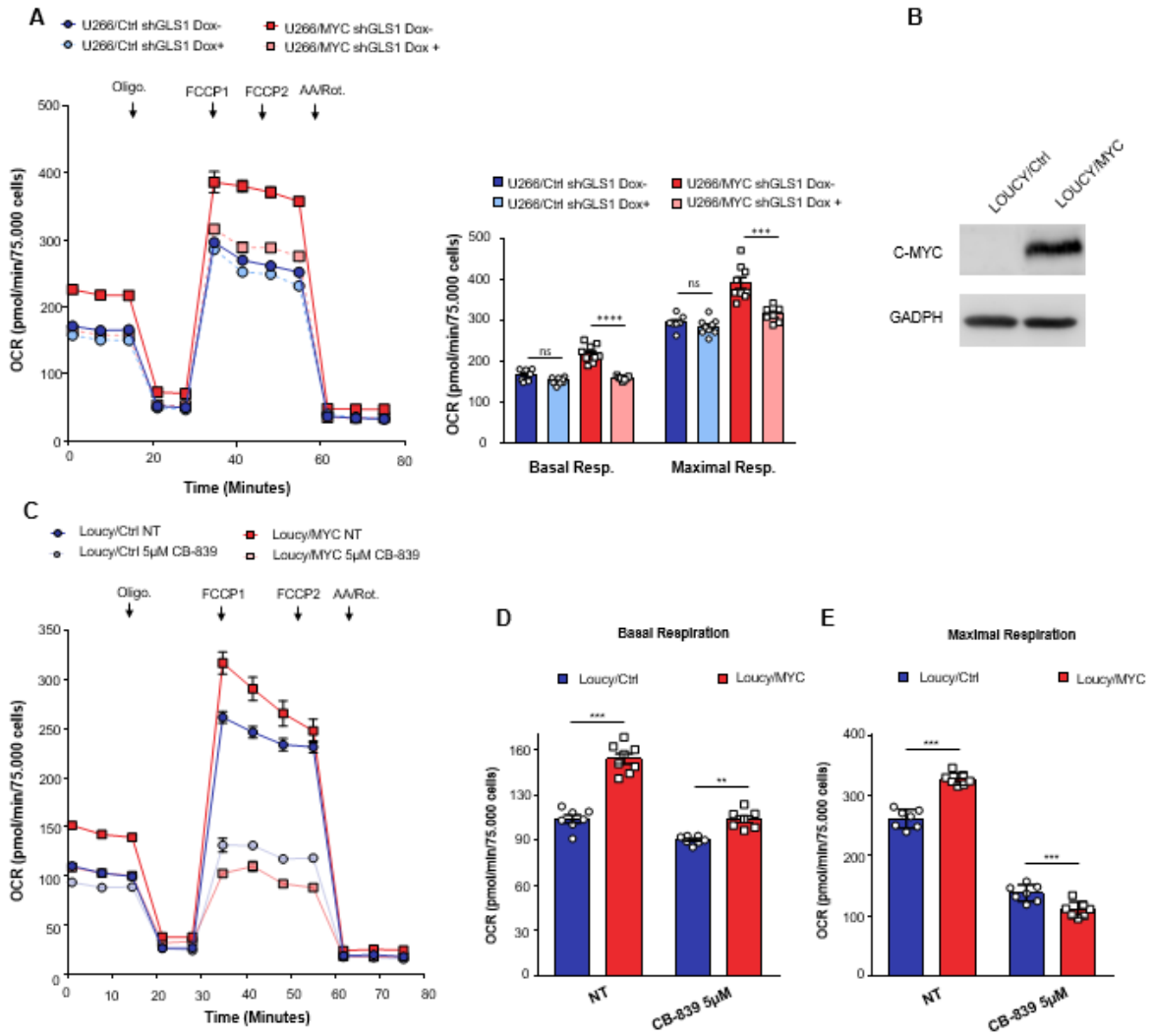

Figure S2. Glutamine role in essential in maintaining mitochondrial function in MYC OE cells. Related to Figure 3. A. Kinetic plot and corresponding bar graphs of normalized OCR obtained during mitochondrial stress test of U266 isogenic model expressing a doxycycline-inducible GLS1 shRNA, treated with or without doxycycline (1µg/ml) for 72 hours, cells were exposed sequentially to each mitochondrial modulator of mitochondrial activity at the indicated times to assess. **B.** MYC expression was assessed by western blot in the indicated cell lines. GAPDH served as an internal control. **C.** Kinetic plot and corresponding bar graphs of normalized OCR obtained during mitochondrial stress test of Loucy/Ctrl and Loucy/MYC treated with or without the 5µM CB-839 for 4 hours, cells were exposed sequentially to each mitochondrial modulator of mitochondrial activity at the indicated times to assess **D.** Basal respiration. **E.** Maximal respiration**.** Data are presented as mean ± SEM calculated from 3 technical replicates. * Indicates p values < 0.05, ** indicates p-value < 0.01, *** indicates p-value < 0.001; Student *t* test. DMSO-treated cells were used as a non-treated control (NT).

Figure S3

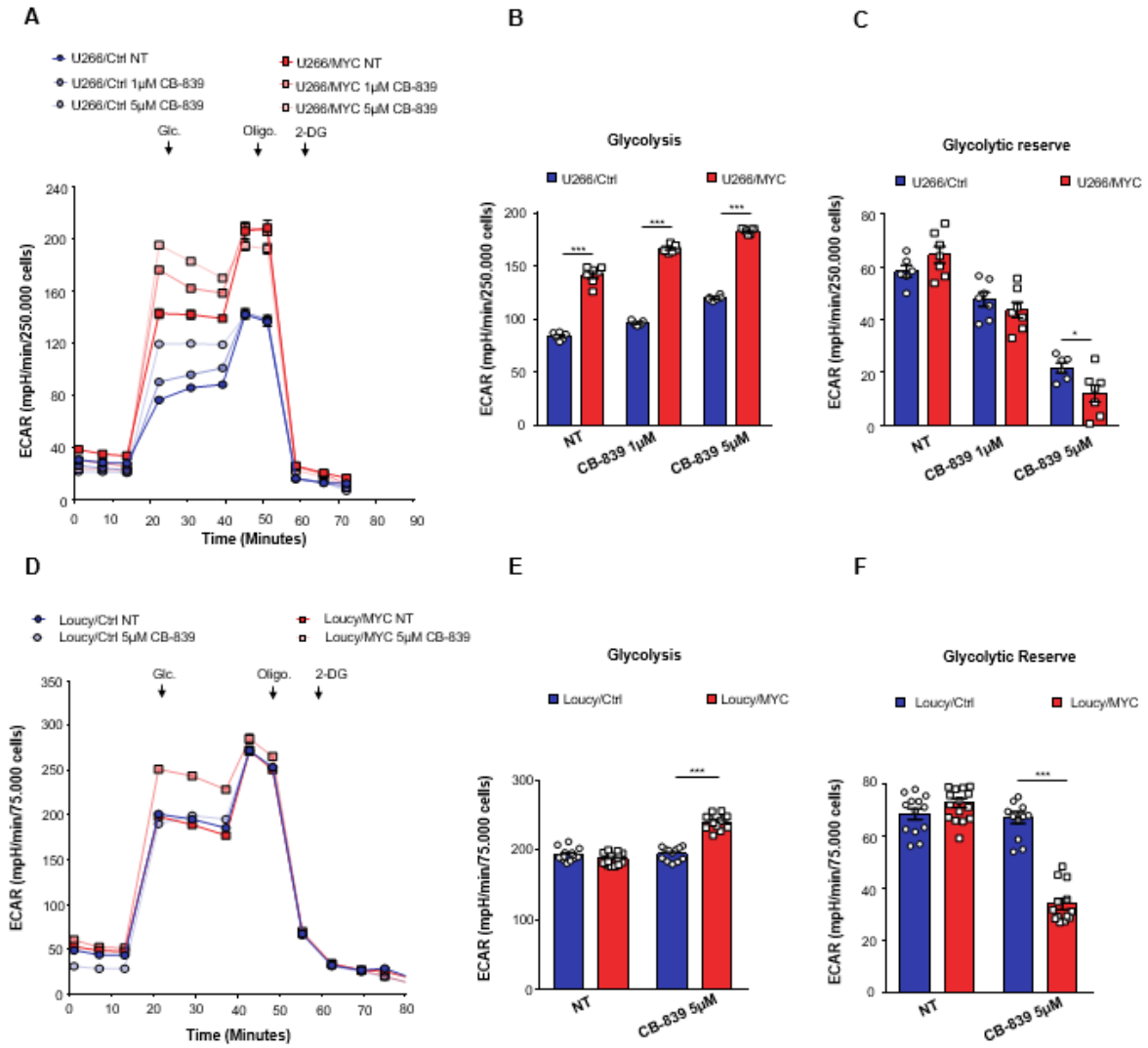

Figure S3. MYC OE cells failed to shift to glycolysis under GLS1 inhibition to maintain cellular energy metabolism. Related to Figure 3. A. Kinetic plot and corresponding bar graphs of normalized ECAR obtained during glycolysis stress test of U266/Ctrl and U266/MYC with or without the indicated concentrations of CB-839 for 4 hours, test was started in a glucose-free medium before cells were exposed sequentially to glycolysis, oligomycin, 2-DG and rotenone/actinomycin A at the indicated times to assess **B.** Glycolysis. **C.** Glycolytic capacity. **D**. Kinetic plot and corresponding bar graphs of normalized ECAR obtained during glycolysis stress test of Loucy/Ctrl and Loucy/MYC with or without 5µM CB-839 for 4 hours, test was started in a glucose-free medium before cells were exposed sequentially to glycolysis, oligomycin, 2-DG and rotenone/actinomycin A at the indicated times to assess **E.** Glycolysis. **F.** Glycolytic capacity. Data are presented as mean ± SEM calculated from 3 technical replicates. * Indicates p values < 0.05, ** indicates p-value < 0.01, *** indicates p-value < 0.001; Student *t* test. DMSO-treated cells were used as a non-treated control (NT).

Figure S4

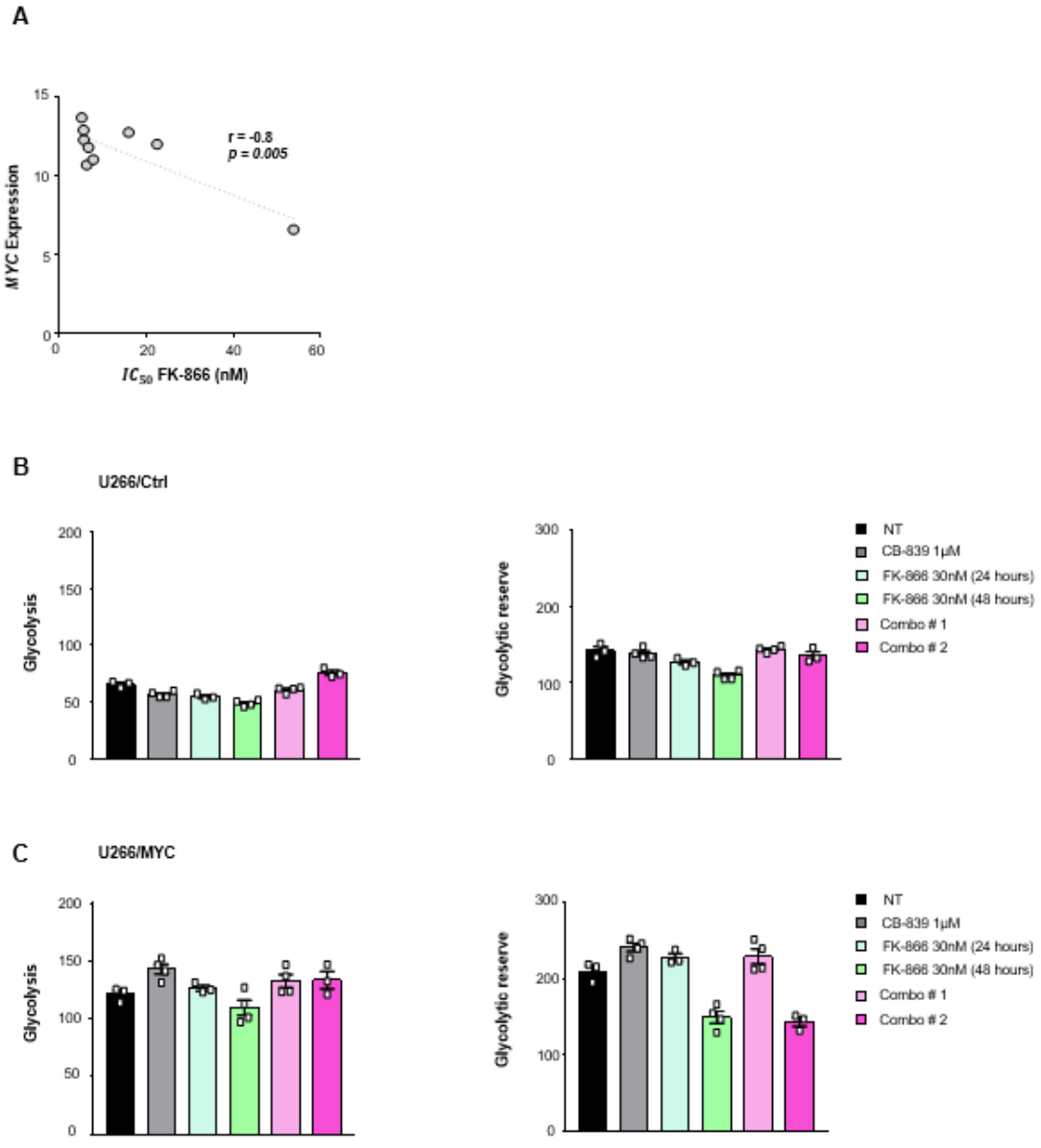

Figure S4. Effects of the combinatorial treatment of CB-839 and FK-866 on mitochondrial functions. Related to Figure 6. A. Correlation between MYC gene expression levels from CCLE database and the IC50 values of FK-866. **B.** Normalized glycolysis and glycolytic reserve obtained during glycolysis stress test of U266/Ctrl and **C.** U266/MYC with or without the indicated concentration of: CB-839 (1µM) for 4 hours, FK-866 (30nM) for 24 and 48 hours and combined treatment. Data are presented as mean ± SEM calculated from 3 technical replicates. DMSO-treated cells were used as a non-treated control (NT). *P < 0.05; **P < 0.01; ***P < 0.001 ; Student's t-test.

Figure S5

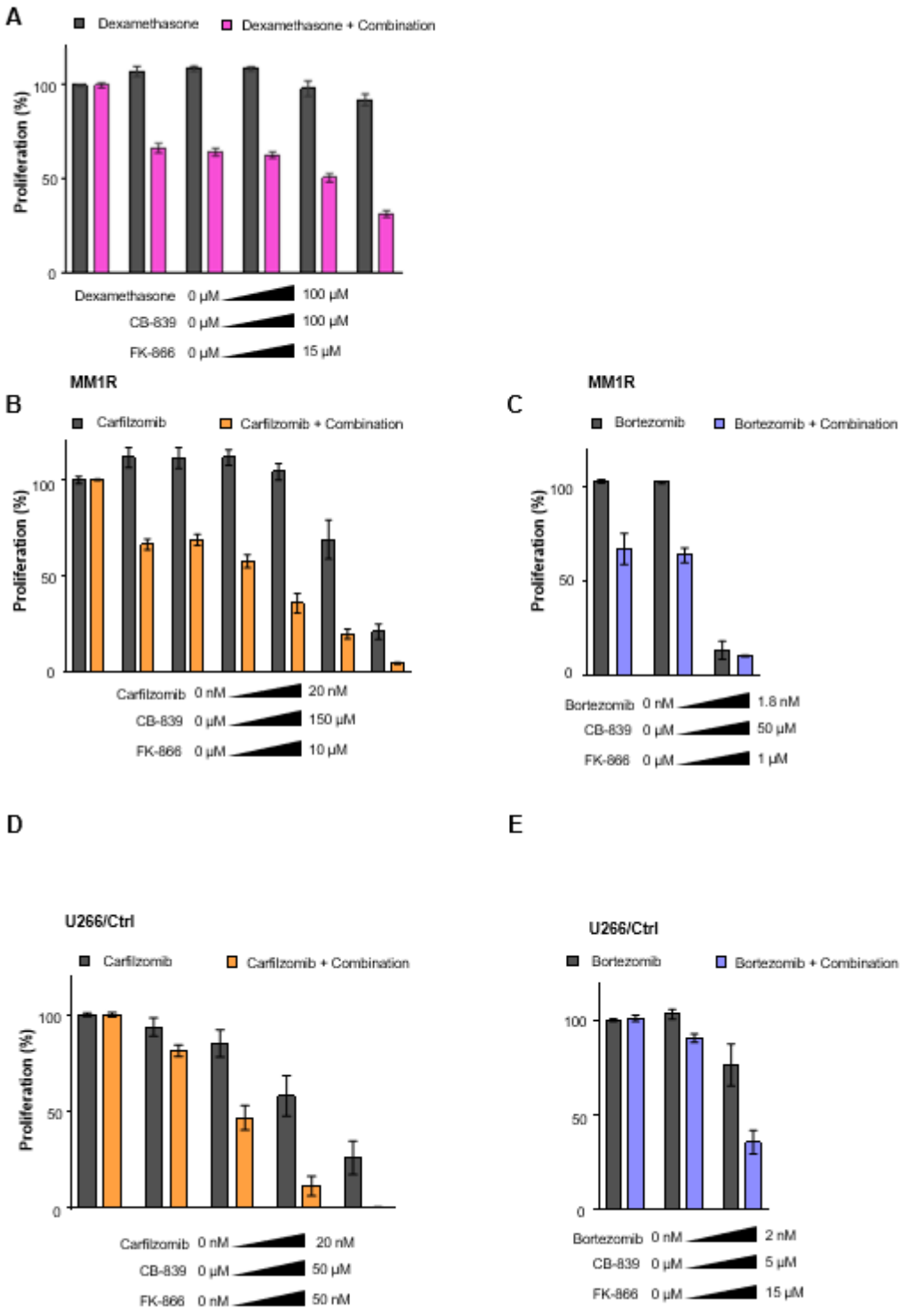
A
Dexamethasone
Dexamethasone + Combination
Proliferation (%)
100
50
0
Dexamethasone 0 µM 100 µM
CB-839 0 µM 100 µM
FK-866 0 µM 15 µM
MM1R
B
Carfilzomib
Carfilzomib + Combination
Proliferation (%)
100
50
0
Carfilzomib 0 nM 20 nM
CB-839 0 µM 150 µM
FK-866 0 µM 10 µM
MM1R
C
Bortezomib
Bortezomib + Combination
Proliferation (%)
100
50
0
Bortezomib 0 nM 1.8 nM
CB-839 0 µM 50 µM
FK-866 0 µM 1 µM
D
U266/Ctrl
Carfilzomib
Carfilzomib + Combination
Proliferation (%)
100
50
0
Carfilzomib 0 nM 20 nM
CB-839 0 µM 50 µM
FK-866 0 nM 50 nM
E
U266/Ctrl
Bortezomib
Bortezomib + Combination
100
50
0
Bortezomib 0 nM 2 nM
CB-839 0 µM 5 µM
FK-866 0 µM 15 µM

Figure S5

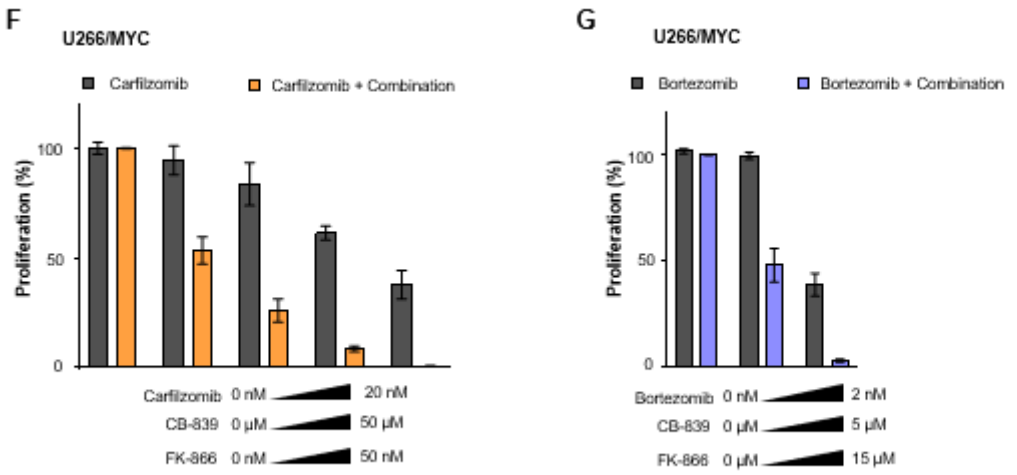

Figure S5. CB-839 and FK-866 combinatorial treatment improves the resistance and sensitivity profile of MM cell lines. A. Dose-response effect of increased doses of Dexamethasone (0-100µM) with or without increased doses of CB-839 and FK-866 combinatorial treatment in MM1R cell line for 72h. **B.** Dose-response effect of increased doses of the currently used drugs in MM, Carlfizomib and Bortazomib in **B&C** MM1R, **D&E** U266/Ctrl and **F&G** U266/MYC without or without increased dosses of CB-839 and FK-866 combinatorial treatment for 72h. Data are presented as mean ± SEM calculated from 3 technical replicates.

List of supplemental tables

Table S1. Pooled shRNA screen analysis to identify genes selectively required for the proliferation of MYC overexpressing cells.

Table S2. Pooled shRNA screen analysis to identify genes selectively required for the proliferation of the cells with the highest MYC signature score.

Table S3. RNA sequencing - Genes up/down regulated in U266/MYC.

Table S4. TMT Proteomics - up/down-regulated proteins in U266/MYC.

Table S5. Gene set enrichment analysis demonstrating the most significantly up-regulated genes in the context of high MYC expression against C5 gene set in; U266 isogenic model, 169 CCLE cell lines and patient datasets.

Table S6. Intracellular metabolite levels were measured by CE/MS-MS in U266/Ctrl and U266/MYC cells treated with DMSO or CB-83.

Table S7. Large-scale small molecule screening to identify compound with potent effects in MYC overexpressing cells.

Chapter VI

General discussion

12. General discussion

Being a key driver in the progression of MM, MYC represents a critical focal point for intervention. However, MYC remains undruggable in clinic due to several challenges associated with its localization, structure, and essential role in normal cellular functions including proliferation, cell cycle regulation, and metabolism. In this study, we aimed to address this challenge by indirectly targeting MYC through targeting its core dependencies.

Cancer dependency map is a research project towards building a comprehensive catalog of cancer genomic vulnerabilities. In this regard, researchers conducted large-scale shRNA or RNAi library screens, enabling the systematic interrogation of gene essentiality. These libraries represent a transformative tool to quantify the phenotypic value, which provides an intuitive measurement of the effect of gene suppression in specific cellular contexts (e.g., expression pattern, mutation, gene copy numbers). This powerful approach grants the possibility of identifying new therapeutic targets for preclinical cancer research.

We hypothesized that the proliferative advantage triggered by *MYC* overexpression induces differential genomic dependencies on specific signaling pathways, creating vulnerabilities that can be further therapeutically exploited. To that end, we have combined two large-scale screens to identify new therapeutic candidates with synergistic properties in this specific cellular context. At first, we uncovered genomic vulnerabilities associated with MYC overexpression by leveraging genome-scale pooled shRNA screen in a panel of 236 cancer cell lines from Project Achilles to identify the genes essential for the proliferation and survival of *MYC* overexpressing cell lines. This analysis reveals a main dependency on glutamine metabolism and specifically GLS1 associated with MYC expression.

Previous studies aimed to describe the link between MYC and the glutaminolysis activity. Gao et al. found no transcriptional regulatory mechanism between *MYC* and *GLS1* despite an E-box element on *GLS1* first intron. However, *MYC* was shown to regulate *GLS1* at a post-transcriptional level, implicating microRNAs [351] . In later research, Haikala et al. reported that *MYC* directly transcriptionally regulates *GLS1* [368]. Therefore, the association between MYC and GLS1 is worth further studies. In this regard, our transcriptome and translational profiles of the U266 isogenic model, the analysis of two main MM patients' data sets, and the expression profiles of 169 hem cell lines showed no significant upregulation in the glutamine metabolism-related genes. Therefore, our data suggests GLS1 as a non-oncogenic dependency in MYC-driven cells.

We functionally explored these dependencies as a selective targetable vulnerability using CB-839, a potent and selective GLS1 inhibitor. We demonstrated through different approaches the heightened sensitivity of *MYC* overexpressing cells to perturbed glutaminolysis. In our present study, we pinpointed the essential role of glutamine in maintaining mitochondrial-centric bioenergetics in *MYC* overexpressing cells. Moreover, we have studied the metabolic rewiring in *MYC* overexpressing cells and identified the enriched pathways under GLS1 inhibition. We observed a notable energy debt in *MYC* overexpressing cells arising from changes in the TCA cycle. We have also observed differential effects of CB-839 on redox homeostasis and macromolecule biosynthesis.

We next applied a small-molecule screen composed of 1869 well-annotated small molecules, including FDA-approved compounds, chemotherapeutic agents, as well as some natural products to improve the translational potential of the data. We have marked a potent effect of NAMPT inhibition on *MYC* overexpressing cells. Preclinically, FK866 exerts potent antitumor activity on various tumor models due to depleting NAD levels, the crucial cofactor in various cellular processes. We have further validated and investigated the metabolic mechanism of the NAMPT inhibitor FK866 in *MYC* overexpressing cells. Previously, Tateishi K et al. reported that FK866 results in the accumulation of glycolytic intermediates and attenuates glycolysis by depleting NAD+ required for the activity of glyceraldehyde 3-phosphate dehydrogenase, which was found to be more potent in *MYC*-driven cells due to the metabolic reprogramming that renders these cells more dependent on glycolysis [369]. Aligned with prior investigation by Tateishi K et al., we observed an enhanced effect of FK-866 on *MYC*-overexpressing cells using different approaches. While FK866 MM toxic effects were observed at low doses, many clinical trials reported dose-limiting toxicity including thrombocytopenia and gastrointestinal symptoms [367,370]; thus, we thought of using FK-866 as a complement agent to enhance the efficacy and improve tolerability, and we uncover for the first time a potent synergy between the two metabolic inhibitors, CB-839 and FK-866, both *in vitro* and *in vivo*.

The integration of a cancer dependency map is essential in the realm of selectively targeting cancer cells while sparing normal tissues. This is exemplified by Kryukov et al. in identifying differential dependency triggered by methylthioadenosine phosphorylase (MTAP) loss. *MTAP* loss is frequently observed in solid and hematological malignancies due to its promoter methylation or co-deletion with the tumor suppressor *CDKN2A*. Therefore, identifying novel therapeutic interventions is of high importance. Kryukov et al. have investigated the changes that follow *MTAP* deficiency to identify vulnerabilities to be further

targeted, and they successfully revealed a pivotal dependency on the arginine methyltransferase, PRMT5 [132]. Furthermore, other studies developed *in vitro* loss-of-function screens to offer better approximation to *in vivo* conditions and consequently run an *in vivo* pooled shRNA screen to unravel vulnerabilities in intact tissues and organs. In this regard, B Roux et al. have effectively shed light on an alternative therapeutic approach in AML. They have uncovered a stress-related AML dependency on the ATPase protein chaperone, VCP. VCP inhibition was shown to disrupt DNA repair and, consequently cell death in AML cells [371].

Drawing inspiration from the previous work mentioned, we have successfully employed a cancer dependency map and identified a high-fidelity dependency on GLS1 in MYC overexpressing cells. Owing to the presence of CB-839, this dependency can be translated into actionable therapeutic intervention. CB-839 is currently administered in phase I/II clinical against different cancer types. However, combining CB-839 with other anti-cancer agents to target multiple mechanisms is receiving more significant interest to overcome metabolic adaptation. Herein, we have exacerbated the differential metabolic vulnerability on glutaminolysis in *MYC* overexpressing cells by inhibiting NAD biosynthesis and combining CB-839 and FK-866. A combination that allowed higher efficacy and dose reduction

In conclusion, our research was marked by applying both dependency maps and drug screens to identify therapeutic vulnerabilities of *MYC* overexpressing myeloma cells as well as to identify therapeutic candidates in other specific molecular subsets that remain undruggable. Moreover, our research opens up the opportunity to repurpose the use of FK866 to overcome its dose-limiting toxicity and to improve the anti-myeloma activity of CB-839 through the co-administration of both metabolic inhibitors. This powerful combination of two clinically tested compounds paves the road to translating preclinical findings into potential clinical applications.

References

1. Metcalf D. On Hematopoietic Stem Cell Fate. *Immunity*. 2007;26(6):669-673. doi:10.1016/j.immuni.2007.05.012

2. Tajer P, Pike-Overzet K, Arias S, Havenga M, Staal F. Ex Vivo Expansion of Hematopoietic Stem Cells for Therapeutic Purposes: Lessons from Development and the Niche. *Cells*. 2019;8(2):169. doi:10.3390/cells8020169

3. Bretscher P, Cohn M. A theory of self-nonself discrimination. *Science*. 1970;169(3950):1042-1049. doi:10.1126/science.169.3950.1042

4. Rock KL, Benacerraf B, Abbas AK. Antigen presentation by hapten-specific B lymphocytes. I. Role of surface immunoglobulin receptors. *J Exp Med*. 1984;160(4):1102-1113. doi:10.1084/jem.160.4.1102

5. Bai Y, Orfao A, Chim CS. Molecular detection of minimal residual disease in multiple myeloma. *Br J Haematol*. 2018;181(1):11-26. doi:10.1111/bjh.15075

6. Stavnezer J, Schrader CE. IgH Chain Class Switch Recombination: Mechanism and Regulation. *The Journal of Immunology*. 2014;193(11):5370-5378. doi:10.4049/jimmunol.1401849

7. Landgren O, Kyle RA, Pfeiffer RM, et al. Monoclonal gammopathy of undetermined significance (MGUS) consistently precedes multiple myeloma: a prospective study. *Blood*. 2009;113(22):5412-5417. doi:10.1182/blood-2008-12-194241

8. Weiss BM, Abadie J, Verma P, Howard RS, Kuehl WM. A monoclonal gammopathy precedes multiple myeloma in most patients. *Blood*. 2009;113(22):5418-5422. doi:10.1182/blood-2008-12-195008

9. Rajkumar SV, Dimopoulos MA, Palumbo A, et al. International Myeloma Working Group updated criteria for the diagnosis of multiple myeloma. *The Lancet Oncology*. 2014;15(12):e538-e548. doi:10.1016/S1470-2045(14)70442-5

10. Greipp PR, Miguel JS, Durie BGM, et al. International Staging System for Multiple Myeloma. *JCO*. 2005;23(15):3412-3420. doi:10.1200/JCO.2005.04.242

11. Rajkumar SV. Updated Diagnostic Criteria and Staging System for Multiple Myeloma. Published online 2016.

12. Palumbo A, Anderson K. Multiple myeloma. *N Engl J Med*. 2011;364(11):1046-1060. doi:10.1056/NEJMra1011442

13. ECIS - European Cancer Information System. https://ecis.jrc.ec.europa.eu, accessed on 04/01/2024

14. Leleu X, Gorsh B, Bessou A, et al. Survival outcomes for patients with multiple myeloma in France: A retrospective cohort study using the Système National des Données de Santé

national healthcare database. *Eur J Haematol*. 2023;111(1):125-134. doi:10.1111/ejh.13976

15. Barwick BG, Gupta VA, Vertino PM, Boise LH. Cell of Origin and Genetic Alterations in the Pathogenesis of Multiple Myeloma. *Front Immunol*. 2019;10:1121. doi:10.3389/fimmu.2019.01121

16. Fonseca R, Bailey RJ, Ahmann GJ, et al. Genomic abnormalities in monoclonal gammopathy of undetermined significance. *Blood*. 2002;100(4):1417-1424. doi:10.1182/blood.V100.4.1417.h81602001417_1417_1424

17. Hassan H, Szalat R. Genetic Predictors of Mortality in Patients with Multiple Myeloma. *TACG*. 2021;Volume 14:241-254. doi:10.2147/TACG.S262866

18. Bergsagel PL, Mateos MV, Gutierrez NC, Rajkumar SV, San Miguel JF. Improving overall survival and overcoming adverse prognosis in the treatment of cytogenetically high-risk multiple myeloma. *Blood*. 2013;121(6):884-892. doi:10.1182/blood-2012-05-432203

19. Kuehl WM, Bergsagel PL. Multiple myeloma: evolving genetic events and host interactions. *Nat Rev Cancer*. 2002;2(3):175-187. doi:10.1038/nrc746

20. Corre J, Perrot A, Caillot D, et al. del(17p) without TP53 mutation confers a poor prognosis in intensively treated newly diagnosed patients with multiple myeloma. *Blood*. 2021;137(9):1192-1195. doi:10.1182/blood.2020008346

21. Hanamura I, Stewart JP, Huang Y, et al. Frequent gain of chromosome band 1q21 in plasma-cell dyscrasias detected by fluorescence in situ hybridization: incidence increases from MGUS to relapsed myeloma and is related to prognosis and disease progression following tandem stem-cell transplantation. *Blood*. 2006;108(5):1724-1732. doi:10.1182/blood-2006-03-009910

22. Clarke SE, Fuller KA, Erber WN. Chromosomal defects in multiple myeloma. *Blood Rev*. 2024;64:101168. doi:10.1016/j.blre.2024.101168

23. Lannes R, Samur M, Perrot A, et al. In Multiple Myeloma, High-Risk Secondary Genetic Events Observed at Relapse Are Present From Diagnosis in Tiny, Undetectable Subclonal Populations. *J Clin Oncol*. 2023;41(9):1695-1702. doi:10.1200/JCO.21.01987

24. Marcon C, Simeon V, Deias P, et al. Experts' consensus on the definition and management of high risk multiple myeloma. *Front Oncol*. 2022;12:1096852. doi:10.3389/fonc.2022.1096852

25. Muylaert C, Van Hemelrijck LA, Maes A, et al. Aberrant DNA methylation in multiple myeloma: A major obstacle or an opportunity? *Front Oncol*. 2022;12:979569. doi:10.3389/fonc.2022.979569

26. Schütt J, Nägler T, Schenk T, Brioli A. Investigating the Interplay between Myeloma Cells and Bone Marrow Stromal Cells in the Development of Drug Resistance: Dissecting the Role of Epigenetic Modifications. *Cancers*. 2021;13(16):4069. doi:10.3390/cancers13164069

27. Chng WJ, Huang GF, Chung TH, et al. Clinical and biological implications of MYC activation: a common difference between MGUS and newly diagnosed multiple myeloma. *Leukemia*. 2011;25(6):1026-1035. doi:10.1038/leu.2011.53

28. Sharma N, Smadbeck JB, Abdallah N, et al. The Prognostic Role of MYC Structural Variants Identified by NGS and FISH in Multiple Myeloma. *Clin Cancer Res*. 2021;27(19):5430-5439. doi:10.1158/1078-0432.CCR-21-0005

29. Chesi M, Robbiani DF, Sebag M, et al. AID-Dependent Activation of a MYC Transgene Induces Multiple Myeloma in a Conditional Mouse Model of Post-Germinal Center Malignancies. *Cancer Cell*. 2008;13(2):167-180. doi:10.1016/j.ccr.2008.01.007

30. Rahmat M, Clement K, Alberge JB, et al. *Novel Mechanism of* MYC *Deregulation in Multiple Myeloma*. Cancer Biology; 2023. doi:10.1101/2023.05.19.541506

31. Sudha P, Ahsan A, Ashby C, et al. Myeloma Genome Project Panel is a Comprehensive Targeted Genomics Panel for Molecular Profiling of Patients with Multiple Myeloma. *Clin Cancer Res*. 2022;28(13):2854-2864. doi:10.1158/1078-0432.CCR-21-3695

32. Sheiness D, Bishop JM. DNA and RNA from Uninfected Vertebrate Cells Contain Nucleotide Sequences Related to the Putative Transforming Gene of Avian Myelocytomatosis Virus. *J Virol*. 1979;31(2):514-521. doi:10.1128/jvi.31.2.514-521.1979

33. Vennstrom B, Sheiness D, Zabielski J, Bishop JM. Isolation and characterization of c-myc, a cellular homolog of the oncogene (v-myc) of avian myelocytomatosis virus strain 29. *J Virol*. 1982;42(3):773-779. doi:10.1128/jvi.42.3.773-779.1982

34. Carabet L, Rennie P, Cherkasov A. Therapeutic Inhibition of Myc in Cancer. Structural Bases and Computer-Aided Drug Discovery Approaches. *IJMS*. 2018;20(1):120. doi:10.3390/ijms20010120

35. Carter PS, Jarquin-Pardo M, Benedetti AD. Differential expression of Myc1 and Myc2 isoforms in cells transformed by eIF4E: evidence for internal ribosome repositioning in the human c-myc 5'UTR. Published online 1999. doi:https://doi-org.proxy.insermbiblio.inist.fr/10.1038/sj.onc.1202890

36. Hann SR, King MW, Bentley DL, Anderson CW, Eisenman RN. A non-AUG translational initiation in c-myc exon 1 generates an N-terminally distinct protein whose synthesis is disrupted in Burkitt's lymphomas. *Cell*. 1988;52(2):185-195. doi:10.1016/0092-8674(88)90507-7

37. Neel BG, JHANWARt SC, CHAGANTIt RSK, HAYWARDtt WS. Two human c-one genes are located on the long arm of chromosome 8. *Proc Natl Acad Sci USA*. Published online 1982.

38. Llombart V, Mansour MR. Therapeutic targeting of "undruggable" MYC. *eBioMedicine*. 2022;75:103756. doi:10.1016/j.ebiom.2021.103756

39. Cowling VH, Chandriani S, Whitfield ML, Cole MD. A Conserved Myc Protein Domain, MBIV, Regulates DNA Binding, Apoptosis, Transformation, and G $_2$ Arrest. *Molecular and Cellular Biology*. 2006;26(11):4226-4239. doi:10.1128/MCB.01959-05

40. Cowling VH, Cole MD. Mechanism of transcriptional activation by the Myc oncoproteins. *Seminars in Cancer Biology*. 2006;16(4):242-252. doi:10.1016/j.semcancer.2006.08.001

41. Koh CM, Sabò A, Guccione E. Targeting MYC in cancer therapy: RNA processing offers new opportunities. *BioEssays*. 2016;38(3):266-275. doi:10.1002/bies.201500134

42. Meyer N, Penn LZ. Reflecting on 25 years with MYC. *Nat Rev Cancer*. 2008;8(12):976-990. doi:10.1038/nrc2231

43. Amati B, Brooks MW, Levy N, Littlewood TD, Evan GI, Land H. Oncogenic activity of the c-Myc protein requires dimerization with Max. *Cell*. 1993;72(2):233-245. doi:10.1016/0092-8674(93)90663-B

44. Blackwood EM, Eisenman RN. Max: A Helix-Loop-Helix Zipper Protein That Forms a Sequence-Specific DNA-Binding Complex with Myc. *Science*. 1991;251(4998):1211-1217. doi:10.1126/science.2006410

45. Allevato M, Bolotin E, Grossman M, Mane-Padros D, Sladek FM, Martinez E. Sequence-specific DNA binding by MYC/MAX to low-affinity non-E-box motifs. Hayes F, ed. *PLoS ONE*. 2017;12(7):e0180147. doi:10.1371/journal.pone.0180147

46. Cawley S, Bekiranov S, Ng HH, et al. Unbiased Mapping of Transcription Factor Binding Sites along Human Chromosomes 21 and 22 Points to Widespread Regulation of Noncoding RNAs. *Cell*. 2004;116(4):499-509. doi:10.1016/S0092-8674(04)00127-8

47. Fernandez PC, Frank SR, Wang L, et al. Genomic targets of the human c-Myc protein. *Genes Dev*. 2003;17(9):1115-1129. doi:10.1101/gad.1067003

48. Kretzner L, Blackwood EM, Eisenman RN. Myc and Max proteins possess distinct transcriptional activities. *Nature*. 1992;359(6394):426-429. doi:10.1038/359426a0

49. Hatton KS, Mahon K, Chin L, et al. Expression and Activity of L-Myc in Normal Mouse Development. *Molecular and Cellular Biology*. 1996;16(4):1794-1804. doi:10.1128/MCB.16.4.1794

50. Obaya AJ, Mateyak MK, Sedivy JM. Mysterious liaisons: the relationship between c-Myc and the cell cycle. *Oncogene*. 1999;18(19):2934-2941. doi:10.1038/sj.onc.1202749

51. Breit S, Schwab M. Suppression ofMYC by high expression ofNMYC in human neuroblastoma cells. *J Neurosci Res*. 1989;24(1):21-28. doi:10.1002/jnr.490240105

52. Nisen PD, Zimmerman KA, Cotter SV, Gilbert F, Alt FW. Enhanced Expression of the N-myc Gene in Wilms' Tumors. Published online 1986.

53. Davis AC, Wims M, Spotts GD, Hann SR, Bradley A. A null c-myc mutation causes lethality before 10.5 days of gestation in homozygotes and reduced fertility in heterozygous female mice. *Genes Dev*. 1993;7(4):671-682. doi:10.1101/gad.7.4.671

54. Malynn BA, De Alboran IM, O'Hagan RC, et al. N- *myc* can functionally replace c- *myc* in murine development, cellular growth, and differentiation. *Genes Dev*. 2000;14(11):1390-1399. doi:10.1101/gad.14.11.1390

55. Patel JH, Loboda AP, Showe MK, Showe LC, McMahon SB. Analysis of genomic targets reveals complex functions of MYC. *Nat Rev Cancer*. 2004;4(7):562-568. doi:10.1038/nrc1393

56. McMahon SB. MYC and the Control of Apoptosis. *Cold Spring Harbor Perspectives in Medicine*. 2014;4(7):a014407-a014407. doi:10.1101/cshperspect.a014407

57. Kress TR, Sabò A, Amati B. MYC: connecting selective transcriptional control to global RNA production. *Nat Rev Cancer*. 2015;15(10):593-607. doi:10.1038/nrc3984

58. Roussel MF, Cleveland JL, Shurtleff SA, Sherr CJ. Myc rescue of a mutant CSF-1 receptor impaired in mitogenic signalling. *Nature*. 1991;353(6342):361-363. doi:10.1038/353361a0

59. Mateyak MK, Obaya AJ, Adachi S, Sedivy JM. Phenotypes of c-Myc-deficient rat fibroblasts isolated by targeted homologous recombination. *Cell Growth Differ*. 1997;8(10):1039-1048.

60. Roussel MF, Theodoras AM, Pagano M, Sherr CJ. Rescue of defective mitogenic signaling by D-type cyclins. *Proc Natl Acad Sci USA*. 1995;92(15):6837-6841. doi:10.1073/pnas.92.15.6837

61. Scafuro M, Capasso L, Carafa V, Altucci L, Nebbioso A. Gene Transactivation and Transrepression in MYC-Driven Cancers. *IJMS*. 2021;22(7):3458. doi:10.3390/ijms22073458

62. Bouchard C. Direct induction of cyclin D2 by Myc contributes to cell cycle progression and sequestration of p27. *The EMBO Journal*. 1999;18(19):5321-5333. doi:10.1093/emboj/18.19.5321

63. Perez-Roger I. Cyclins D1 and D2 mediate Myc-induced proliferation via sequestration of p27Kip1 and p21Cip1. *The EMBO Journal*. 1999;18(19):5310-5320. doi:10.1093/emboj/18.19.5310

64. Bretones G, Acosta JC, Caraballo JM, et al. SKP2 Oncogene Is a Direct MYC Target Gene and MYC Down-regulates p27KIP1 through SKP2 in Human Leukemia Cells. *Journal of Biological Chemistry*. 2011;286(11):9815-9825. doi:10.1074/jbc.M110.165977

65. Stine ZE, Walton ZE, Altman BJ, Hsieh AL, Dang CV. MYC, Metabolism, and Cancer. *Cancer Discovery*. 2015;5(10):1024-1039. doi:10.1158/2159-8290.CD-15-0507

66. Oskarsson T, Essers MAG, Dubois N, et al. Skin epidermis lacking the *c-myc* gene is resistant to Ras-driven tumorigenesis but can reacquire sensitivity upon additional loss of the p21 ^{Cip1} gene. *Genes Dev*. 2006;20(15):2024-2029. doi:10.1101/gad.381206

67. Wiese KE, Walz S, Von Eyss B, et al. The Role of MIZ-1 in MYC-Dependent Tumorigenesis. *Cold Spring Harbor Perspectives in Medicine*. 2013;3(12):a014290-a014290. doi:10.1101/cshperspect.a014290

68. Grandori C, Gomez-Roman N, Felton-Edkins ZA, et al. c-Myc binds to human ribosomal DNA and stimulates transcription of rRNA genes by RNA polymerase I. *Nat Cell Biol*. 2005;7(3):311-318. doi:10.1038/ncb1224

69. Schlosser I. A role for c-Myc in the regulation of ribosomal RNA processing. *Nucleic Acids Research*. 2003;31(21):6148-6156. doi:10.1093/nar/gkg794

70. Van Riggelen J, Yetil A, Felsher DW. MYC as a regulator of ribosome biogenesis and protein synthesis. *Nat Rev Cancer*. 2010;10(4):301-309. doi:10.1038/nrc2819

71. Schmidt EV. The role of c-myc in regulation of translation initiation. *Oncogene*. 2004;23(18):3217-3221. doi:10.1038/sj.onc.1207548

72. Gao P, Tchernyshyov I, Chang TC, et al. c-Myc suppression of miR-23a/b enhances mitochondrial glutaminase expression and glutamine metabolism. *Nature*. 2009;458(7239):762-765. doi:10.1038/nature07823

73. Wise DR, DeBerardinis RJ, Mancuso A, et al. Myc regulates a transcriptional program that stimulates mitochondrial glutaminolysis and leads to glutamine addiction. *Proc Natl Acad Sci USA*. 2008;105(48):18782-18787. doi:10.1073/pnas.0810199105

74. Gao P, Tchernyshyov I, Chang TC, et al. c-Myc suppression of miR-23a/b enhances mitochondrial glutaminase expression and glutamine metabolism. *Nature*. 2009;458(7239):762-765. doi:10.1038/nature07823

75. Felix JB, Cox AR, Hartig SM. Acetyl-CoA and Metabolite Fluxes Regulate White Adipose Tissue Expansion. *Trends in Endocrinology & Metabolism*. 2021;32(5):320-332. doi:10.1016/j.tem.2021.02.008

76. Dong Y, Tu R, Liu H, Qing G. Regulation of cancer cell metabolism: oncogenic MYC in the driver's seat. *Sig Transduct Target Ther*. 2020;5(1):124. doi:10.1038/s41392-020-00235-2

77. Yue M, Jiang J, Gao P, Liu H, Qing G. Oncogenic MYC Activates a Feedforward Regulatory Loop Promoting Essential Amino Acid Metabolism and Tumorigenesis. *Cell Reports*. 2017;21(13):3819-3832. doi:10.1016/j.celrep.2017.12.002

78. Clark RA, Qiao J, Jacobson JC, Chung DH. Induction of serine hydroxymethyltransferase 2 promotes tumorigenesis and metastasis in neuroblastoma. *Oncotarget*. 2022;13(1):32-45. doi:10.18632/oncotarget.28168

79. Sun L, Song L, Wan Q, et al. cMyc-mediated activation of serine biosynthesis pathway is critical for cancer progression under nutrient deprivation conditions. *Cell Res*. 2015;25(4):429-444. doi:10.1038/cr.2015.33

80. Dhanasekaran R, Deutzmann A, Mahauad-Fernandez WD, Hansen AS, Gouw AM, Felsher DW. The MYC oncogene — the grand orchestrator of cancer growth and immune evasion. *Nat Rev Clin Oncol*. 2022;19(1):23-36. doi:10.1038/s41571-021-00549-2

81. Denis N, Kitzis A, Kruh J, Dautry F, Corcos D. Stimulation of methotrexate resistance and dihydrofolate reductase gene amplification by c-myc. *Oncogene*. 1991;6(8):1453-1457.

82. Kuzyk A, Mai S. c-MYC-Induced Genomic Instability. *Cold Spring Harbor Perspectives in Medicine*. 2014;4(4):a014373-a014373. doi:10.1101/cshperspect.a014373

83. Bian X, Lin W. Targeting DNA Replication Stress and DNA Double-Strand Break Repair for Optimizing SCLC Treatment. *Cancers*. 2019;11(9):1289. doi:10.3390/cancers11091289

84. Campaner S, Amati B. Two sides of the Myc-induced DNA damage response: from tumor suppression to tumor maintenance. *Cell Div*. 2012;7(1):6. doi:10.1186/1747-1028-7-6

85. Caracciolo D, Scionti F, Juli G, et al. Exploiting MYC-induced PARPness to target genomic instability in multiple myeloma. *haematol*. 2020;106(1):185-195. doi:10.3324/haematol.2019.240713

86. Meškytė EM, Keskas S, Ciribilli Y. MYC as a Multifaceted Regulator of Tumor Microenvironment Leading to Metastasis. *IJMS*. 2020;21(20):7710. doi:10.3390/ijms21207710

87. Mundim FGL, Pasini FS, Brentani MM, Soares FA, Nonogaki S, Waitzberg AFL. MYC is expressed in the stromal and epithelial cells of primary breast carcinoma and paired nodal metastases. *Molecular and Clinical Oncology*. 2015;3(3):506-514. doi:10.3892/mco.2015.526

88. He L, Thomson JM, Hemann MT, et al. A microRNA polycistron as a potential human oncogene. *Nature*. 2005;435(7043):828-833. doi:10.1038/nature03552

89. Mendell JT. MicroRNAs: Critical Regulators of Development, Cellular Physiology and Malignancy. *Cell Cycle*. 2005;4(9):1179-1184. doi:10.4161/cc.4.9.2032

90. Ventura A, Young AG, Winslow MM, et al. Targeted Deletion Reveals Essential and Overlapping Functions of the miR-17∼92 Family of miRNA Clusters. *Cell*. 2008;132(5):875-886. doi:10.1016/j.cell.2008.02.019

91. Chang TC, Yu D, Lee YS, et al. Widespread microRNA repression by Myc contributes to tumorigenesis. *Nat Genet*. 2008;40(1):43-50. doi:10.1038/ng.2007.30

92. Sampson VB, Rong NH, Han J, et al. MicroRNA Let-7a Down-regulates MYC and Reverts MYC-Induced Growth in Burkitt Lymphoma Cells. *Cancer Research*. 2007;67(20):9762-9770. doi:10.1158/0008-5472.CAN-07-2462

93. Jovanović KK, Roche-Lestienne C, Ghobrial IM, Facon T, Quesnel B, Manier S. Targeting MYC in multiple myeloma. *Leukemia*. 2018;32(6):1295-1306. doi:10.1038/s41375-018-0036-x

94. Viswanathan SR, Powers JT, Einhorn W, et al. Lin28 promotes transformation and is associated with advanced human malignancies. *Nat Genet*. 2009;41(7):843-848. doi:10.1038/ng.392

95. Zech L, Haglund U, Nilsson K, Klein G. Characteristic chromosomal abnormalities in biopsies and lymphoid-cell lines from patients with burkitt and non-burkitt lymphomas. *Int J Cancer*. 1976;17(1):47-56. doi:10.1002/ijc.2910170108

96. Avet-Loiseau H, Li C, Magrangeas F, et al. Prognostic Significance of Copy-Number Alterations in Multiple Myeloma. *JCO*. 2009;27(27):4585-4590. doi:10.1200/JCO.2008.20.6136

97. Kalkat M, De Melo J, Hickman KA, et al. MYC Deregulation in Primary Human Cancers. *Genes (Basel)*. 2017;8(6):151. doi:10.3390/genes8060151

98. Sears R, Leone G, DeGregori J, Nevins JR. Ras Enhances Myc Protein Stability. *Molecular Cell*. 1999;3(2):169-179. doi:10.1016/S1097-2765(00)80308-1

99. Manier S, Salem KZ, Park J, Landau DA, Getz G, Ghobrial IM. Genomic complexity of multiple myeloma and its clinical implications. *Nat Rev Clin Oncol*. 2017;14(2):100-113. doi:10.1038/nrclinonc.2016.122

100. Shaffer AL, Emre NCT, Lamy L, et al. IRF4 addiction in multiple myeloma. *Nature*. 2008;454(7201):226-231. doi:10.1038/nature07064

101. Allen-Petersen BL, Sears RC. Mission Possible: Advances in MYC Therapeutic Targeting in Cancer. *BioDrugs*. 2019;33(5):539-553. doi:10.1007/s40259-019-00370-5

102. Ba M, Long H, Yan Z, et al. BRD4 promotes gastric cancer progression through the transcriptional and epigenetic regulation of c-MYC. *J Cell Biochem*. 2018;119(1):973-982. doi:10.1002/jcb.26264

103. Chen H, Liu H, Qing G. Targeting oncogenic Myc as a strategy for cancer treatment. *Sig Transduct Target Ther*. 2018;3(1):5. doi:10.1038/s41392-018-0008-7

104. Filippakopoulos P, Qi J, Picaud S, et al. Selective inhibition of BET bromodomains. *Nature*. 2010;468(7327):1067-1073. doi:10.1038/nature09504

105. Delmore JE, Issa GC, Lemieux ME, et al. BET Bromodomain Inhibition as a Therapeutic Strategy to Target c-Myc. *Cell*. 2011;146(6):904-917. doi:10.1016/j.cell.2011.08.017

106. Mazur PK, Herner A, Mello SS, et al. Combined inhibition of BET family proteins and histone deacetylases as a potential epigenetics-based therapy for pancreatic ductal adenocarcinoma. *Nat Med*. 2015;21(10):1163-1171. doi:10.1038/nm.3952

107. Mertz JA, Conery AR, Bryant BM, et al. Targeting MYC dependence in cancer by inhibiting BET bromodomains. *Proc Natl Acad Sci USA*. 2011;108(40):16669-16674. doi:10.1073/pnas.1108190108

108. Lebraud H, Wright DJ, Johnson CN, Heightman TD. Protein Degradation by In-Cell Self-Assembly of Proteolysis Targeting Chimeras. *ACS Cent Sci*. 2016;2(12):927-934. doi:10.1021/acscentsci.6b00280

109. Li X, Pu W, Zheng Q, Ai M, Chen S, Peng Y. Proteolysis-targeting chimeras (PROTACs) in cancer therapy. *Mol Cancer*. 2022;21(1):99. doi:10.1186/s12943-021-01434-3

110. Constantin TA, Greenland KK, Varela-Carver A, Bevan CL. Transcription associated cyclin-dependent kinases as therapeutic targets for prostate cancer. *Oncogene*. 2022;41(24):3303-3315. doi:10.1038/s41388-022-02347-1

111. Garcia-Cuellar MP, Füller E, Mäthner E, et al. Efficacy of cyclin-dependent-kinase 9 inhibitors in a murine model of mixed-lineage leukemia. *Leukemia*. 2014;28(7):1427-1435. doi:10.1038/leu.2014.40

112. Deng C, Lipstein MR, Scotto L, et al. Silencing c-Myc translation as a therapeutic strategy through targeting PI3Kδ and CK1ε in hematological malignancies. *Blood*. 2017;129(1):88-99. doi:10.1182/blood-2016-08-731240

113. Pourdehnad M, Truitt ML, Siddiqi IN, Ducker GS, Shokat KM, Ruggero D. Myc and mTOR converge on a common node in protein synthesis control that confers synthetic lethality in Myc-driven cancers. *Proc Natl Acad Sci USA*. 2013;110(29):11988-11993. doi:10.1073/pnas.1310230110

114. Rodrigo CM, Cencic R, Roche SP, Pelletier J, Porco JA. Synthesis of Rocaglamide Hydroxamates and Related Compounds as Eukaryotic Translation Inhibitors: Synthetic and Biological Studies. *J Med Chem*. 2012;55(1):558-562. doi:10.1021/jm201263k

115. Manier S, Huynh D, Shen YJ, et al. Inhibiting the oncogenic translation program is an effective therapeutic strategy in multiple myeloma. *Sci Transl Med*. 2017;9(389):eaal2668. doi:10.1126/scitranslmed.aal2668

116. Lee HC, Wang H, Baladandayuthapani V, et al. RNA Polymerase I Inhibition with CX-5461 as a Novel Therapeutic Strategy to Target *MYC* in Multiple Myeloma. *Br J Haematol*. 2017;177(1):80-94. doi:10.1111/bjh.14525

117. Hann SR, Eisenman RN. Proteins Encoded by the Human c-myc Oncogene: Differential Expression in Neoplastic Cells. *MOL CELL BIOL*. 1984;4.

118. Paul I, Ahmed SF, Bhowmik A, Deb S, Ghosh MK. The ubiquitin ligase CHIP regulates c-Myc stability and transcriptional activity. *Oncogene*. 2013;32(10):1284-1295. doi:10.1038/onc.2012.144

119. Kategaya L, Di Lello P, Rougé L, et al. USP7 small-molecule inhibitors interfere with ubiquitin binding. *Nature*. 2017;550(7677):534-538. doi:10.1038/nature24006

120. Altun M, Kramer HB, Willems LI, et al. Activity-Based Chemical Proteomics Accelerates Inhibitor Development for Deubiquitylating Enzymes. *Chemistry & Biology*. 2011;18(11):1401-1412. doi:10.1016/j.chembiol.2011.08.018

121. Tavana O, Li D, Dai C, et al. HAUSP deubiquitinates and stabilizes N-Myc in neuroblastoma. *Nat Med*. 2016;22(10):1180-1186. doi:10.1038/nm.4180

122. Zhang W, Zhang J, Xu C, et al. Ubiquitin-specific protease 7 is a drug-able target that promotes hepatocellular carcinoma and chemoresistance. *Cancer Cell Int*. 2020;20(1):28. doi:10.1186/s12935-020-1109-2

123. Castell A, Yan Q, Fawkner K, et al. A selective high affinity MYC-binding compound inhibits MYC:MAX interaction and MYC-dependent tumor cell proliferation. *Sci Rep*. 2018;8(1):10064. doi:10.1038/s41598-018-28107-4

124. Wang H, Hammoudeh DI, Follis AV, et al. Improved low molecular weight Myc-Max inhibitors. *Molecular Cancer Therapeutics*. 2007;6(9):2399-2408. doi:10.1158/1535-7163.MCT-07-0005

125. Struntz NB, Chen A, Deutzmann A, et al. Stabilization of the Max Homodimer with a Small Molecule Attenuates Myc-Driven Transcription. *Cell Chemical Biology*. 2019;26(5):711-723.e14. doi:10.1016/j.chembiol.2019.02.009

126. Jeong KC, Ahn KO, Yang CH. Small-molecule inhibitors of c-Myc transcriptional factor suppress proliferation and induce apoptosis of promyelocytic leukemia cell via cell cycle arrest. *Mol BioSyst*. 2010;6(8):1503. doi:10.1039/c002534h

127. Jeong KC, Kim KT, Seo HH, et al. Intravesical Instillation of c-MYC Inhibitor KSI-3716 Suppresses Orthotopic Bladder Tumor Growth. *Journal of Urology*. 2014;191(2):510-518. doi:10.1016/j.juro.2013.07.019

128. Gao J, Wang Y, Li K, Zhang J, Geng X. Comparative analysis of compound NSC13728 as Omomyc homodimer stabilizer by molecular dynamics simulation and MM/GBSA free energy calculation. *J Mol Model*. 2022;28(4):92. doi:10.1007/s00894-022-05082-2

129. Demma MJ, Mapelli C, Sun A, et al. Omomyc Reveals New Mechanisms To Inhibit the MYC Oncogene. *Molecular and Cellular Biology*. 2019;39(22):e00248-19. doi:10.1128/MCB.00248-19

130. Behan FM, Iorio F, Picco G, et al. Prioritization of cancer therapeutic targets using CRISPR–Cas9 screens. *Nature*. 2019;568(7753):511-516. doi:10.1038/s41586-019-1103-9

131. Tsherniak A, Vazquez F, Montgomery PG, et al. Defining a Cancer Dependency Map. *Cell*. 2017;170(3):564-576.e16. doi:10.1016/j.cell.2017.06.010

132. Kryukov GV, Wilson FH, Ruth JR, et al. *MTAP* deletion confers enhanced dependency on the PRMT5 arginine methyltransferase in cancer cells. *Science*. 2016;351(6278):1214-1218. doi:10.1126/science.aad5214

133. Kim KH, Kim W, Howard TP, et al. SWI/SNF-mutant cancers depend on catalytic and non-catalytic activity of EZH2. *Nat Med*. 2015;21(12):1491-1496. doi:10.1038/nm.3968

134. Cowley GS, Weir BA, Vazquez F, et al. Parallel genome-scale loss of function screens in 216 cancer cell lines for the identification of context-specific genetic dependencies. *Sci Data*. 2014;1(1):140035. doi:10.1038/sdata.2014.35

135. Shao DD, Tsherniak A, Gopal S, et al. ATARiS: Computational quantification of gene suppression phenotypes from multisample RNAi screens. *Genome Res*. 2013;23(4):665-678. doi:10.1101/gr.143586.112

136. Bender T, Martinou JC. The mitochondrial pyruvate carrier in health and disease: To carry or not to carry? *Biochimica et Biophysica Acta (BBA) - Molecular Cell Research*. 2016;1863(10):2436-2442. doi:10.1016/j.bbamcr.2016.01.017

137. Lin R, Tao R, Gao X, et al. Acetylation Stabilizes ATP-Citrate Lyase to Promote Lipid Biosynthesis and Tumor Growth. *Molecular Cell*. 2013;51(4):506-518. doi:10.1016/j.molcel.2013.07.002

138. Siekevitz P. Powerhouse of the Cell. *Scientific American*. July 1957:131-140.

139. Heinz S, Freyberger A, Lawrenz B, Schladt L, Schmuck G, Ellinger-Ziegelbauer H. Mechanistic Investigations of the Mitochondrial Complex I Inhibitor Rotenone in the Context of Pharmacological and Safety Evaluation. *Sci Rep*. 2017;7(1):45465. doi:10.1038/srep45465

140. Fullerton M, McFarland R, Taylor RW, Alston CL. The genetic basis of isolated mitochondrial complex II deficiency. *Molecular Genetics and Metabolism*. 2020;131(1-2):53-65. doi:10.1016/j.ymgme.2020.09.009

141. Miyadera H, Shiomi K, Ui H, et al. Atpenins, potent and specific inhibitors of mitochondrial complex II (succinate-ubiquinone oxidoreductase). *Proc Natl Acad Sci USA*. 2003;100(2):473-477. doi:10.1073/pnas.0237315100

142. Klimova T, Chandel NS. Mitochondrial complex III regulates hypoxic activation of HIF. *Cell Death Differ*. 2008;15(4):660-666. doi:10.1038/sj.cdd.4402307

143. Ma X, Jin M, Cai Y, et al. Mitochondrial Electron Transport Chain Complex III Is Required for Antimycin A to Inhibit Autophagy. *Chemistry & Biology*. 2011;18(11):1474-1481. doi:10.1016/j.chembiol.2011.08.009

144. Gandhirajan RK, Rödder K, Bodnar Y, et al. Cytochrome C oxidase Inhibition and Cold Plasma-derived Oxidants Synergize in Melanoma Cell Death Induction. *Sci Rep*. 2018;8(1):12734. doi:10.1038/s41598-018-31031-2

145. Randi EB, Zuhra K, Pecze L, Panagaki T, Szabo C. Physiological concentrations of cyanide stimulate mitochondrial Complex IV and enhance cellular bioenergetics. *Proc Natl Acad Sci USA*. 2021;118(20):e2026245118. doi:10.1073/pnas.2026245118

146. Lardy HA, Johnson D, McMurray WC. Antibiotics as tools for metabolic studies. I. A survey of toxic antibiotics in respiratory, phosphorylative and glycolytic systems. *Archives of Biochemistry and Biophysics*. 1958;78(2):587-597. doi:10.1016/0003-9861(58)90383-7

147. Symersky J, Osowski D, Walters DE, Mueller DM. Oligomycin frames a common drug-binding site in the ATP synthase. *Proc Natl Acad Sci USA*. 2012;109(35):13961-13965. doi:10.1073/pnas.1207912109

148. Klingenberg M. Membrane protein oligomeric structure and transport function. *Nature*. 1981;290(5806):449-454. doi:10.1038/290449a0

149. Stepien G, Torroni A, Chung AB, Hodge JA, Wallace DC. Differential expression of adenine nucleotide translocator isoforms in mammalian tissues and during muscle cell differentiation. *Journal of Biological Chemistry*. 1992;267(21):14592-14597. doi:10.1016/S0021-9258(18)42082-0

150. Yang Y, Sauve AA. NAD + metabolism: Bioenergetics, signaling and manipulation for therapy. *Biochimica et Biophysica Acta (BBA) - Proteins and Proteomics*. 2016;1864(12):1787-1800. doi:10.1016/j.bbapap.2016.06.014

151. Sheeran FL, Angerosa J, Liaw NY, Cheung MM, Pepe S. Adaptations in Protein Expression and Regulated Activity of Pyruvate Dehydrogenase Multienzyme Complex in

Human Systolic Heart Failure. *Oxidative Medicine and Cellular Longevity*. 2019;2019:1-11. doi:10.1155/2019/4532592

152. Strumiło S. Short-term regulation of the mammalian pyruvate dehydrogenase complex. *Acta Biochim Pol*. 2005;52(4):759-764. doi:10.18388/abp.2005_3387

153. Jornayvaz FR, Shulman GI. Regulation of mitochondrial biogenesis. Brown GC, Murphy MP, eds. *Essays in Biochemistry*. 2010;47:69-84. doi:10.1042/bse0470069

154. Valero T. Editorial: Mitochondrial Biogenesis: Pharmacological Approaches. *CPD*. 2014;21(999):1-1. doi:10.2174/1381612819999140307101132

155. Rasmo DD, Palmisano G, Scacco S, et al. Phosphorylation pattern of the NDUFS4 subunit of complex I of the mammalian respiratory chain. *Mitochondrion*. 2010;10(5):464-471. doi:10.1016/j.mito.2010.04.005

156. Yadava N, Potluri P, Scheffler IE. Investigations of the potential effects of phosphorylation of the MWFE and ESSS subunits on complex I activity and assembly. *The International Journal of Biochemistry & Cell Biology*. 2008;40(3):447-460. doi:10.1016/j.biocel.2007.08.015

157. Bennett CF, Latorre-Muro P, Puigserver P. Mechanisms of mitochondrial respiratory adaptation. *Nat Rev Mol Cell Biol*. 2022;23(12):817-835. doi:10.1038/s41580-022-00506-6

158. Kim SC, Sprung R, Chen Y, et al. Substrate and Functional Diversity of Lysine Acetylation Revealed by a Proteomics Survey. *Molecular Cell*. 2006;23(4):607-618. doi:10.1016/j.molcel.2006.06.026

159. Ahn BH, Kim HS, Song S, et al. A role for the mitochondrial deacetylase Sirt3 in regulating energy homeostasis. *Proc Natl Acad Sci USA*. 2008;105(38):14447-14452. doi:10.1073/pnas.0803790105

160. Kurmi K, Haigis MC. Nitrogen Metabolism in Cancer and Immunity. *Trends in Cell Biology*. 2020;30(5):408-424. doi:10.1016/j.tcb.2020.02.005

161. Bode BP. Recent Molecular Advances in Mammalian Glutamine Transport.

162. Oxender DL, Christensen HN. Distinct Mediating Systems for the Transport of Neutral Amino Acids by the Ehrlich Cell. *Journal of Biological Chemistry*. 1963;238(11):3686-3699. doi:10.1016/S0021-9258(19)75327-7

163. Pochini L, Scalise M, Galluccio M, Indiveri C. Membrane transporters for the special amino acid glutamine: structure/function relationships and relevance to human health. *Front Chem*. 2014;2. doi:10.3389/fchem.2014.00061

164. Indiveri C, Pochini L, Galluccio M, Scalise M. SLC1A5 (solute carrier family 1 (neutral amino acid transporter), member 5). *Atlas of Genetics and Cytogenetics in Oncology and Haematology*. 2014;(9). doi:10.4267/2042/54036

165. Masson J, Darmon M, Conjard A, et al. Mice Lacking Brain/Kidney Phosphate-Activated Glutaminase Have Impaired Glutamatergic Synaptic Transmission, Altered Breathing,

Disorganized Goal-Directed Behavior and Die Shortly after Birth. *J Neurosci*. 2006;26(17):4660-4671. doi:10.1523/JNEUROSCI.4241-05.2006

166. Mock B, Kozak C, Szpirer C, Seuane H, O'Brien S, Banners C. A Glutaminase (G/s) Gene Maps to Mouse Chromosome 1, Rat Chromosome 9, and Human Chromosome 2. *Genomics*. 1989;5(2):291-297. doi:10.1016/0888-7543(89)90060-8.

167. Elgadi KM, Meguid RA, Qian M, Souba WW, Abcouwer SF. Cloning and analysis of unique human glutaminase isoforms generated by tissue-specific alternative splicing. *Physiological Genomics*. 1999;1(2):51-62. doi:10.1152/physiolgenomics.1999.1.2.51

168. Ferreira APS, Cassago A, Gonçalves K de A, et al. Active Glutaminase C Self-assembles into a Supratetrameric Oligomer That Can Be Disrupted by an Allosteric Inhibitor. *Journal of Biological Chemistry*. 2013;288(39):28009-28020. doi:10.1074/jbc.M113.501346

169. Pasquali CC, Islam Z, Adamoski D, et al. The origin and evolution of human glutaminases and their atypical C-terminal ankyrin repeats. *Journal of Biological Chemistry*. 2017;292(27):11572-11585. doi:10.1074/jbc.M117.787291

170. Cassago A, Ferreira APS, Ferreira IM, et al. Mitochondrial localization and structure-based phosphate activation mechanism of Glutaminase C with implications for cancer metabolism. *Proc Natl Acad Sci USA*. 2012;109(4):1092-1097. doi:10.1073/pnas.1112495109

171. Fan X, Ross DD, Arakawa H, Ganapathy V, Tamai I, Nakanishi T. Impact of system L amino acid transporter 1 (LAT1) on proliferation of human ovarian cancer cells: A possible target for combination therapy with anti-proliferative aminopeptidase inhibitors. *Biochemical Pharmacology*. 2010;80(6):811-818. doi:10.1016/j.bcp.2010.05.021

172. Patel D, Menon D, Bernfeld E, et al. Aspartate Rescues S-phase Arrest Caused by Suppression of Glutamine Utilization in KRas-driven Cancer Cells. *Journal of Biological Chemistry*. 2016;291(17):9322-9329. doi:10.1074/jbc.M115.710145

173. Barve, Vega, Shah, et al. Perturbation of Methionine/S-adenosylmethionine Metabolism as a Novel Vulnerability in MLL Rearranged Leukemia. *Cells*. 2019;8(11):1322. doi:10.3390/cells8111322

174. Chello PL, Bertino JR. Dependence of 5-Methyltetrahydrofolate Utilization by L5178Y Murine Leukemia Cells in Vitro on the Presence of Hydroxycobalamin and Transcobalamin II'. 1973;33.

175. Kaiser P. Methionine Dependence of Cancer. *Biomolecules*. 2020;10(4):568. doi:10.3390/biom10040568

176. Lu SC. Regulation of glutathione synthesis. *Molecular Aspects of Medicine*. 2009;30(1-2):42-59. doi:10.1016/j.mam.2008.05.005

177. Koju N, Qin Z hong, Sheng R. Reduced nicotinamide adenine dinucleotide phosphate in redox balance and diseases: a friend or foe? *Acta Pharmacol Sin*. 2022;43(8):1889-1904. doi:10.1038/s41401-021-00838-7

178. Kulikova V, Shabalin K, Nerinovski K, et al. Generation, Release, and Uptake of the NAD Precursor Nicotinic Acid Riboside by Human Cells. *Journal of Biological Chemistry*. 2015;290(45):27124-27137. doi:10.1074/jbc.M115.664458

179. Houtkooper RH, Cantó C, Wanders RJ, Auwerx J. The Secret Life of NAD+: An Old Metabolite Controlling New Metabolic Signaling Pathways. *Endocrine Reviews*. 2010;31(2):194-223. doi:10.1210/er.2009-0026

180. Okabe K, Yaku K, Tobe K, Nakagawa T. Implications of altered NAD metabolism in metabolic disorders. *J Biomed Sci*. 2019;26(1):34. doi:10.1186/s12929-019-0527-8

181. Kawai S, Murata K. Structure and Function of NAD Kinase and NADP Phosphatase: Key Enzymes That Regulate the Intracellular Balance of NAD(H) and NADP(H). *Bioscience, Biotechnology, and Biochemistry*. 2008;72(4):919-930. doi:10.1271/bbb.70738

182. Ronchi JA, Francisco A, Passos LAC, Figueira TR, Castilho RF. The Contribution of Nicotinamide Nucleotide Transhydrogenase to Peroxide Detoxification Is Dependent on the Respiratory State and Counterbalanced by Other Sources of NADPH in Liver Mitochondria. *Journal of Biological Chemistry*. 2016;291(38):20173-20187. doi:10.1074/jbc.M116.730473

183. Wang T, Zhang X, Bheda P, Revollo JR, Imai S ichiro, Wolberger C. Structure of Nampt/PBEF/visfatin, a mammalian NAD+ biosynthetic enzyme. *Nat Struct Mol Biol*. 2006;13(7):661-662. doi:10.1038/nsmb1114

184. Revollo JR, Körner A, Mills KF, et al. Nampt/PBEF/Visfatin Regulates Insulin Secretion in β Cells as a Systemic NAD Biosynthetic Enzyme. *Cell Metabolism*. 2007;6(5):363-375. doi:10.1016/j.cmet.2007.09.003

185. Liao X, Huang X, Li X, et al. AMPK phosphorylates NAMPT to regulate NAD^+ homeostasis under ionizing radiation. *Open Biol*. 2022;12(10):220213. doi:10.1098/rsob.220213

186. Imai S, Yoshino J. The importance of NAMPT / NAD / SIRT1 in the systemic regulation of metabolism and ageing. *Diabetes Obesity Metabolism*. 2013;15(s3):26-33. doi:10.1111/dom.12171

187. Garten A, Schuster S, Penke M, Gorski T, De Giorgis T, Kiess W. Physiological and pathophysiological roles of NAMPT and NAD metabolism. *Nat Rev Endocrinol*. 2015;11(9):535-546. doi:10.1038/nrendo.2015.117

188. Xing S, Hu Y, Huang X, Shen D, Chen C. Nicotinamide phosphoribosyltransferase-related signaling pathway in early Alzheimer's disease mouse models. *Mol Med Report*. Published online October 30, 2019. doi:10.3892/mmr.2019.10782

189. Berger F, Lau C, Dahlmann M, Ziegler M. Subcellular Compartmentation and Differential Catalytic Properties of the Three Human Nicotinamide Mononucleotide Adenylyltransferase Isoforms. *Journal of Biological Chemistry*. 2005;280(43):36334-36341. doi:10.1074/jbc.M508660200

190. Stein LR, Imai S ichiro. The dynamic regulation of NAD metabolism in mitochondria. *Trends in Endocrinology & Metabolism*. 2012;23(9):420-428. doi:10.1016/j.tem.2012.06.005

191. Xiao W, Wang RS, Handy DE, Loscalzo J. NAD(H) and NADP(H) Redox Couples and Cellular Energy Metabolism. *Antioxidants & Redox Signaling*. 2018;28(3):251-272. doi:10.1089/ars.2017.7216

192. Hanahan D, Weinberg RA. The Hallmarks of Cancer. *Cell*. 2000;100(1):57-70. doi:10.1016/S0092-8674(00)81683-9

193. Hanahan D, Weinberg RA. Hallmarks of Cancer: The Next Generation. *Cell*. 2011;144(5):646-674. doi:10.1016/j.cell.2011.02.013

194. Cori CF, Cori GT. THE CARBOHYDRATE METABOLISM OF TUMORS: II. CHANGES IN THE SUGAR, LACTIC ACID, AND CO2-COMBINING POWER OF BLOOD PASSING THROUGH A TUMOR. *Journal of Biological Chemistry*. 1925;65(2):397-405. doi:10.1016/S0021-9258(18)84849-9

195. Warburg O. On the Origin of Cancer Cells. 1956;123.

196. Warburg O, Wind F, Negelein E. THE METABOLISM OF TUMORS IN THE BODY. *Journal of General Physiology*. 1927;8(6):519-530. doi:10.1085/jgp.8.6.519

197. DeBerardinis RJ, Chandel NS. We need to talk about the Warburg effect. *Nat Metab*. 2020;2(2):127-129. doi:10.1038/s42255-020-0172-2

198. Koppenol WH, Bounds PL, Dang CV. Otto Warburg's contributions to current concepts of cancer metabolism. *Nat Rev Cancer*. 2011;11(5):325-337. doi:10.1038/nrc3038

199. Osthus RC, Shim H, Kim S, et al. Deregulation of Glucose Transporter 1 and Glycolytic Gene Expression by c-Myc. *Journal of Biological Chemistry*. 2000;275(29):21797-21800. doi:10.1074/jbc.C000023200

200. Kim J whan, Zeller KI, Wang Y, et al. Evaluation of Myc E-Box Phylogenetic Footprints in Glycolytic Genes by Chromatin Immunoprecipitation Assays. *Molecular and Cellular Biology*. 2004;24(13):5923-5936. doi:10.1128/MCB.24.13.5923-5936.2004

201. Cencioni C, Scagnoli F, Spallotta F, Nasi S, Illi B. The "Superoncogene" Myc at the Crossroad between Metabolism and Gene Expression in Glioblastoma Multiforme. *Int J Mol Sci*. 2023;24(4):4217. doi:10.3390/ijms24044217

202. He TL, Zhang YJ, Jiang H, Li XH, Zhu H, Zheng KL. The c-Myc-LDHA axis positively regulates aerobic glycolysis and promotes tumor progression in pancreatic cancer. *Med Oncol*. 2015;32(7):187. doi:10.1007/s12032-015-0633-8

203. Maiso P, Huynh D, Moschetta M, et al. Metabolic signature identifies novel targets for drug resistance in multiple myeloma. *Cancer Res*. 2015;75(10):2071-2082. doi:10.1158/0008-5472.CAN-14-3400

204. Zhang B, Wang Q, Lin Z, et al. A novel glycolysis-related gene signature for predicting the prognosis of multiple myeloma. *Front Cell Dev Biol*. 2023;11:1198949. doi:10.3389/fcell.2023.1198949

205. David CJ, Chen M, Assanah M, Canoll P, Manley JL. HnRNP proteins controlled by c-Myc deregulate pyruvate kinase mRNA splicing in cancer. *Nature*. 2010;463(7279):364-368. doi:10.1038/nature08697

206. Zahra K, Dey T, Ashish, Mishra SP, Pandey U. Pyruvate Kinase M2 and Cancer: The Role of PKM2 in Promoting Tumorigenesis. *Front Oncol*. 2020;10:159. doi:10.3389/fonc.2020.00159

207. Elstrom RL, Bauer DE, Buzzai M, et al. Akt Stimulates Aerobic Glycolysis in Cancer Cells. *Cancer Research*. 2004;64(11):3892-3899. doi:10.1158/0008-5472.CAN-03-2904

208. Bloedjes TA, de Wilde G, Khan GH, et al. AKT supports the metabolic fitness of multiple myeloma cells by restricting FOXO activity. *Blood Adv*. 2023;7(9):1697-1712. doi:10.1182/bloodadvances.2022007383

209. Kierans SJ, Taylor CT. Regulation of glycolysis by the hypoxia-inducible factor (HIF): implications for cellular physiology. *J Physiol*. 2021;599(1):23-37. doi:10.1113/JP280572

210. Li Y, Sun XX, Qian DZ, Dai MS. Molecular Crosstalk Between MYC and HIF in Cancer. *Front Cell Dev Biol*. 2020;8:590576. doi:10.3389/fcell.2020.590576

211. Semenza GL. Targeting HIF-1 for cancer therapy. *Nat Rev Cancer*. 2003;3(10):721-732. doi:10.1038/nrc1187

212. Zhong H, De Marzo AM, Laughner E, et al. Overexpression of hypoxia-inducible factor 1alpha in common human cancers and their metastases. *Cancer Res*. 1999;59(22):5830-5835.

213. Birner P, Schindl M, Obermair A, Breitenecker G, Oberhuber G. Expression of hypoxia-inducible factor 1alpha in epithelial ovarian tumors: its impact on prognosis and on response to chemotherapy. *Clin Cancer Res*. 2001;7(6):1661-1668.

214. Bos R, van der Groep P, Greijer AE, et al. Levels of hypoxia-inducible factor-1alpha independently predict prognosis in patients with lymph node negative breast carcinoma. *Cancer*. 2003;97(6):1573-1581. doi:10.1002/cncr.11246

215. Takahashi R, Tanaka S, Hiyama T, et al. Hypoxia-inducible factor-1alpha expression and angiogenesis in gastrointestinal stromal tumor of the stomach. *Oncol Rep*. 2003;10(4):797-802.

216. Volm M, Koomägi R. Hypoxia-inducible factor (HIF-1) and its relationship to apoptosis and proliferation in lung cancer. *Anticancer Res*. 2000;20(3A):1527-1533.

217. Maschek G, Savaraj N, Priebe W, et al. 2-Deoxy- D -glucose Increases the Efficacy of Adriamycin and Paclitaxel in Human Osteosarcoma and Non-Small Cell Lung Cancers ***In Vivo*** . *Cancer Research*. 2004;64(1):31-34. doi:10.1158/0008-5472.CAN-03-3294

218. Zhao Y, Liu H, Liu Z, et al. Overcoming Trastuzumab Resistance in Breast Cancer by Targeting Dysregulated Glucose Metabolism. *Cancer Research*. 2011;71(13):4585-4597. doi:10.1158/0008-5472.CAN-11-0127

219. Chan DA, Sutphin PD, Nguyen P, et al. Targeting GLUT1 and the Warburg Effect in Renal Cell Carcinoma by Chemical Synthetic Lethality. *Sci Transl Med*. 2011;3(94). doi:10.1126/scitranslmed.3002394

220. Liu Y, Cao Y, Zhang W, et al. A Small-Molecule Inhibitor of Glucose Transporter 1 Downregulates Glycolysis, Induces Cell-Cycle Arrest, and Inhibits Cancer Cell Growth *In Vitro* and *In Vivo*. *Molecular Cancer Therapeutics*. 2012;11(8):1672-1682. doi:10.1158/1535-7163.MCT-12-0131

221. Anastasiou D, Yu Y, Israelsen WJ, et al. Pyruvate kinase M2 activators promote tetramer formation and suppress tumorigenesis. *Nat Chem Biol*. 2012;8(10):839-847. doi:10.1038/nchembio.1060

222. Bonnet S, Archer SL, Allalunis-Turner J, et al. A Mitochondria-K+ Channel Axis Is Suppressed in Cancer and Its Normalization Promotes Apoptosis and Inhibits Cancer Growth. *Cancer Cell*. 2007;11(1):37-51. doi:10.1016/j.ccr.2006.10.020

223. Garon EB, Christofk HR, Hosmer W, et al. Dichloroacetate should be considered with platinum-based chemotherapy in hypoxic tumors rather than as a single agent in advanced non-small cell lung cancer. *J Cancer Res Clin Oncol*. 2014;140(3):443-452. doi:10.1007/s00432-014-1583-9

224. Halford S, Veal GJ, Wedge SR, et al. A Phase I Dose-escalation Study of AZD3965, an Oral Monocarboxylate Transporter 1 Inhibitor, in Patients with Advanced Cancer. *Clinical Cancer Research*. 2023;29(8):1429-1439. doi:10.1158/1078-0432.CCR-22-2263

225. Noble RA, Bell N, Blair H, et al. Inhibition of monocarboxyate transporter 1 by AZD3965 as a novel therapeutic approach for diffuse large B-cell lymphoma and Burkitt lymphoma. *Haematologica*. 2017;102(7):1247-1257. doi:10.3324/haematol.2016.163030

226. Cluntun AA, Lukey MJ, Cerione RA, Locasale JW. Glutamine Metabolism in Cancer: Understanding the Heterogeneity. *Trends in Cancer*. 2017;3(3):169-180. doi:10.1016/j.trecan.2017.01.005

227. Snaebjornsson MT, Janaki-Raman S, Schulze A. Greasing the Wheels of the Cancer Machine: The Role of Lipid Metabolism in Cancer. *Cell Metabolism*. 2020;31(1):62-76. doi:10.1016/j.cmet.2019.11.010

228. Vyas S, Zaganjor E, Haigis MC. Mitochondria and Cancer. *Cell*. 2016;166(3):555-566. doi:10.1016/j.cell.2016.07.002

229. Eagle H. Nutrition Needs of Mammalian Cells in Tissue Culture. *Science*. 1955;122(3168):501-504. doi:10.1126/science.122.3168.501

230. Scalise M, Pochini L, Galluccio M, Console L, Indiveri C. Glutamine Transport and Mitochondrial Metabolism in Cancer Cell Growth. *Front Oncol*. 2017;7:306. doi:10.3389/fonc.2017.00306

231. Kurayama R, Ito N, Nishibori Y, et al. Role of amino acid transporter LAT2 in the activation of mTORC1 pathway and the pathogenesis of crescentic glomerulonephritis. *Lab Invest*. 2011;91(7):992-1006. doi:10.1038/labinvest.2011.43

232. Thangavelu K, Pan CQ, Karlberg T, et al. Structural basis for the allosteric inhibitory mechanism of human kidney-type glutaminase (KGA) and its regulation by Raf-Mek-Erk signaling in cancer cell metabolism. *Proc Natl Acad Sci USA*. 2012;109(20):7705-7710. doi:10.1073/pnas.1116573109

233. Bolzoni M, Chiu M, Accardi F, et al. Dependence on glutamine uptake and glutamine addiction characterize myeloma cells: a new attractive target. *Blood*. 2016;128(5):667-679. doi:10.1182/blood-2016-01-690743

234. Giuliani N, Chiu M, Bolzoni M, et al. The potential of inhibiting glutamine uptake as a therapeutic target for multiple myeloma. *Expert Opin Ther Targets*. 2017;21(3):231-234. doi:10.1080/14728222.2017.1279148

235. Bajpai R, Matulis SM, Wei C, et al. Targeting glutamine metabolism in multiple myeloma enhances BIM binding to BCL-2 eliciting synthetic lethality to venetoclax. *Oncogene*. 2016;35(30):3955-3964. doi:10.1038/onc.2015.464

236. Nguyen TV, Lee JE, Sweredoski MJ, et al. Glutamine Triggers Acetylation-Dependent Degradation of Glutamine Synthetase via the Thalidomide Receptor Cereblon. *Mol Cell*. 2016;61(6):809-820. doi:10.1016/j.molcel.2016.02.032

237. Jin J, Byun JK, Choi YK, Park KG. Targeting glutamine metabolism as a therapeutic strategy for cancer. *Exp Mol Med*. 2023;55(4):706-715. doi:10.1038/s12276-023-00971-9

238. Venkateswaran N, Lafita-Navarro MC, Hao YH, et al. MYC promotes tryptophan uptake and metabolism by the kynurenine pathway in colon cancer. *Genes Dev*. 2019;33(17-18):1236-1251. doi:10.1101/gad.327056.119

239. Gaglio D, Soldati C, Vanoni M, Alberghina L, Chiaradonna F. Glutamine Deprivation Induces Abortive S-Phase Rescued by Deoxyribonucleotides in K-Ras Transformed Fibroblasts. Blagosklonny MV, ed. *PLoS ONE*. 2009;4(3):e4715. doi:10.1371/journal.pone.0004715

240. Pupo E, Avanzato D, Middonti E, Bussolino F, Lanzetti L. KRAS-Driven Metabolic Rewiring Reveals Novel Actionable Targets in Cancer. *Front Oncol*. 2019;9:848. doi:10.3389/fonc.2019.00848

241. Son J, Lyssiotis CA, Ying H, et al. Glutamine supports pancreatic cancer growth through a KRAS-regulated metabolic pathway. *Nature*. 2013;496(7443):101-105. doi:10.1038/nature12040

242. Coloff JL, Murphy JP, Braun CR, et al. Differential Glutamate Metabolism in Proliferating and Quiescent Mammary Epithelial Cells. *Cell Metabolism*. 2016;23(5):867-880. doi:10.1016/j.cmet.2016.03.016

243. Dang CV. Links between metabolism and cancer. *Genes Dev*. 2012;26(9):877-890. doi:10.1101/gad.189365.112

244. Csibi A, Fendt SM, Li C, et al. The mTORC1 Pathway Stimulates Glutamine Metabolism and Cell Proliferation by Repressing SIRT4. *Cell*. 2013;153(4):840-854. doi:10.1016/j.cell.2013.04.023

245. Csibi A, Lee G, Yoon SO, et al. The mTORC1/S6K1 Pathway Regulates Glutamine Metabolism through the eIF4B-Dependent Control of c-Myc Translation. *Current Biology*. 2014;24(19):2274-2280. doi:10.1016/j.cub.2014.08.007

246. Esslinger CS, Cybulski KA, Rhoderick JF. Nγ-Aryl glutamine analogues as probes of the ASCT2 neutral amino acid transporter binding site. *Bioorganic & Medicinal Chemistry*. 2005;13(4):1111-1118. doi:10.1016/j.bmc.2004.11.028

247. Schulte ML, Fu A, Zhao P, et al. Pharmacological blockade of ASCT2-dependent glutamine transport leads to antitumor efficacy in preclinical models. *Nat Med*. 2018;24(2):194-202. doi:10.1038/nm.4464

248. Edwards DN, Ngwa VM, Raybuck AL, et al. Selective glutamine metabolism inhibition in tumor cells improves antitumor T lymphocyte activity in triple-negative breast cancer. *Journal of Clinical Investigation*. 2021;131(4):e140100. doi:10.1172/JCI140100

249. Böhme-Schäfer I, Lörentz S, Bosserhoff AK. Role of Amino Acid Transporter SNAT1/SLC38A1 in Human Melanoma. *Cancers*. 2022;14(9):2151. doi:10.3390/cancers14092151

250. Imai H, Kaira K, Oriuchi N, et al. Inhibition of L-type Amino Acid Transporter 1 Has Antitumor Activity in Non-small Cell Lung Cancer. *ANTICANCER RESEARCH*. Published online 2010.

251. Shennan. Inhibition of system L (LAT1/CD98hc) reduces the growth of cultured human breast cancer cells. *Oncol Rep*. 1994;20(4). doi:10.3892/or_00000087

252. Seltzer MJ, Bennett BD, Joshi AD, et al. Inhibition of Glutaminase Preferentially Slows Growth of Glioma Cells with Mutant IDH1. *Cancer Research*. 2010;70(22):8981-8987. doi:10.1158/0008-5472.CAN-10-1666

253. Wu C, Chen L, Jin S, Li H. Glutaminase inhibitors: a patent review. *Expert Opinion on Therapeutic Patents*. 2018;28(11):823-835. doi:10.1080/13543776.2018.1530759

254. Stalnecker CA, Ulrich SM, Li Y, et al. Mechanism by which a recently discovered allosteric inhibitor blocks glutamine metabolism in transformed cells. *Proc Natl Acad Sci USA*. 2015;112(2):394-399. doi:10.1073/pnas.1414056112

255. Ramachandran S, Pan CQ, Zimmermann SC, et al. Structural basis for exploring the allosteric inhibition of human kidney type glutaminase. *Oncotarget*. 2016;7(36):57943-57954. doi:10.18632/oncotarget.10791

256. Lemberg KM, Vornov JJ, Rais R, Slusher BS. We're Not "DON" Yet: Optimal Dosing and Prodrug Delivery of *6-Diazo-5-oxo-L-norleucine*. *Molecular Cancer Therapeutics*. 2018;17(9):1824-1832. doi:10.1158/1535-7163.MCT-17-1148

257. Hsu BY, Marshall CM, McNamara PD, Segal S. The effect of azaserine on glutamine uptake by rat renal brush-border membranes. *Biochemical Journal*. 1980;192(1):119-126. doi:10.1042/bj1920119

258. Smulski DR, Huang LL, McCluskey MP, et al. Combined, Functional Genomic-Biochemical Approach to Intermediary Metabolism: Interaction of Acivicin, a Glutamine Amidotransferase Inhibitor, with *Escherichia coli* K-12. *J Bacteriol*. 2001;183(11):3353-3364. doi:10.1128/JB.183.11.3353-3364.2001

259. Kidd BJG. REGRESSION OF TRANSPLANTED LYMPHOMAS INDUCED IN VIVO BY MEANS OF NORMAL GUINEA PIG SERUM.

260. Broome D. EVIDENCE THAT THE L-ASPARAGINASE OF GUINEA PIG SERUM IS RESPONSIBLE FOR ITS ANTILYMPHOMA EFFECTS*,$.

261. Broome JD. EVIDENCE THAT THE L-ASPARAGINASE OF GUINEA PIG SERUM IS RESPONSIBLE FOR ITS ANTILYMPHOMA EFFECTS. *Journal of Experimental Medicine*. 1963;118(1):121-148. doi:10.1084/jem.118.1.121

262. Chan WK, Lorenzi PL, Anishkin A, et al. The glutaminase activity of l-asparaginase is not required for anticancer activity against ASNS-negative cells. *Blood*. 2014;123(23):3596-3606. doi:10.1182/blood-2013-10-535112

263. Pieters R, Hunger SP, Boos J, et al. L-asparaginase treatment in acute lymphoblastic leukemia: A focus on Erwinia asparaginase. *Cancer*. 2011;117(2):238-249. doi:10.1002/cncr.25489

264. Distasio JA, Salazar AM, Nadji M, Durden DL. Glutaminase-free asparaginase fromvibrio succinogenes: An antilymphoma enzyme lacking hepatotoxicity. *Int J Cancer*. 1982;30(3):343-347. doi:10.1002/ijc.2910300314

265. Ehsanipour EA, Sheng X, Behan JW, et al. Adipocytes Cause Leukemia Cell Resistance to L -Asparaginase via Release of Glutamine. *Cancer Research*. 2013;73(10):2998-3006. doi:10.1158/0008-5472.CAN-12-4402

266. Li C, Feng Y, Wang W, et al. Targeting Glutaminolysis to Treat Multiple Myeloma: An In Vitro Evaluation of GlutaminaseInhibitors Telaglenastat and Epigallocatechin-3-gallate. *ACAMC*. 2023;23(7):779-785. doi:10.2174/1871520622666220905142338

267. Sbirkov Y, Vergov B, Dzharov V, Schenk T, Petrie K, Sarafian V. Targeting Glutaminolysis Shows Efficacy in Both Prednisolone-Sensitive and in Metabolically Rewired Prednisolone-Resistant B-Cell Childhood Acute Lymphoblastic Leukaemia Cells. *IJMS*. 2023;24(4):3378. doi:10.3390/ijms24043378

268. Gao M, Monian P, Quadri N, Ramasamy R, Jiang X. Glutaminolysis and Transferrin Regulate Ferroptosis. *Molecular Cell*. 2015;59(2):298-308. doi:10.1016/j.molcel.2015.06.011

269. Clancy KP, Berger R, Cox M, et al. Localization of theL-Glutamine Synthetase Gene to Chromosome 1q23. *Genomics*. 1996;38(3):418-420. doi:10.1006/geno.1996.0645

270. Berlicki L. Inhibitors of Glutamine Synthetase and their Potential Application in Medicine. *MRMC*. 2008;8(9):869-878. doi:10.2174/138955708785132800

271. Currie E, Schulze A, Zechner R, Walther TC, Farese RV. Cellular Fatty Acid Metabolism and Cancer. *Cell Metabolism*. 2013;18(2):153-161. doi:10.1016/j.cmet.2013.05.017

272. Nieman KM, Kenny HA, Penicka CV, et al. Adipocytes promote ovarian cancer metastasis and provide energy for rapid tumor growth. *Nat Med*. 2011;17(11):1498-1503. doi:10.1038/nm.2492

273. DeFilippis RA, Chang H, Dumont N, et al. CD36 Repression Activates a Multicellular Stromal Program Shared by High Mammographic Density and Tumor Tissues. *Cancer Discovery*. 2012;2(9):826-839. doi:10.1158/2159-8290.CD-12-0107

274. Ladanyi A, Mukherjee A, Kenny HA, et al. Adipocyte-induced CD36 expression drives ovarian cancer progression and metastasis. *Oncogene*. 2018;37(17):2285-2301. doi:10.1038/s41388-017-0093-z

275. Watt MJ, Clark AK, Selth LA, et al. Suppressing fatty acid uptake has therapeutic effects in preclinical models of prostate cancer. *Sci Transl Med*. 2019;11(478):eaau5758. doi:10.1126/scitranslmed.aau5758

276. Shurbaji MS, Kalbfleisch JH, Thurmond TS. Immunohistochemical detection of a fatty acid synthase (OA-519) as a predictor of progression of prostate cancer. *Human Pathology*. 1996;27(9):917-921. doi:10.1016/S0046-8177(96)90218-X

277. Ogino S, Nosho K, Meyerhardt JA, et al. Cohort Study of Fatty Acid Synthase Expression and Patient Survival in Colon Cancer. *JCO*. 2008;26(35):5713-5720. doi:10.1200/JCO.2008.18.2675

278. Visca P, Sebastiani V, Botti C, et al. Fatty Acid Synthase (FAS) is a Marker of Increased Risk of Recurrence in Lung Carcinoma. *ANTICANCER RESEARCH*. Published online 2004.

279. Wellen KE, Hatzivassiliou G, Sachdeva UM, Bui TV, Cross JR, Thompson CB. ATP-Citrate Lyase Links Cellular Metabolism to Histone Acetylation. *Science*. 2009;324(5930):1076-1080. doi:10.1126/science.1164097

280. Svensson RU, Parker SJ, Eichner LJ, et al. Inhibition of acetyl-CoA carboxylase suppresses fatty acid synthesis and tumor growth of non-small-cell lung cancer in preclinical models. *Nat Med*. 2016;22(10):1108-1119. doi:10.1038/nm.4181

281. Che XM. Overexpression of Nampt in gastric cancer and chemopotentiating effects of the Nampt inhibitor FK866 in combination with fluorouracil. *Oncol Rep*. Published online July 4, 2011. doi:10.3892/or.2011.1378

282. Lucena-Cacace A, Otero-Albiol D, Jiménez-García MP, Muñoz-Galvan S, Carnero A. *NAMPT* Is a Potent Oncogene in Colon Cancer Progression that Modulates Cancer Stem Cell Properties and Resistance to Therapy through Sirt1 and PARP. *Clinical Cancer Research*. 2018;24(5):1202-1215. doi:10.1158/1078-0432.CCR-17-2575

283. Olesen UH, Hastrup N, Sehested M. Expression patterns of nicotinamide phosphoribosyltransferase and nicotinic acid phosphoribosyltransferase in human malignant lymphomas. *APMIS*. 2011;119(4-5):296-303. doi:10.1111/j.1600-0463.2011.02733.x

284. Shackelford RE, Bui MM, Coppola D, Hakam A. Over-expression of nicotinamide phosphoribosyl- transferase in ovarian cancers. *Int J Cli Exp Pathol*. 2010;3(5):522-527.

285. Wang B, Hasan MK, Alvarado E, Yuan H, Wu H, Chen WY. NAMPT overexpression in prostate cancer and its contribution to tumor cell survival and stress response. *Oncogene*. 2011;30(8):907-921. doi:10.1038/onc.2010.468

286. Zhu Y, Guo M, Zhang L, Xu T, Wang L, Xu G. Biomarker triplet NAMPT/VEGF/HER2 as a de novo detection panel for the diagnosis and prognosis of human breast cancer. *Oncology Reports*. 2016;35(1):454-462. doi:10.3892/or.2015.4391

287. Zhang C, Tong J, Huang G. Nicotinamide Phosphoribosyl Transferase (Nampt) Is a Target of MicroRNA-26b in Colorectal Cancer Cells. El-Rifai W, ed. *PLoS ONE*. 2013;8(7):e69963. doi:10.1371/journal.pone.0069963

288. Hesari Z, Nourbakhsh M, Hosseinkhani S, et al. Down-regulation of NAMPT expression by mir-206 reduces cell survival of breast cancer cells. *Gene*. 2018;673:149-158. doi:10.1016/j.gene.2018.06.021

289. Ju HQ, Zhuang ZN, Li H, et al. Regulation of the Nampt-mediated NAD salvage pathway and its therapeutic implications in pancreatic cancer. *Cancer Letters*. 2016;379(1):1-11. doi:10.1016/j.canlet.2016.05.024

290. Zhang H, Zhang N, Liu Y, et al. Epigenetic Regulation of *NAMPT* by *NAMPT-AS* Drives Metastatic Progression in Triple-Negative Breast Cancer. *Cancer Research*. 2019;79(13):3347-3359. doi:10.1158/0008-5472.CAN-18-3418

291. Lee J, Kim H, Lee JE, et al. Selective Cytotoxicity of the NAMPT Inhibitor FK866 Toward Gastric Cancer Cells With Markers of the Epithelial-Mesenchymal Transition, Due to Loss of NAPRT. *Gastroenterology*. 2018;155(3):799-814.e13. doi:10.1053/j.gastro.2018.05.024

292. Li X qin, Lei J, Mao L hong, et al. NAMPT and NAPRT, Key Enzymes in NAD Salvage Synthesis Pathway, Are of Negative Prognostic Value in Colorectal Cancer. *Front Oncol*. 2019;9:736. doi:10.3389/fonc.2019.00736

293. Watson M, Roulston A, Bélec L, et al. The Small Molecule GMX1778 Is a Potent Inhibitor of NAD $^{+}$ Biosynthesis: Strategy for Enhanced Therapy in Nicotinic Acid Phosphoribosyltransferase 1-Deficient Tumors. *Molecular and Cellular Biology*. 2009;29(21):5872-5888. doi:10.1128/MCB.00112-09

294. Chowdhry S, Zanca C, Rajkumar U, et al. NAD metabolic dependency in cancer is shaped by gene amplification and enhancer remodelling. *Nature*. 2019;569(7757):570-575. doi:10.1038/s41586-019-1150-2

295. Piacente F, Caffa I, Ravera S, et al. Nicotinic Acid Phosphoribosyltransferase Regulates Cancer Cell Metabolism, Susceptibility to NAMPT Inhibitors, and DNA Repair. *Cancer Research*. 2017;77(14):3857-3869. doi:10.1158/0008-5472.CAN-16-3079

296. Fortunato C, Mazzola F, Raffaelli N. The key role of the NAD biosynthetic enzyme nicotinamide mononucleotide adenylyltransferase in regulating cell functions. *IUBMB Life*. 2022;74(7):562-572. doi:10.1002/iub.2584

297. Zhou T, Kurnasov O, Tomchick DR, et al. Structure of Human Nicotinamide/Nicotinic Acid Mononucleotide Adenylyltransferase. *Journal of Biological Chemistry*. 2002;277(15):13148-13154. doi:10.1074/jbc.M111469200

298. Song T, Yang L, Kabra N, et al. The NAD+ Synthesis Enzyme Nicotinamide Mononucleotide Adenylyltransferase (NMNAT1) Regulates Ribosomal RNA Transcription. *Journal of Biological Chemistry*. 2013;288(29):20908-20917. doi:10.1074/jbc.M113.470302

299. Kiss A, Ráduly AP, Regdon Z, et al. Targeting Nuclear NAD+ Synthesis Inhibits DNA Repair, Impairs Metabolic Adaptation and Increases Chemosensitivity of U-2OS Osteosarcoma Cells. *Cancers*. 2020;12(5):1180. doi:10.3390/cancers12051180

300. Berger NA, Berger SJ, Catino DM, Petzold SJ, Robins RK. Modulation of nicotinamide adenine dinucleotide and poly(adenosine diphosphoribose) metabolism by the synthetic "C" nucleoside analogs, tiazofurin and selenazofurin. A new strategy for cancer chemotherapy. *J Clin Invest*. 1985;75(2):702-709. doi:10.1172/JCI111750

301. Hovstadius P, Larsson R, Jonsson E, et al. A Phase I study of CHS 828 in patients with solid tumor malignancy. *Clin Cancer Res*. 2002;8(9):2843-2850.

302. von Heideman A, Berglund A, Larsson R, Nygren P. Safety and efficacy of NAD depleting cancer drugs: results of a phase I clinical trial of CHS 828 and overview of published data. *Cancer Chemother Pharmacol*. 2010;65(6):1165-1172. doi:10.1007/s00280-009-1125-3

303. Hasmann M, Schemainda I. FK866, a Highly Specific Noncompetitive Inhibitor of Nicotinamide Phosphoribosyltransferase, Represents a Novel Mechanism for Induction of Tumor Cell Apoptosis. *Cancer Research*. 2003;63(21):7436-7442.

304. O'Brien T, Oeh J, Xiao Y, et al. Supplementation of Nicotinic Acid with NAMPT Inhibitors Results in Loss of In Vivo Efficacy in NAPRT1-Deficient Tumor Models. *Neoplasia*. 2013;15(12):1314-IN3. doi:10.1593/neo.131718

305. Gibson AE, Yeung C, Issaq SH, et al. Inhibition of nicotinamide phosphoribosyltransferase (NAMPT) with OT-82 induces DNA damage, cell death, and suppression of tumor growth in preclinical models of Ewing sarcoma. *Oncogenesis*. 2020;9(9):80. doi:10.1038/s41389-020-00264-0

306. Wei Y, Xiang H, Zhang W. Review of various NAMPT inhibitors for the treatment of cancer. *Front Pharmacol*. 2022;13:970553. doi:10.3389/fphar.2022.970553

307. Gaut ZN, Solomon HM. Uptake and metabolism of nicotinic acid by human blood platelets. Effects of structure analogs and metabolic inhibitors. *Biochim Biophys Acta*. 1970;201(2):316-322. doi:10.1016/0304-4165(70)90306-5

308. Gaut ZN, Solomon HM. Inhibition of nicotinate phosphoribosyl transferase by nonsteroidal anti-inflammatory drugs: a possible mechanism of action. *J Pharm Sci*. 1971;60(12):1887-1888. doi:10.1002/jps.2600601230

309. Ghanem MS, Caffa I, Del Rio A, et al. Identification of NAPRT Inhibitors with Anti-Cancer Properties by In Silico Drug Discovery. *Pharmaceuticals*. 2022;15(7):848. doi:10.3390/ph15070848

310. Buonvicino D, Mazzola F, Zamporlini F, et al. Identification of the Nicotinamide Salvage Pathway as a New Toxification Route for Antimetabolites. *Cell Chemical Biology*. 2018;25(4):471-482.e7. doi:10.1016/j.chembiol.2018.01.012

311. Ghanem MS, Monacelli F, Nencioni A. Advances in NAD-Lowering Agents for Cancer Treatment. *Nutrients*. 2021;13(5):1665. doi:10.3390/nu13051665

312. Haubrich BA, Ramesha C, Swinney DC. Development of a Bioluminescent High-Throughput Screening Assay for Nicotinamide Mononucleotide Adenylyltransferase (NMNAT). *SLAS Discovery*. 2020;25(1):33-42. doi:10.1177/2472555219879644

313. Palumbo A, Anderson K. Multiple Myeloma. *N Engl J Med*. 2011;364(11):1046-1060. doi:10.1056/NEJMra1011442

314. Landgren O, Kyle RA, Pfeiffer RM, et al. Monoclonal gammopathy of undetermined significance (MGUS) consistently precedes multiple myeloma: a prospective study. *Blood*. 2009;113(22):5412-5417. doi:10.1182/blood-2008-12-194241

315. Weiss BM, Abadie J, Verma P, Howard RS, Kuehl WM. A monoclonal gammopathy precedes multiple myeloma in most patients. *Blood*. 2009;113(22):5418-5422. doi:10.1182/blood-2008-12-195008

316. Manier S, Salem KZ, Park J, Landau DA, Getz G, Ghobrial IM. Genomic complexity of multiple myeloma and its clinical implications. *Nat Rev Clin Oncol*. 2017;14(2):100-113. doi:10.1038/nrclinonc.2016.122

317. Kuehl WM, Bergsagel PL. Multiple myeloma: evolving genetic events and host interactions. *Nat Rev Cancer*. 2002;2(3):175-187. doi:10.1038/nrc746

318. Chng WJ, Huang GF, Chung TH, et al. Clinical and biological implications of MYC activation: a common difference between MGUS and newly diagnosed multiple myeloma. *Leukemia*. 2011;25(6):1026-1035. doi:10.1038/leu.2011.53

319. Hideshima T, Mitsiades C, Tonon G, Richardson PG, Anderson KC. Understanding multiple myeloma pathogenesis in the bone marrow to identify new therapeutic targets. *Nat Rev Cancer*. 2007;7(8):585-598. doi:10.1038/nrc2189

320. Shou Y, Martelli ML, Gabrea A, et al. Diverse karyotypic abnormalities of the c *-myc* locus associated with c *-myc* dysregulation and tumor progression in multiple myeloma. *Proc Natl Acad Sci USA*. 2000;97(1):228-233. doi:10.1073/pnas.97.1.228

321. Affer M, Chesi M, Chen WD, et al. Promiscuous MYC locus rearrangements hijack enhancers but mostly super-enhancers to dysregulate MYC expression in multiple myeloma. *Leukemia*. 2014;28(8):1725-1735. doi:10.1038/leu.2014.70

322. Allevato M, Bolotin E, Grossman M, Mane-Padros D, Sladek FM, Martinez E. Sequence-specific DNA binding by MYC/MAX to low-affinity non-E-box motifs. Hayes F, ed. *PLoS ONE*. 2017;12(7):e0180147. doi:10.1371/journal.pone.0180147

323. Dang CV, O'Donnell KA, Zeller KI, Nguyen T, Osthus RC, Li F. The c-Myc target gene network. *Seminars in Cancer Biology*. 2006;16(4):253-264. doi:10.1016/j.semcancer.2006.07.014

324. Chen H, Liu H, Qing G. Targeting oncogenic Myc as a strategy for cancer treatment. *Sig Transduct Target Ther*. 2018;3(1):5. doi:10.1038/s41392-018-0008-7

325. Rajagopalan KN, DeBerardinis RJ. Role of Glutamine in Cancer: Therapeutic and Imaging Implications: FIGURE 1. *J Nucl Med*. 2011;52(7):1005-1008. doi:10.2967/jnumed.110.084244

326. DeBerardinis RJ, Cheng T. Q's next: the diverse functions of glutamine in metabolism, cell biology and cancer. *Oncogene*. 2010;29(3):313-324. doi:10.1038/onc.2009.358

327. Revollo JR, Grimm AA, Imai S ichiro. The NAD Biosynthesis Pathway Mediated by Nicotinamide Phosphoribosyltransferase Regulates Sir2 Activity in Mammalian Cells. *Journal of Biological Chemistry*. 2004;279(49):50754-50763. doi:10.1074/jbc.M408388200

328. Liberzon A, Birger C, Thorvaldsdóttir H, Ghandi M, Mesirov JP, Tamayo P. The Molecular Signatures Database Hallmark Gene Set Collection. *Cell Systems*. 2015;1(6):417-425. doi:10.1016/j.cels.2015.12.004

329. Schlosser I. A role for c-Myc in the regulation of ribosomal RNA processing. *Nucleic Acids Research*. 2003;31(21):6148-6156. doi:10.1093/nar/gkg794

330. Van Riggelen J, Yetil A, Felsher DW. MYC as a regulator of ribosome biogenesis and protein synthesis. *Nat Rev Cancer*. 2010;10(4):301-309. doi:10.1038/nrc2819

331. Schmidt EV. The role of c-myc in regulation of translation initiation. *Oncogene*. 2004;23(18):3217-3221. doi:10.1038/sj.onc.1207548

332. Manier S, Huynh D, Shen YJ, et al. Inhibiting the oncogenic translation program is an effective therapeutic strategy in multiple myeloma. *Sci Transl Med*. 2017;9(389):eaal2668. doi:10.1126/scitranslmed.aal2668

333. Tambay V, Raymond VA, Bilodeau M. MYC Rules: Leading Glutamine Metabolism toward a Distinct Cancer Cell Phenotype. *Cancers*. 2021;13(17):4484. doi:10.3390/cancers13174484

334. Lu SC. Regulation of glutathione synthesis. *Molecular Aspects of Medicine*. 2009;30(1-2):42-59. doi:10.1016/j.mam.2008.05.005

335. Yang D, Liu H, Goga A, Kim S, Yuneva M, Bishop JM. Therapeutic potential of a synthetic lethal interaction between the *MYC* proto-oncogene and inhibition of aurora-B kinase. *Proc Natl Acad Sci USA*. 2010;107(31):13836-13841. doi:10.1073/pnas.1008366107

336. Pourdehnad M, Truitt ML, Siddiqi IN, Ducker GS, Shokat KM, Ruggero D. Myc and mTOR converge on a common node in protein synthesis control that confers synthetic lethality in Myc-driven cancers. *Proc Natl Acad Sci USA*. 2013;110(29):11988-11993. doi:10.1073/pnas.1310230110

337. Stein LR, Imai S ichiro. The dynamic regulation of NAD metabolism in mitochondria. *Trends in Endocrinology & Metabolism*. 2012;23(9):420-428. doi:10.1016/j.tem.2012.06.005

338. Garten A, Schuster S, Penke M, Gorski T, de Giorgis T, Kiess W. Physiological and pathophysiological roles of NAMPT and NAD metabolism. *Nat Rev Endocrinol*. 2015;11(9):535-546. doi:10.1038/nrendo.2015.117

339. Hong SM, Park CW, Kim SW, et al. NAMPT suppresses glucose deprivation-induced oxidative stress by increasing NADPH levels in breast cancer. *Oncogene*. 2016;35(27):3544-3554. doi:10.1038/onc.2015.415

340. Heske CM. Beyond Energy Metabolism: Exploiting the Additional Roles of NAMPT for Cancer Therapy. *Front Oncol*. 2020;9:1514. doi:10.3389/fonc.2019.01514

341. Thompson RM, Dytfeld D, Reyes L, et al. Glutaminase inhibitor CB-839 synergizes with carfilzomib in resistant multiple myeloma cells. *Oncotarget*. 2017;8(22):35863-35876. doi:10.18632/oncotarget.16262

342. Llombart V, Mansour MR. Therapeutic targeting of "undruggable" MYC. *eBioMedicine*. 2022;75:103756. doi:10.1016/j.ebiom.2021.103756

343. Allen-Petersen BL, Sears RC. Mission Possible: Advances in MYC Therapeutic Targeting in Cancer. *BioDrugs*. 2019;33(5):539-553. doi:10.1007/s40259-019-00370-5

344. Ba M, Long H, Yan Z, et al. BRD4 promotes gastric cancer progression through the transcriptional and epigenetic regulation of c-MYC. *J Cell Biochem*. 2018;119(1):973-982. doi:10.1002/jcb.26264

345. Constantin TA, Greenland KK, Varela-Carver A, Bevan CL. Transcription associated cyclin-dependent kinases as therapeutic targets for prostate cancer. *Oncogene*. 2022;41(24):3303-3315. doi:10.1038/s41388-022-02347-1

346. Viswanathan SR, Powers JT, Einhorn W, et al. Lin28 promotes transformation and is associated with advanced human malignancies. *Nat Genet*. 2009;41(7):843-848. doi:10.1038/ng.392

347. Delmore JE, Issa GC, Lemieux ME, et al. BET Bromodomain Inhibition as a Therapeutic Strategy to Target c-Myc. *Cell*. 2011;146(6):904-917. doi:10.1016/j.cell.2011.08.017

348. Mazur PK, Herner A, Mello SS, et al. Combined inhibition of BET family proteins and histone deacetylases as a potential epigenetics-based therapy for pancreatic ductal adenocarcinoma. *Nat Med*. 2015;21(10):1163-1171. doi:10.1038/nm.3952

349. Effenberger M, Bommert KS, Kunz V, et al. Glutaminase inhibition in multiple myeloma induces apoptosis *via* MYC degradation. *Oncotarget*. 2017;8(49):85858-85867. doi:10.18632/oncotarget.20691

350. Wise DR, DeBerardinis RJ, Mancuso A, et al. Myc regulates a transcriptional program that stimulates mitochondrial glutaminolysis and leads to glutamine addiction. *Proc Natl Acad Sci USA*. 2008;105(48):18782-18787. doi:10.1073/pnas.0810199105

351. Gao P, Tchernyshyov I, Chang TC, et al. c-Myc suppression of miR-23a/b enhances mitochondrial glutaminase expression and glutamine metabolism. *Nature*. 2009;458(7239):762-765. doi:10.1038/nature07823

352. Gross MI, Demo SD, Dennison JB, et al. Antitumor Activity of the Glutaminase Inhibitor CB-839 in Triple-Negative Breast Cancer. *Molecular Cancer Therapeutics*. 2014;13(4):890-901. doi:10.1158/1535-7163.MCT-13-0870

353. Galan-Cobo A, Sitthideatphaiboon P, Qu X, et al. LKB1 and KEAP1/NRF2 Pathways Cooperatively Promote Metabolic Reprogramming with Enhanced Glutamine Dependence in *KRAS* -Mutant Lung Adenocarcinoma. *Cancer Research*. 2019;79(13):3251-3267. doi:10.1158/0008-5472.CAN-18-3527

354. Jacque N, Ronchetti AM, Larrue C, et al. Targeting glutaminolysis has antileukemic activity in acute myeloid leukemia and synergizes with BCL-2 inhibition. *Blood*. 2015;126(11):1346-1356. doi:10.1182/blood-2015-01-621870

355. Matre P, Velez J, Jacamo R, et al. Inhibiting glutaminase in acute myeloid leukemia: metabolic dependency of selected AML subtypes. *Oncotarget*. 2016;7(48):79722-79735. doi:10.18632/oncotarget.12944

356. Gonsalves WI, Jang JS, Jessen E, et al. In vivo assessment of glutamine anaplerosis into the TCA cycle in human pre-malignant and malignant clonal plasma cells. *Cancer Metab*. 2020;8(1):29. doi:10.1186/s40170-020-00235-4

357. Muir A, Danai LV, Gui DY, Waingarten CY, Lewis CA, Vander Heiden MG. Environmental cystine drives glutamine anaplerosis and sensitizes cancer cells to glutaminase inhibition. *eLife*. 2017;6:e27713. doi:10.7554/eLife.27713

358. Jin H, Wang S, Zaal EA, et al. A powerful drug combination strategy targeting glutamine addiction for the treatment of human liver cancer. *eLife*. 2020;9:e56749. doi:10.7554/eLife.56749

359. Sayin VI, LeBoeuf SE, Singh SX, et al. Activation of the NRF2 antioxidant program generates an imbalance in central carbon metabolism in cancer. *eLife*. 2017;6:e28083. doi:10.7554/eLife.28083

360. Varghese S, Pramanik S, Williams LJ, et al. The Glutaminase Inhibitor CB-839 (Telaglenastat) Enhances the Antimelanoma Activity of T-Cell–Mediated

Immunotherapies. *Molecular Cancer Therapeutics*. 2021;20(3):500-511. doi:10.1158/1535-7163.MCT-20-0430

361. Momcilovic M, Bailey ST, Lee JT, et al. The GSK3 Signaling Axis Regulates Adaptive Glutamine Metabolism in Lung Squamous Cell Carcinoma. *Cancer Cell*. 2018;33(5):905-921.e5. doi:10.1016/j.ccell.2018.04.002

362. Hasmann M, Schemainda I. FK866, a highly specific noncompetitive inhibitor of nicotinamide phosphoribosyltransferase, represents a novel mechanism for induction of tumor cell apoptosis. *Cancer Res*. 2003;63(21):7436-7442.

363. Nahimana A, Attinger A, Aubry D, et al. The NAD biosynthesis inhibitor APO866 has potent antitumor activity against hematologic malignancies. *Blood*. 2009;113(14):3276-3286. doi:10.1182/blood-2008-08-173369

364. Olesen UH, Thougaard AV, Jensen PB, Sehested M. A Preclinical Study on the Rescue of Normal Tissue by Nicotinic Acid in High-Dose Treatment with APO866, a Specific Nicotinamide Phosphoribosyltransferase Inhibitor. *Molecular Cancer Therapeutics*. 2010;9(6):1609-1617. doi:10.1158/1535-7163.MCT-09-1130

365. Billington RA, Genazzani AA, Travelli C, Condorelli F. NAD depletion by FK866 induces autophagy. *Autophagy*. 2008;4(3):385-387. doi:10.4161/auto.5635

366. Pogrebniak A, Schemainda I, Azzam K, Pelka-Fleischer R, Nüssler V, Hasmann M. CHEMOPOTENTIATING EFFECTS OF A NOVEL NAD BIOSYNTHESIS INHIBITOR, FK866, IN COMBINATION WITH ANTINEOPLASTIC AGENTS. *EUROPEAN JOURNAL OF MEDICAL RESEARCH*. Published online 2006.

367. Tan B, Young DA, Lu ZH, et al. Pharmacological Inhibition of Nicotinamide Phosphoribosyltransferase (NAMPT), an Enzyme Essential for NAD+ Biosynthesis, in Human Cancer Cells. *Journal of Biological Chemistry*. 2013;288(5):3500-3511. doi:10.1074/jbc.M112.394510

368. Haikala HM, Marques E, Turunen M, Klefström J. Myc requires RhoA/SRF to reprogram glutamine metabolism. *Small GTPases*. 2018;9(3):274-282. doi:10.1080/21541248.2016.1224287

369. Tateishi K, Iafrate AJ, Ho Q, et al. Myc-Driven Glycolysis Is a Therapeutic Target in Glioblastoma. *Clin Cancer Res*. 2016;22(17):4452-4465. doi:10.1158/1078-0432.CCR-15-2274

370. Ravaud A, Cerny T, Terret C, et al. Phase I study and pharmacokinetic of CHS-828, a guanidino-containing compound, administered orally as a single dose every 3 weeks in solid tumours: an ECSG/EORTC study. *Eur J Cancer*. 2005;41(5):702-707. doi:10.1016/j.ejca.2004.12.023

371. Roux B, Vaganay C, Vargas JD, et al. Targeting acute myeloid leukemia dependency on VCP-mediated DNA repair through a selective second-generation small-molecule inhibitor. *Sci Transl Med*. 2021;13(587):eabg1168. doi:10.1126/scitranslmed.abg1168